

**PEPTIDE NUCLEIC ACID (PNA) HYBRIDIZATION TO
NUCLEIC ACID TARGETS**

APPROVED BY SUPERVISORY COMMITTEE

David R. Corey, Ph.D., Advisor

Michael J. Gale, Jr., Ph.D., Chairman

Donald L. Sodora, Ph.D.

Thomas Kodadek, Ph.D.

Kristen W. Lynch, Ph.D.

Dedication

To my parents; Marilyn J. Nulf and Larry L. Nulf

**PEPTIDE NUCLEIC ACID (PNA) HYBRIDIZATION TO
NUCLEIC ACID TARGETS**

By

Christopher J. Nulf

DISSERTATION

Presented to the Faculty of the Graduate School of Biomedical Sciences

In Partial Fulfillment of the Requirements

For the Degree of

DOCTOR OF PHILOSOPHY

The University of Texas Southwestern Medical Center at Dallas

Dallas, Texas

July 2004

ACKNOWLEDGEMENTS

I would like to thank my mentor, Dr. David Corey, who has dedicated a generous amount of time in teaching me the scientific philosophy. His continuous optimism drove me to pursue experiments that I may not have otherwise chased.

I would also like to thank the members of my committee: Dr. Michael Gale Jr., Dr. Donald Sodora, Dr. Thomas Kodadek, and Dr. Kristen Lynch for their time, guidance, and scientific suggestions.

I am also grateful to the members of the lab who have contributed many interesting ideas and suggestions for the progress of my projects over the years. Special thanks goes to Lynn Mayfield who taught me the finer points of PNA synthesis. Also, Dr. Dwaine Braasch spent countless hours teaching me the transfection protocols and luciferase assays. His troubleshooting expertise and mechanical skills were an invaluable contribution to the success of my project.

I would also thank the collaborators who provided me the essential materials to pursue my own experimentation and who had faith in my synthesis abilities to use my PNAs in their own studies: Dr. Khalil Arar and Alex Amiet (Proligo LLC.) for providing the chimeric LNA oligonucleotides used in the HCV IRES studies; Dr. Michael Gale (University of Texas Southwestern Medical Center at Dallas) for generously providing the pRL-HL (bicistronic transcript) vector used in the HCV IRES antisense experiments; Dr. Yinghui Liu who used my PNAs in her experiments as a comparison to siRNA in inhibiting isoform-specific gene expression of human caveolin; Dr. Brett Monia (ISIS Pharmaceuticals) who used my PNAs in his experiments toward altering splicing events

of the insulin receptor α -subunit pre-mRNA; Dr. Stephen Ekker (The University of Minnesota) who used my PNAs in his experiments as a comparison to antisense morpholinos in altering gene expression during embryogenesis of the Zebrafish.

Last, but certainly not least, I would like to extend a special thanks to Chrissy Webber for her love, enthusiasm, and patience. She has stood by me through the highs and the lows of my education with an infinite amount of understanding for my career ambitions. Chrissy, thank-you for being there when I needed you.

**PEPTIDE NUCLEIC ACID (PNA) HYBRIDIZATION TO
NUCLEIC ACID TARGETS**

Publication No. _____

Christopher J. Nulf, Ph.D.

The University of Texas Southwestern Medical Center at Dallas, 2004

Supervising Professor: David R. Corey, Ph.D.

Peptide nucleic acid (PNA) is a DNA/RNA mimic that offers many advantages for hybridization to nucleic acid targets. The simple premise of Watson-Crick base-pairing presents PNAs with a number of diverse applications ranging from nanotechnology to antisense therapeutics.

I studied the synthesis and characterization of novel tethered PNA molecules (bisPNAs) designed to assemble two individual DNA molecules through Watson-Crick base pairing. The spacer regions linking the PNAs were varied in length and contained amino acids with different electrostatic properties. I observed that bisPNAs effectively assembled oligonucleotides that were either the exact length of the PNA or that contained overhanging regions that projected outwards. In contrast, DNA assembly was much less efficient if the oligonucleotides contained overhanging regions that projected inwards. Surprisingly, the length of the spacer region between the PNA sequences did not greatly affect the efficiency of DNA assembly. Reasons for inefficient assembly of inward projecting DNA oligonucleotides include non-sequence-specific intramolecular interactions between the overhanging region of the bisPNA and steric conflicts that complicate binding of two inward projecting strands. These results suggested that bisPNA molecules can be used for self-assembling DNA nanostructures.

The Hepatitis C Virus (HCV) RNA genome contains a conserved tertiary structure known as the internal ribosomal entry site (IRES) necessary for cap-independent translation. I tested the hypothesis that antisense peptide nucleic acid (PNA) and locked nucleic acid (LNA) oligomers can bind IRES sequences and block translation. Using a lipid-mediated approach to introduce antisense PNAs and LNAs into cells, my data suggested that PNAs and LNAs could inhibit HCV IRES-dependent translation. PNA or LNA oligomers targeting different regions of the HCV IRES demonstrated a sequence-specific dose-response inhibition of translation with EC_{50} values of 50-150 nM. IRES-directed inhibition of gene expression widens the range of mechanisms for antisense

inhibition by PNAs and LNAs and may provide further therapeutic lead compounds for the treatment of HCV.

It is important to compare and contrast the biological activities of PNAs against other nucleotide analogs. Presented herein are collaborations involving comparisons of my PNAs against siRNA, 2'-O-methoxyethyl RNA, and morpholinos. Antisense PNAs were demonstrated to cause isoform-specific inhibition of protein expression of Caveolin. Similarly, PNAs demonstrated the ability to re-direct splicing activity of Insulin Receptor α -Subunit pre-mRNA. Also, antisense PNAs targeting the Chordino gene demonstrated “knock-down” morphologies similar to “knock-out” mutants in developing Zebrafish embryos. Collectively, these results suggest that PNAs are comparable in function to other oligonucleotide analogs and across many experimental platforms.

TABLE OF CONTENTS

	<u>Page</u>
ABSTRACT	vi
TABLE OF CONTENTS	ix
PUBLICATIONS	xvi
LIST OF FIGURES	xvii
LIST OF TABLES	xx
GLOSSARY	xxi

CHAPTER 1 - THE BASICS OF PEPTIDE NUCLEIC ACIDS (PNAs)

	<u>Page</u>
Chemical structure of PNAs	2
Biophysical properties of PNAs	
The First report	2
Stability of PNA hybridization	6
Specificity of PNA hybridization	10
Ion-independence of PNA hybridization	12
Biophysical structures of PNA duplexes	12
Design, synthesis, analysis and handling of PNAs	15
Current uses of PNAs	25
PNAs as antisense molecules	28
Delivery of PNAs into cells	31
References for Chapter 1	36

CHAPTER 2 - DNA ASSEMBLY BY BIS-PEPTIDE NUCLEIC ACIDS (bisPNAs)

	<u>Page</u>
Introduction	50
DNA in nano-biotechnology	50
PNA potentials in nano-biotechnology	54
Rational design of novel bisPNAs	56
Chemical synthesis and analysis of PNA and bisPNA molecules	56
Models of dual DNA oligonucleotide hybridization	
Melting temperature (T_m) analysis of exact complement and overhanging DNA oligonucleotides to bisPNAs	58
Assembly of short, complementary oligonucleotides by bisPNA	62
Assembly of oligonucleotides that project beyond the bisPNA	62
DNA assembly by bisPNAs connected by spacers of differing lengths	64
Reasons for inefficient assembly of oligonucleotides that project inward	69
Applications of PNAs for the assembly of DNA structures	72
BisPNAs strand-invasion into duplex DNA	75
Uses of bisPNA to strand invade at two individual duplex DNA locations	78
Conclusions	80
References for Chapter 2	84

**CHAPTER 3 - INTRACELLULAR INHIBITION OF HEPATITIS C VIRUS
(HCV) INTERNAL RIBOSOMAL ENTRY SITE (IRES)-DEPENDENT
TRANSLATION BY PEPTIDE NUCLEIC ACIDS (PNAs) AND
CHIMERIC LOCKED NUCLEIC ACIDS (LNAs)**

	<u>Page</u>
Background and relevance	89
Design of PNAs and chimeric LNAs to target sequences within the HCV IRES	95
Cellular delivery of PNA and chimeric LNA oligonucleotides	100
Fluorescent microscopy of PNAs transfected into CV-1 cells	100
Analysis of lipid-mediated delivery of LNAs by flow cytometry	103
Inhibition of IRES-dependent translation by PNAs	103
Carrier DNA does not appear to influence IRES-dependent translation inhibition by antisense PNAs	108
Effect of PNA length on inhibition of gene expression	110
PNA length and mechanisms of antisense inhibition	111
Inhibition of IRES-dependent translation by chimeric LNAs	113
Factors governing the potencies of anti-IRES PNAs and LNAs	115
IRES sequences as targets for PNAs and chimeric LNAs	116
Future Directions	118
References for Chapter 3	120

CHAPTER 4 - OTHER MODELS AND APPLICATIONS FOR PNAs IN REGULATING GENE EXPRESSION (COLLABORATIONS)

	<u>Page</u>
Introduction	131
Comparison of PNAs with siRNA towards inhibiting isoform-specific expression of human caveolin-1 (Collaboration with Dr. Yinghui Liu, UT Southwestern Medical Center at Dallas)	133
The model target: Human caveolin-1	135
Design of PNAs and siRNAs to target sequences within the hCav-1 transcript	136
Inhibition of expression of hCav-1 isoforms by PNAs	136
Inhibition of expression of hCav-1 by siRNAs	139
The potency and duration of PNAs and siRNAs	139
Conclusions of comparisons	141
Comparison of PNAs with morpholinos for the inhibition of developmental genes in Zebrafish (collaboration with Dr. Stephen Egger, The University of Minnesota)	145
Background and chemistry of morpholino oligomers	145
Potential phenotypic outcomes of antisense experiments	147
Antisense effects of morpholinos and PNAs on Zebrafish development	148

Comparison of PNAs with 2'-<i>O</i>-(2-methoxyethyl) oligoribonucleotides	152
(2'-MOE) for re-directing pre-mRNA splicing events (collaboration with Dr. Brett Monia, ISIS Pharmaceuticals)	
Background and chemistry of 2'-<i>O</i>-(2-methoxyethyl) oligoribonucleotides (2'-MOE)	152
The model target: Human insulin receptor α-subunit	154
Efficiency of re-directing splicing events by PNAs and 2'MOE	156
The future of 2'MOE and PNAs as therapeutics	159
References for Chapter 4	161

CHAPTER 5 – WORDS OF WISDOM FOR THE NEW USER

	<u>Page</u>
Introduction	172
Commit to details	173
Design simple protocols with sensitive assays	173
Oligomers as controls	175
Critique the work	176
Progress towards complexity	178
References for Chapter 5	180

CHAPTER 6 – EXPERIMENTAL PROCEDURES

	<u>Page</u>
The Expedite 8909 PNA Synthesizer	183
Automated Synthesis of PNAs and bisPNAs	184
Manual Synthesis of PNAs	185
Reverse-Phase High Performance Liquid Chromatography	190
(RP-HPLC) for the analysis and purification of PNAs	
Matrix-Assisted Laser Desorption-Ionization Time-of-Flight	191
(MALDI-TOF) Mass Spectroscopy of PNAs	
Lyophilization of purified PNAs	192
Quantification of PNA concentrations by UV absorbance	192
spectroscopy	
Annealing of PNAs to complementary DNA oligonucleotides	193
(PNA:DNA Duplex Formation)	
Melting temperature analysis (T_m)	193
Preparation of radiolabeled (^{32}P) DNA oligonucleotides	194
Polyacrylamide gel electrophoresis of bisPNA:DNA hybridizations	195
Cesium-Chloride gradient preparation of supercoiled	195
plasmid DNA	
Detection of strand-invasion of PNA and bisPNA by the	196
modified T7 Sequenase assay	
Solution-phase N-terminal labeling of PNAs with Cy3 fluorophore	197
Thin-Layer Chromatography (TLC) detection of uncoupled Cy3	197

Maintenance and passaging of the CV-1 Cell Line	198
Cationic lipid-mediated transfection of PNA:DNA duplexes and chimeric LNA oligonucleotides into CV-1 cells	198
Cationic lipid-mediated transfection of reporter plasmid pRL-HL into CV-1 cells	199
Assessing Firefly luciferase and Renilla luciferase expression levels	201
Confocal fluorescence microscopy of cationic lipid-mediated uptake of PNA-Cy3 into live CV-1 cells	202
FACS analysis of LNA-Cy3 cellular uptake into CV-1 cells	202
References for Chapter 5	204

Publications

Nulf C.J., Corey D.R. (In Press) Intracellular inhibition of hepatitis C virus (HCV) internal ribosomal entry site (IRES)-dependent translation by peptide nucleic acids (PNAs) and locked nucleic acids (LNAs). *Nucleic Acids Research*.

Liu Y., Braasch D.A., **Nulf C.J.**, Corey D.R. (2004) Efficient and isoform-selective inhibition of cellular gene expression by peptide nucleic acids. *Biochemistry*. 43(7):1921-1927.

Gamper H.B., **Nulf C.J.**, Corey D.R., Kmiec E.B. (2003) The synaptic complex of RecA protein participates in hybridization and inverse strand exchange reactions. *Biochemistry*. 42(9):2643-55.

Nulf C.J., Corey D.R. (2002) DNA assembly using bis-peptide nucleic acids (bisPNAs). *Nucleic Acids Research*. 30(13):2782-9.

Braasch D.A., **Nulf C.J.**, and Corey D.R. (2002) *Current Protocols in Nucleic Acid Chemistry. Unit 4.11 Synthesis and Purification of Peptide Nucleic Acids*. pp.14.11.11-14.11.18, John Wiley & Sons, New York.

Abstracts and Posters

Nulf C.J., Corey D.R. Rules for Using Peptide Nucleic Acids (PNAs) to Bind and Assemble 'Complex' Nucleic Acid Targets. *2003 Keystone Symposia, Drug Target Validation: Gene Suppression*. Jan 17-22, 2003.

Nulf C.J., Corey D.R. Use of Complex Peptide Nucleic Acids to Assemble DNA Nanostructures. *Biotechnology and Nano-Biotechnology: Challenges and Opportunities of Drug Targeting in the Post-Genomic Era*. Oct. 18, 2002.

List of Figures

	<u>Page</u>
Figure 1-1. The PNA monomer.	3
Figure 1-2. Comparison of the chemical structures of peptides, PNA, and DNA molecules.	4
Figure 1-3. Watson-Crick and Hoogsteen hydrogen bonding between duplex and triplex oligonucleotide.	5
Figure 1-4. P-loop formation.	7
Figure 1-5. Structural features of PNA:RNA, PNA:DNA, PNA ₂ :DNA triplex, PNA:PNA.	14
Figure 1-6. Chemical structures of the protected monomers used for automated synthesis.	16
Figure 1-7. Automated PNA synthesis on the Expedite 8909 (Cycles).	19
Figure 1-8. Automated PNA synthesis on the Expedite 8909 (Chemistries).	21
Figure 1-9. RP-HPLC and MALDI-TOF MS of PNA.	22
Figure 1-10. Hyperchromic/Hypochromic effect of PNA:DNA hybridization.	24
Figure 1-11. Fluorescence <i>in situ</i> hybridization (FISH) of telomeres with PNA-Cy3.	26
Figure 1-12. Steric blocking of PNAs to nucleic acid targets.	30
Figure 1-13. Lipid-mediated cellular delivery of PNAs .	34
Figure 2-1. Chemical and physical dimensions of duplex DNA.	51
Figure 2-2. DNA Molecular "Tweezers" and "Switches".	53
Figure 2-3. The bisPNA design.	55
Figure 2-4. Models of bisPNA hybridized to DNA oligonucleotides.	59
Figure 2-5. Non-denaturing polyacrylamide gel electrophoresis of bisPNA-AEEA ₃ with exact complement DNA oligonucleotides.	63

Figure 2-6.	Comparison of each half of bisPNA-AEEA₃ for hybridization to one or two outward projecting DNA oligonucleotides.	64
Figure 2-7.	Comparison of bisPNA-AEEA₃ hybridization to DNA oligonucleotides that project outwards, partially project inwards, and project inwards.	66
Figure 2-8.	Comparison of oligonucleotide assembly by bisPNAs that contain spacers with varying numbers of AEEA spacers and amino acids.	68
Figure 2-9.	Non-specific interactions of bisPNA and DNA oligonucleotides.	70
Figure 2-10.	“DNA motifs” and “PNA motifs” for supramolecular oligonucleotide assembly.	73
Figure 2-11.	Strand-invasion target sites: Cruciform structure of supercoiled pUC19.	76
Figure 2-12.	Detection of PNA strand-invasion into supercoiled plasmid DNA: T7 Sequenase assay.	77
Figure 2-13.	T7 Sequenase assay demonstrating strand-invasion of bisPNA-AEEA₃ into dsDNA.	79
Figure 2-14.	Schematic of a bridging oligonucleotide targeting deleted mtDNA molecules.	81
Figure 2-15.	Schematic of a tethered DNA fragment being targeted to chromosomal DNA to encourage recombination.	82
Figure 3-1.	Lifecycle of HCV.	90
Figure 3-2.	The RNA secondary structure of the HCV 5'UTR/IRES.	91
Figure 3-3.	Comparisons of PNAs with LNAs.	93
Figure 3-4.	PNA and chimeric LNA target sites within the HCV 5'UTR/IRES.	99
Figure 3-5.	Confocal fluorescence microscopy of live cells.	102
Figure 3-6.	FACS analysis of lipid-mediated transfection of LNA-Cy3 into CV-1 cells.	104
Figure 3-7.	Schematic of the HCV bicistronic expression vector.	105

Figure 3-8.	Antisense PNAs targeting the HCV IRES inhibit relative luciferase activity.	107
Figure 3-9.	Effect of PNA length on IRES-dependent translation of Firefly luciferase.	112
Figure 3-10.	Effect of antisense chimeric LNAs on IRES-dependent translation of Firefly luciferase.	114
Figure 4-1.	The RNA interference pathway.	134
Figure 4-2.	Target sites and inhibition of hCav-1 expression by PNAs.	138
Figure 4-3.	Comparison of inhibition of hCav expression by isoform-specific PNA 1 and analogous siRNA 1.	140
Figure 4-4.	Inhibition of hCav-1 expression by varying concentrations of PNA 1, PNA 2, and siRNA 2.	142
Figure 4-5.	Time course of inhibition of hCav-1 expression by PNAs and siRNAs.	143
Figure 4-6.	Comparison of PNAs and morpholinos.	146
Figure 4-7.	Morphologies of wild-type, mutant, and antisense morpholino-treated Zebrafish embryos.	149
Figure 4-8.	Degrees of severity of the mutant chordino morphological phenotype.	150
Figure 4-9.	Comparison of PNAs and 2'-O-methoxyethyl RNA (2'-MOE).	153
Figure 4-10.	Schematic of the alternative splicing mechanism of the human insulin receptor α-subunit.	155
Figure 4-11.	Analysis of re-directed splicing event.	158
Figure 4-12.	Comparison of oligonucleotide splicing inhibition EC₅₀s.	160
Figure 6-1.	The apparatus for manual PNA synthesis	187
Figure 6-2.	Example spreadsheet for manual PNA synthesis	189
Figure 6-3.	The transfection protocol	200

List of Table

	<u>Page</u>
Table 1-1. Duplex stability and melting temperatures.	9
Table 1-2. Increased specificity for PNAs.	11
Table 1-3. PNA hybridization is independent of salt concentration.	13
Table 2-1. BisPNA sequences, expected and observed masses, and melting temperature values (T_m) for hybridization to oligonucleotide complements.	57
Table 2-2. DNA oligonucleotides, T_m Analysis with bisPNA-AEEA₃ and differences in T_m between exact complements and overhanging oligonucleotides.	61
Table 3-1. PNA sequences, expected and found masses, and location of target.	96
Table 3-2. Chimeric LNA sequences, T_m analysis, and target IRES sequences.	97
Table 3-3. Effects of ‘carrier DNA’ on PNA inhibition.	109
Table 4-1. Sequences of PNAs, rational of use, calculated and observed molecular weights.	137
Table 4-2. Comparison of the sequences of 2'-O-methoxyethyl and The PNA sequences and their relative position targeting the intron-exon junction.	157

List of Abbreviations

A	Adenine
ACN	Acetonitrile
AEEA	2-aminoethyl 2-ethoxyacetic acid
Aeg	N-(2-aminoethyl) glycine
Bhoc	Benzhydryloxycarbonyl
Boc	tert-Butyloxycarbonyl
C	Cytosine
Cbz	Benzyloxycarbonyl
DCM	Dichloromethane
DIPEA	Diisopropylethylamine
DMF	N,N-dimethylformamide
Fmoc	9-fluorenylmethoxycarbonyl
G	Guanine
HATU	<i>O</i> -(7-azabenzotriazol-1-yl)-1,1,3,3-tetramethyluronium hexafluorophosphate
HCV	Hepatitis C virus
hCav-1	Human caveolin-1
IRES	Internal ribosomal entry site
LNA	Locked nucleic acid
MALDI-TOF MS	Matrix-assisted laser desorption/ionization time of flight mass spectroscopy
NMP	1-Methyl-2-pyrrolidinone
PNA	Peptide (polyamide) nucleic acid
RP-HPLC	Reverse phase high performance liquid chromatography
siRNA	Short interfering (double-stranded) RNA
T	Thymine
TFA	Trifluoroacetic acid
TFMSA	Trifluoromethanesulfonic acid
XAL-PEG-PS	xanthyloxy alkanoic acid-polyethylene glycol-polystyrene
(T*A:T)	Triplex = Watson-Crick hybridization between A and T, Hoogsteen hybridization of T in the major groove of the double helix.
(C+G:C)	Triplex = Watson-Crick hybridization between G and C, Hoogsteen hybridization of protonated C in the major groove of the double helix.
(PNA:DNA)	Hybridized PNA to DNA oligonucleotide

CHAPTER 1 - THE BASICS OF PEPTIDE NUCLEIC ACIDS (PNAs)

	<u>Page</u>
Chemical structure of PNAs	2
Biophysical properties of PNAs	
The First report	2
Stability of PNA hybridization	6
Specificity of PNA hybridization	10
Ion-independence of PNA hybridization	12
Biophysical structures of PNA duplexes	12
Design, synthesis, analysis and handling of PNAs	15
Current uses of PNAs	25
PNAs as antisense molecules	28
Delivery of PNAs into cells	31
References for Chapter 1	36

Chemical structure of PNAs

Peptide nucleic acids (PNAs) are synthetic oligonucleotide mimics with an achiral backbone containing repeating units of N-(2-aminoethyl)-glycine (Aeg) linked by peptide bonds (1). Each of the four bases adenine, cytosine, guanine, thymine (A, C, G, T) is attached to the charge-neutral backbone by methylenecarbonyl linkages (**Figure 1-1. The PNA monomer**). While possessing neither a true peptide backbone (nor acidic groups), the PNA is sometime referred to as a polyamide nucleic acid. However, unique properties observed from both nucleic acids and peptides can be found within the PNA molecule.

By convention, PNAs have an amine-terminus (or N-terminus) and a carboxy-terminus (or C-terminus), corresponding to the 5'- and 3'-ends of a DNA oligonucleotide, respectively (**Figure 1-2. Comparison of the chemical structures of peptides, PNA, and DNA molecules**). PNA hybridization to complementary nucleic acid targets is reversible and follows normal Watson-Crick hydrogen bonding base-pairing rules (A=T, G≡C) with the anti-parallel formation preferred (2, 3, 4).

Biophysical properties of PNAs

The First report

Using molecular modeling, the PNA was first conceived as a ligand capable of binding into the major groove of double-stranded DNA (dsDNA) (1) (**Figure 1-3. Watson-Crick and Hoogsteen hydrogen bonding between duplex and triplex oligonucleotide**). In designing the ligand, the nucleobase specificity was to remain the

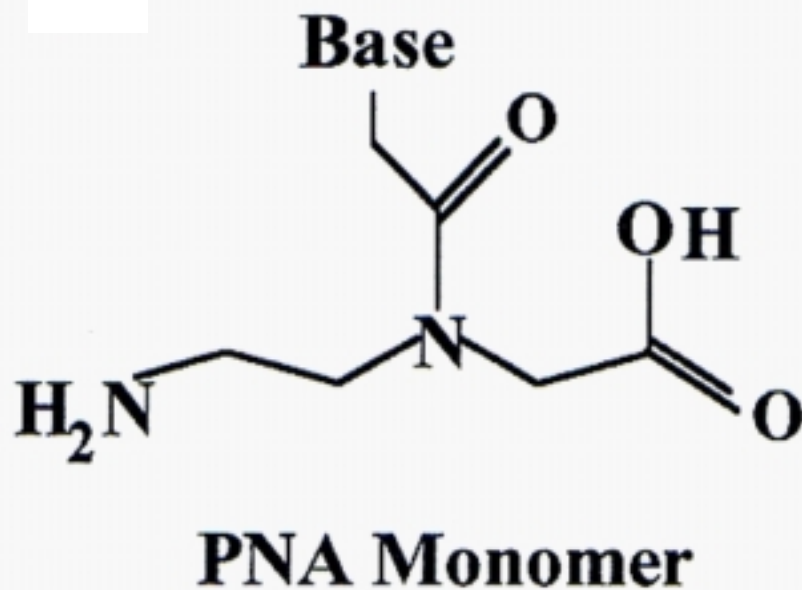


Figure 1-1. The PNA monomer. The backbone is composed of an achiral charge-neutral N-(2-aminoethyl)-glycine. Each of the four bases A, T, G, and C is attached to the backbone by methylenecarbonyl linkages. Each PNA monomer is linked by peptide bonds.

*From Applied Biosystems. (2001) PNA Chemistry for the Expedite 8900 Nucleic Acid Synthesis System User's Guide.

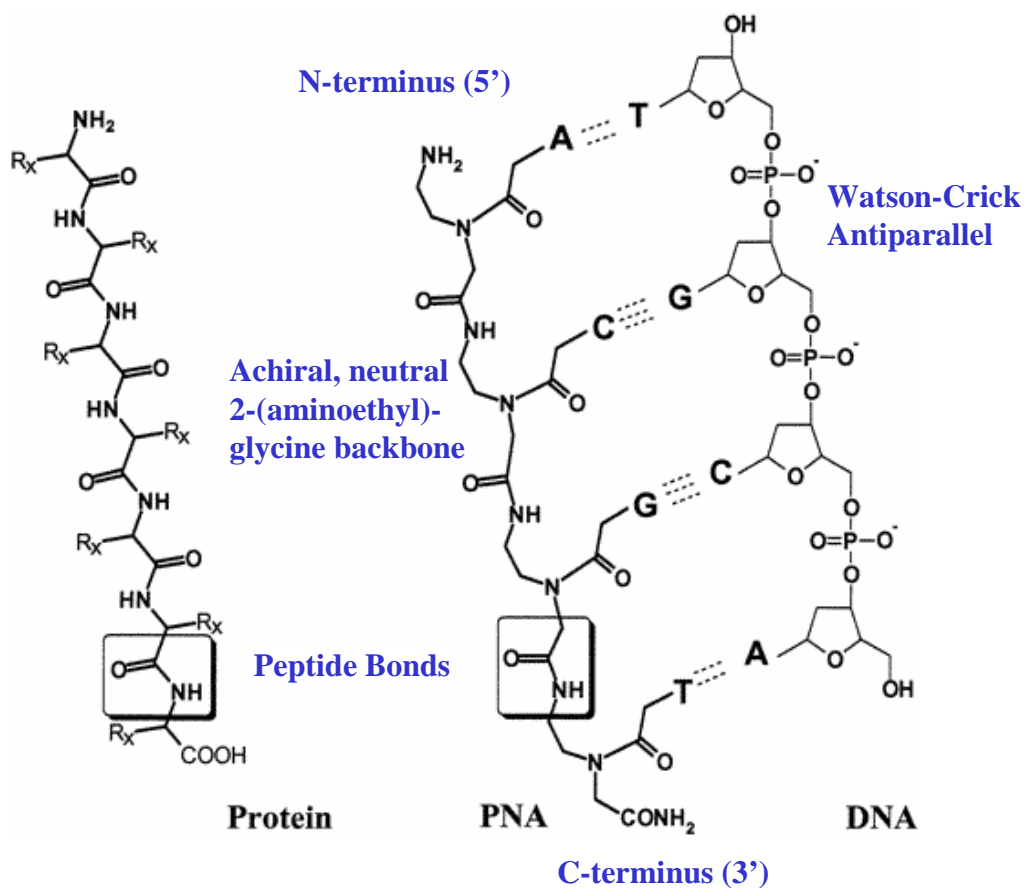
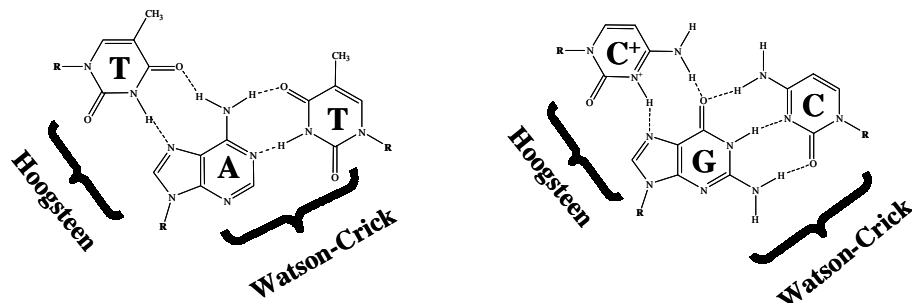


Figure 1-2. Comparison of the chemical structures of peptides, PNA, and DNA molecules. By convention, the C-terminus and N-terminus of the PNA is equivalent to the 3'-end and 5'-end of DNA oligonucleotides, respectively. PNAs hybridize antiparallel to DNA oligonucleotides. PNAs monomers are linked with peptide bonds. At physiological pH, the N-terminus is protonated.

*From Applied Biosystems. (2001) PNA Chemistry for the Expedite 8900 Nucleic Acid Synthesis System User's Guide.

A.



B.

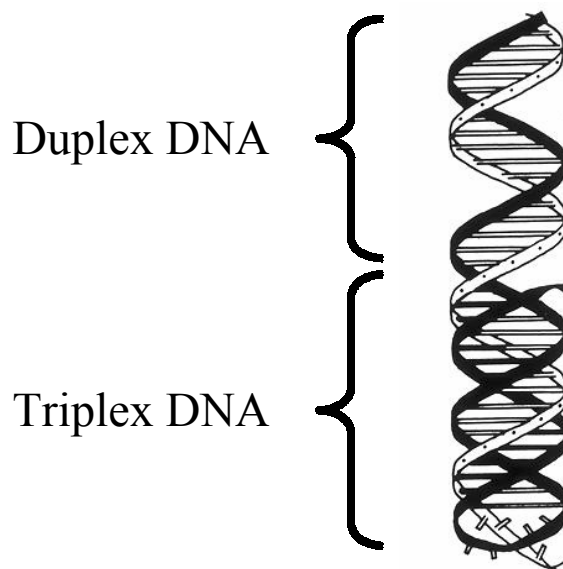


Figure 1-3. Watson-Crick and Hoogsteen hydrogen bonding between duplex and triplex oligonucleotide. A.) Adenine and thymine form two hydrogen bonds of the duplex, with a third thymine hydrogen binding in the major groove (T^{*}A:T); guanine and cytosine forming three hydrogen bonds of the duplex with a protonated cytosine hydrogen bonding in the major groove (C⁺*G:C) R = ribose or deoxyribose. B.) Schematic of the double-stranded helix and a triple-stranded helix.

same, encouraging the same hydrogen donor-acceptor properties found in Hoogsteen base-pairing ($T^*A:T$ or $C^+G:C$; for the purposes of this report, the ":" represent Watson-Crick base-pairing and the "*" represents Hoogsteen base-pairing of a third oligonucleotide bound in the major groove of the double helix). The negatively charged ribose-phosphodiester backbone of the DNA oligonucleotide was replaced with an achiral uncharged polyamide backbone. Theoretically, a neutral PNA ligand bound to dsDNA would have a greater affinity than a negatively charged oligonucleotide.

The first report of PNAs demonstrated that a homothymine PNA 10-mer (T_{10}) bound to homoadenine ssDNA and not homothymine ssDNA, suggesting sequence-specificity (1). The PNA T_{10} :ssDNA duplex was very stable and could withstand denaturing conditions of 80% formamide. The PNA T_{10} also bound to a double-stranded poly-A DNA at a 2:1 ratio (PNA_2 :dsDNA). Photofootprinting of this complex resulted in complete protection of the poly-A DNA strand with no protection within the poly-T DNA strand. Treating the PNA:dsDNA complex with staphylococcal nuclease (which cleaves ssDNA) also resulted in significant cleavage of the poly-T DNA strand with no cleavage in the poly-A strand. These results suggest that two PNA T_{10} s were binding to the poly-A strand of DNA, displacing the other poly-T DNA strand (referred to as a P-loop) (1, 5, 6) (**Figure 1-4. P-loop formation**).

Stability of PNA hybridization

The thermal melting temperature (T_m) of annealed oligonucleotides is defined as the temperature at which 50% of the annealed oligonucleotides have been dissociated as measured by an increase in the UV absorption. The T_m value gives an idea of the stability

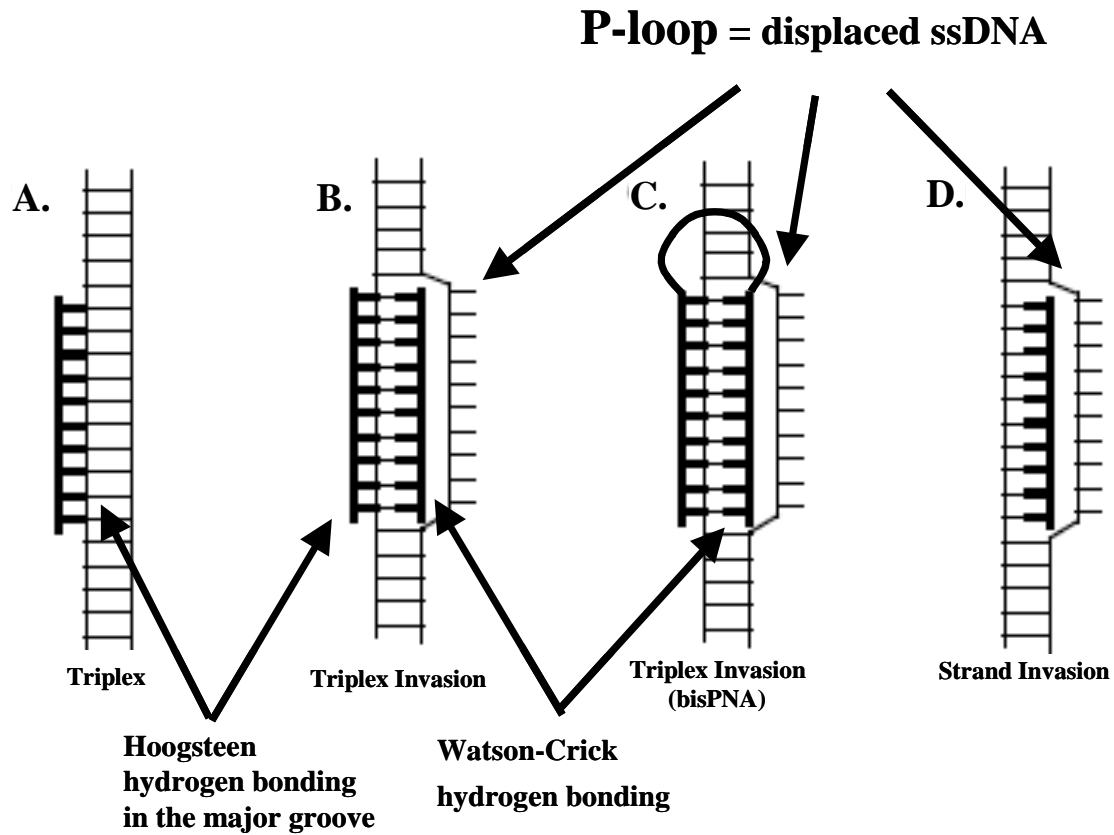


Figure 1-4. P-loop formation. A.) PNA binding parallel in the major groove of dsDNA by Hoogsteen base-pairing rules. B.) Two PNAs binding antiparallel by Watson-Crick base-pairing rules and in parallel by Hoogsteen base-pairing rules, displacing a DNA strand (P-loop). C.) BisPNA binding both antiparallel and parallel, displacing a P-loop. D.) PNA binding antiparallel by Watson-Crick base-pairing rules into dsDNA (A-T rich regions, cruciform structures, supercoiled stress).

*From Nielsen P.E. (2001) Peptide nucleic acid: a versatile tool in genetic diagnostics and molecular biology. *Current Opinion in Biotechnology*. 12:16–20.

of the PNA:DNA or PNA:RNA duplex. Higher T_m values mean a higher duplex stability. PNAs hybridize sequence-specifically to complementary single-stranded DNA and RNA oligonucleotides with greater affinity than corresponding DNA:DNA or RNA:DNA duplexes (3, 7). For example, in melting temperature experiments a PNA 6-mer T (thymines) hybridized to a DNA 6-mer A (adenines) demonstrated a higher melting temperature profile (T_m) of 31°C than the corresponding DNA 6 mer T hybridized to a complement DNA 6-mer A which yielded a T_m of less than 10°C (1, 2) (**Table 1-1. Duplex stability and melting temperatures**). Moreover, the longer the PNA or the greater the GC content, the greater the T_m (the greater the affinity). As a general rule, each base of a PNA oligomer contributes (on average) 1°C to the T_m value, relative to a corresponding DNA oligonucleotide (7).

Triplex formation occurs between two homopyrimidine PNAs and a homopurine DNA sequence (PNA₂:DNA) (1) (see **Figure 1-3**). When targeting polypurine dsDNA, triplex formation (invasion) leads to a displace ssDNA strand called a P-loop. In this case, the affinity is even greater than simple PNA:DNA duplex formation. The higher T_m s are probably a reflection of shorter hydrogen bonds formed between bases as seen by x-ray crystallography (8). Shorter hydrogen bonds results in greater Van der Waals interactions between the backbones of the two individual PNAs and the DNA strand. On average, an increase in T_m of 10°C per base is observed (2).

Two PNA oligomers can be linked with flexible glycol units to form bisPNAs (or bisPNA "clamps"). One half of the bisPNA will be specific for parallel Hoogsteen base-pairing while the other half will be specific for antiparallel Watson-Crick base

Duplex	T_m °C
6-mer PNA-T:DNA-A	31 °C
6-mer DNA-T:DNA-T	<10 °C
10-mer PNA-T:DNA-A	73 °C
10-mer DNA-T:DNA-T	23 °C
15-mer mixed PNA:DNA	69 °C
15-mer mixed DNA:DNA	54 °C
15-mer mixed PNA:RNA	72 °C
15-mer mixed DNA:RNA	50 °C

Table 1-1. Duplex Stability and Melting Temperatures. T_m s of 6-mer and 10-mer duplexes were conducted in 10 mM sodium phosphate, 10 mM MgCl, 140 mM NaCl, pH 7.4. T_m s of 15-mer mixed duplexes conducted in 10 mM phosphate buffer, 0.1 mM EDTA, 100 mM NaCl, pH 7.0. The higher T_m s for the 6-mer and 10-mer PNA-T are due to triplex formation to the DNA oligonucleotide (PNA₂:DNA).

*From:

Egholm M., Buchardt O., Nielsen P.E., Berg R.H. (1992) Peptide Nucleic Acids (PNA): Oligonucleotide analogs with an achiral peptide backbone. *J. Am. Chem. Soc.* 114, 1895-1897.

Nielsen P.E., Egholm M., Berg R.H., Buchardt O. (1991) Sequence-selective recognition of DNA by strand displacement with a thymine-substituted polyamide. *Science*. 254(5037):1497-500.

Egholm M., Buchardt O., Christensen L., Behrens C., Freier S.M., Driver D.A., Berg R.H., Kim S.K., Norden B., Nielsen P.E. (1993) PNA hybridizes to complementary oligonucleotides obeying the Watson-Crick hydrogen-bonding rules. *Nature*. 365(6446):566-8.

pairing, effectively "clamping" around a DNA strand. BisPNAs are better at strand invasion into duplex DNA than monomeric PNAs due to transient triplex formation prior to strand invasion (9). The high affinity and unique binding mode of bisPNAs makes them an ideal molecule for targeting chromosomal DNA (10, 11).

Specificity of PNA hybridization

PNAs have greater specificity for a nucleic acid target than DNA oligonucleotides (3, 12). The specificity is reflected in the differences of the T_m s between a PNA:DNA duplex and a single base mismatch PNA:DNA duplex versus the analogous DNA:DNA duplex or single base mismatch DNA:DNA duplex. A single base mismatch within a PNA:DNA duplex is more destabilizing than a DNA:DNA mismatched duplex (**Table 1-2. Increased specificity for PNAs**). The same phenomenon applies to PNA:RNA duplexes (13, 14). For example, compared to an exact complement 15-mer PNA:DNA duplex, a 15-mer PNA:DNA duplex with a single base mismatch demonstrates a difference in T_m of 15°C, while the corresponding DNA:DNA and mismatch DNA:DNA show a difference of 11°C in the T_m s. The location of the mismatch within a PNA:DNA duplex also affects the stability of the duplex. Mismatched bases in the middle of a PNA:DNA duplex is much more destabilizing than mismatched bases at the end of a duplex (3).

Single-base Mismatch	ΔT_m
15-mer PNA:DNA	8-20°C
15-mer DNA:DNA	4-16°C
15-mer PNA:RNA	9-21°C
10-mer PNA:PNA	14-24°C
10-mer PNA:DNA·PNA (T:A·T, replace A with G)	13°C
7-mer bisPNA:DNA (mismatch in the DNA strand)	23-37°C

Table 1-2. Increased specificity for PNAs. The T_m difference between an exact complement and a single-base mismatch duplex is greater for PNA hybridization compared to a corresponding charged DNA or RNA hybridization. Mismatches in the center of a duplex are more destabilizing than mismatches at the ends of a duplex.

*From:

Egholm M., Buchardt O., Christensen L., Behrens C., Freier S.M., Driver D.A., Berg R.H., Kim S.K., Norden B., Nielsen P.E. (1993) PNA hybridizes to complementary oligonucleotides obeying the Watson-Crick hydrogen-bonding rules. *Nature*. 365(6446):566-8.

Jensen K.K., Ørum, H., Nielsen, P.E. and Nordén, B. (1997) Kinetics for Hybridization of Peptide Nucleic Acids (PNA) with DNA and RNA Studied with the BIAcore Technique. *Biochemistry*. 36, 5072-5077.

Wittung P., Nielsen P.E., Buchardt O., Egholm M., Norden B. (1994) DNA-like double helix formed by peptide nucleic acid. *Nature*. 368(6471):561-3.

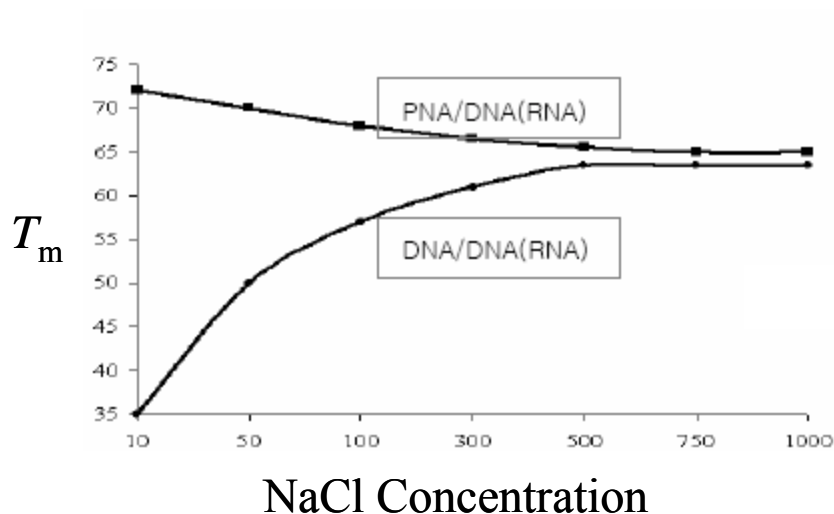
Egholm M., Christensen L., Dueholm K.L., Buchardt O., Coull J., Nielsen P.E. (1995) Efficient pH independent sequence-specific DNA binding by pseudoisocytosine-containing bis-PNA. *Nucleic Acids Res.* 23(2):217-22.

Ion-independence of PNA hybridization

PNA:DNA or PNA:RNA duplex stability is unaffected by the ionic strength (3, 13). Annealed negatively charged oligonucleotides have a charge-charge electrostatic repulsion that can be minimized by the presence of Na^+ counterions. Neutral PNAs hybridized to DNA or RNA do not suffer an electrostatic repulsion and therefore are unaffected by local Na^+ concentrations. For example, the melting temperature T_m of a 15-mer PNA:DNA duplex decreases only 5°C when the NaCl concentration is changed from 10 mM to 500 mM (**Table 1-3. PNA hybridization is independent of salt concentration**). The T_m of the corresponding 15-mer DNA:DNA duplex is significantly increased (ΔT_m of 20°C) when Na^+ concentrations increase (3, 13). These findings are important for using PNAs in applications where experimental conditions are not suitable for anionic oligonucleotides. For example, highly ordered nucleic acid secondary structure will be denatured in the absence of salts, making them accessible to PNA probes (16) or PNA affinity purification (17, 18, 19).

Biophysical structures of PNA duplexes

When annealed the PNA oligomer conforms to its nucleic acid partner (**Figure 1-5. Structural features of PNA:RNA, PNA:DNA, PNA₂:DNA triplex, PNA:PNA**) (for review see 20). The backbone of the PNA oligomer is flexible enough to take on the preferred duplex conformation of its bound nucleic acid complement, but not too flexible as to destabilize hydrogen bond formation. NMR studies revealed that a hexameric PNA:RNA duplex formed an antiparallel, right-handed double helix with Watson-Crick base pairing similar to the "A"



NaCl Concentration	PNA:DNA	DNA:DNA
0 mM	72°C	38°C
100 mM	69°C	54°C
140 mM (physiological)	69°C	56°C
1000 mM	65°C	65°C

Table 1-3. PNA hybridization is independent of salt concentration. Anionic oligonucleotides require counterions to neutralize the charge-charge repulsion of duplexes. Neutrally charged PNAs do not need counterions.

*From:

Egholm M., Buchardt O., Christensen L., Behrens C., Freier S.M., Driver D.A., Berg R.H., Kim S.K., Norden B., Nielsen P.E. (1993) PNA hybridizes to complementary oligonucleotides obeying the Watson-Crick hydrogen-bonding rules. *Nature*. 365(6446):566-8.

Tomac S., Sarkar M., Ratilainen T., Wittung P., Nielsen P.E, Nordén B., Gräslund A. (1996) Ionic effects on the stability and conformation of peptide nucleic acid complexes. *Journal of the American Chemical Society*. 118: 5544-5552.

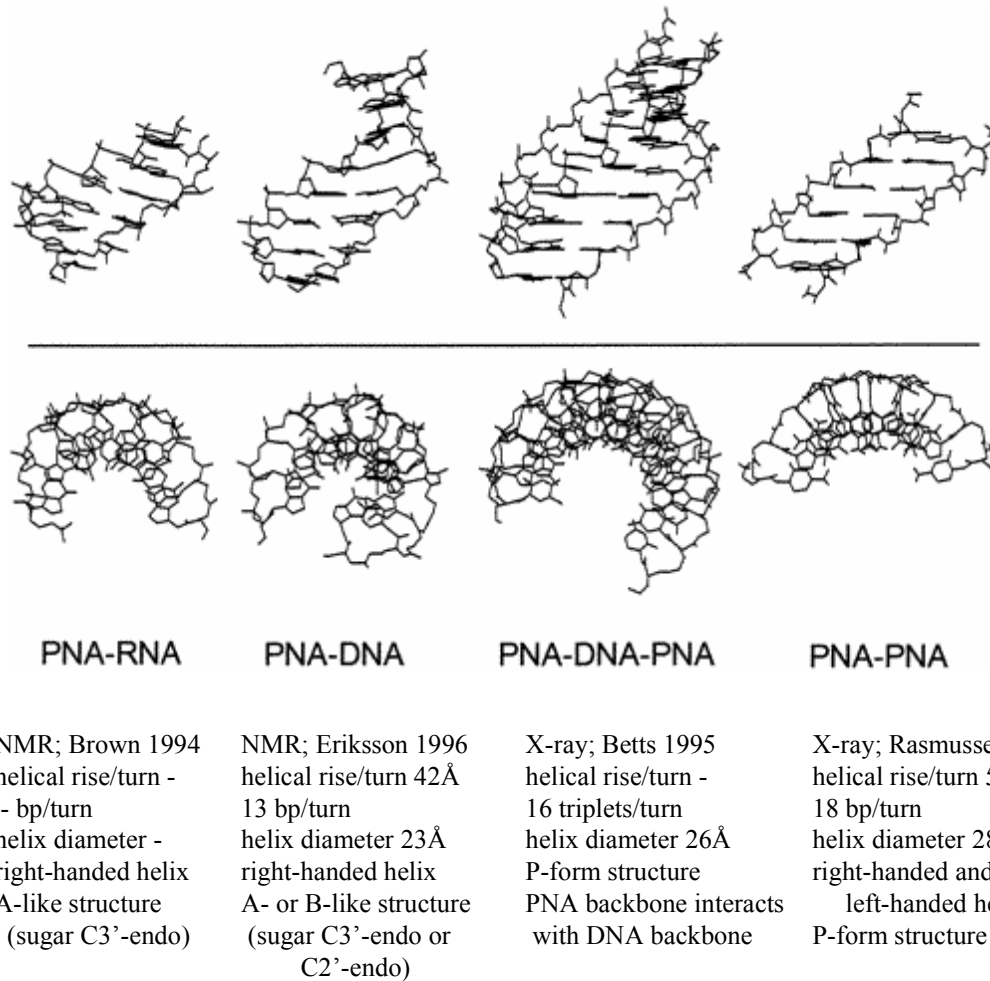


Figure 1-5. Structural features of PNA:RNA, PNA:DNA, PNA₂:DNA triplex, PNA:PNA. The double helix formed by PNA:RNA and PNA:DNA resembles the form of RNA:RNA and DNA:DNA double helices. PNA₂:DNA triplex and PNA:PNA takes on a new form called the P-form (neither A- nor B-form).

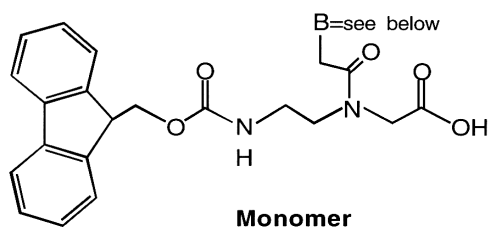
*From: Magdalena Eriksson and Peter Nielsen. (1996) PNA-nucleic acid complexes. Structure, stability and dynamics. *Quarterly Review of Biophysics*. 29, 4, pp369-394.

form structure of RNA:RNA duplexes (21). NMR also demonstrated that a PNA:DNA duplex forms a double helix similar to the "B" form of a duplex DNA:DNA (22, 23). In these two cases, it seems as if the PNA is an excellent DNA/RNA mimic. However, as determined by x-ray crystallography, a PNA:PNA duplex forms a double helix with a wider (28Å) and larger pitch (18 bases per turn) unlike the "A" form of the PNA:RNA duplex or the "B" form of the PNA:DNA duplex. This finding suggests that the PNA is not the perfect mimic of DNA or RNA, but rather has its own unique structural features (24).

Design, synthesis, analysis and handling of PNAs

PNA synthesis uses the same Fmoc- or tBoc-based chemistry as peptide synthesis (25, 26). The four PNA base monomers (A, T, G, C) are commercially available with either Fmoc or tBoc protecting groups on the primary amine and a Bhoc or Cbz protecting group on the exocyclic base (**Figure 1-6. Chemical structures of the protected monomers used for automated synthesis**). The protecting groups must be orthogonal in their requirements for removal from the PNA during synthesis. That is, the Bhoc or Cbz protecting group on the nucleobases must be stable to the conditions used for removal of the Fmoc (using 20% piperidine) or Boc (using 50% TFA) protecting groups from the terminal amine (Bhoc and Cbz protecting groups are removed at the end of synthesis with 95% TFA and 20%TFMSA:60%TFA, respectively). For manual PNA synthesis, Boc/Cbz-PNA monomers are used due to the less stringent requirement for anhydrous conditions during coupling reactions. For automated synthesis, Fmoc/Bhoc-

**Fmoc Protecting Group
of primary amine of backbone
Removed with 20% piperidine**



**Bhoc Protecting Groups
of exocyclic primary amines
Removed with
80% TFA:20% m-cresol**

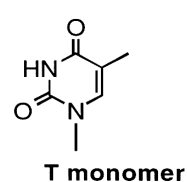
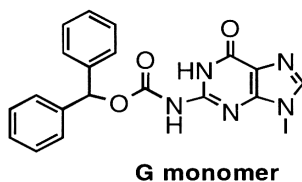
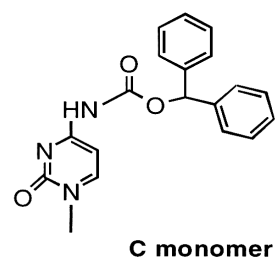
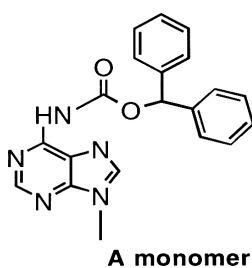


Figure 1-6. Chemical structures of the protected monomers used for automated synthesis. Fmoc is removed from the N-terminus each cycle with piperidine, while the Bhoc is removed from the nucleobase only during final cleavage with TFA.

*From Applied Biosystems. (2001) PNA Chemistry for the Expedite 8900 Nucleic Acid Synthesis System User's Guide.

PNA monomers are routinely used because the conditions for Fmoc removal are less caustic to the instrumentation.

PNAs can be synthesized manually in a chemical hood giving greater yields of PNA product, but with much more labor invested. Manual synthesis of an average PNA of 15 bases takes approximately 12 hours. Automated synthesis of an average PNA oligomer of 15 bases at a 2 μ mole scale takes approximately 6 hours on a modified Expedite 8909 DNA/RNA synthesizer (Applied Biosystems) with only about 1 hour set-up time by the user. The Expedite 8909 PNA synthesizer can synthesize two PNAs oligonucleotides simultaneously if the need for greater quantities or larger numbers of PNAs is necessary.

While PNAs with greater than 25 residues can be synthesized (as will be described in Chapter 2) most applications require PNAs to be only 15-20 bases due to the increased affinity for nucleic acid targets. Theoretically, for antisense applications PNAs of 15-17 bases is necessary for gene specificity from a genome of 3 billion base pairs (27). PNA-peptide conjugates can be synthesized on the Expedite 8909 provided the peptide has no more than 3 different amino acids because the synthesizer has only 3 additional bottle positions for alternative residues (amino acids or linker molecules). For more complicated peptides, a separate peptide synthesizer should be used to complete PNA-peptide conjugates.

Some general guidelines have been developed for optimizing the total product yield of a PNA based on the PNA sequence. As stated previously, increased yields arise from coupling a lysine (or amino acid of choice) to the resin first. For unknown reasons,

PNA monomers are not as efficient as amino acids when chemically coupling directly to the XAL-PEG-PS resins. This generates a PNA with a lysine at the C-terminus.

Some stretches of bases are particularly difficult to synthesize. For example, if a PNA sequence has three or more purines (A or G) in a row, the synthesizer is programmed to "double couple" the third residue. That is, twice the amount of activated monomer is added to the resin prior to the next capping step. It is believed that bulky purine monomers may be the cause of inefficient coupling reactions in these instances. In addition, "double coupling" of monomers near the end (N-terminus) of the synthesis also increase the chances of full-length product. PNA reagents are expensive, so careful attention to details is important in synthesizing a useful PNA.

Starting from a solid support resin, PNA synthesis occurs in a cycle, synthesizing from C-terminus to N-terminus. A single base monomer is coupled to the growing oligonucleotide (chain elongation), followed by washes, a capping step, and deprotection (**Figure 1-7. Automated PNA synthesis on the Expedite 8909 (Cycles)**). The carboxyl group of an Fmoc(Bhoc)-protected PNA monomer is "activated" by HATU. This "activated" carboxyl group is coupled to an exposed reactive primary amine group (uncharged under basic conditions) at the end of the resin-bound PNA. After washing, a capping step is included whereby acetic anhydride acetylates any primary amine groups of the resin-bound PNA that did not get coupled to an "activated" PNA monomer. This step prevents chain elongation of PNA oligomers with missing bases and leads to truncated PNA products. Next, deprotection of the Fmoc protecting group of the newly coupled monomer terminal amine occurs allowing the next incoming "activated" monomer to chemically couple.

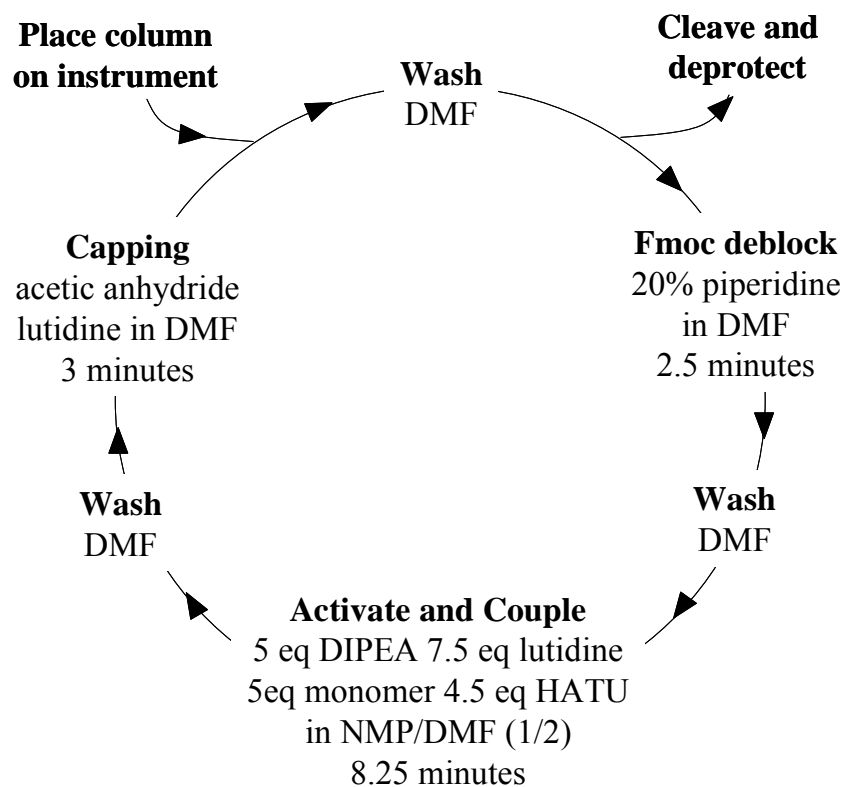


Figure 1-7. Automated PNA synthesis on the Expedite 8909 (Cycles). PNA synthesis is a cyclic process involving activation and coupling of the PNA monomer to the resin bound oligonucleotide, capping of unreacted terminal amines, and deblocking of newly added N-terminal amine.

*From Applied Biosystems. (2001) PNA Chemistry for the Expedite 8900 Nucleic Acid Synthesis System User's Guide.

Upon completion of the synthesis, the PNA is cleaved from the solid-support resin with TFA and simultaneously removes the Bhoc protecting groups from the exocyclic bases. Also included with TFA in the cleavage step is m-cresol that acts as a scavenger for the released protecting groups, preventing undesired side reactions with the PNA oligomer (**Figure 1-8. Automated PNA synthesis on the Expedite 8909 (Chemistries)**). Cleavage from the XAL-PEG-PS resin results a C-terminal amide group. The PNA is then ether precipitated, dried to a solid, and resuspended in water.

Analysis of the crude PNA product is performed by reverse-phase high performance liquid chromatography (RP-HPLC) with a hydrophobic C₁₈ column monitored by UV absorbance spectroscopy at λ_{260} for conformation of a single PNA product (**Figure 1-9a. RP-HPLC of PNAs**). PNAs will adsorb to a C₁₈ column in an aqueous environment (running buffer), but can be eluted off the C₁₈ column with an increasing gradient of non-polar acetonitrile (ACN) (elution buffer). The flow-through is monitored by UV absorbance at λ_{260} , reading the nucleobases of the PNA. Longer PNAs, having greater hydrophobicity, will elute at higher ACN concentrations (longer elution times). Contaminating truncated (acetylated-capped) PNA products from failed coupling reactions, having fewer hydrophobic monomers, will elute at lower ACN concentrations (shorter elution times) making it easy to separate undesired PNA from the full length PNA product. PNA oligomers still retaining the Fmoc protecting group at the N-terminus will elute at later times due to the hydrophobic nature of the protecting group.

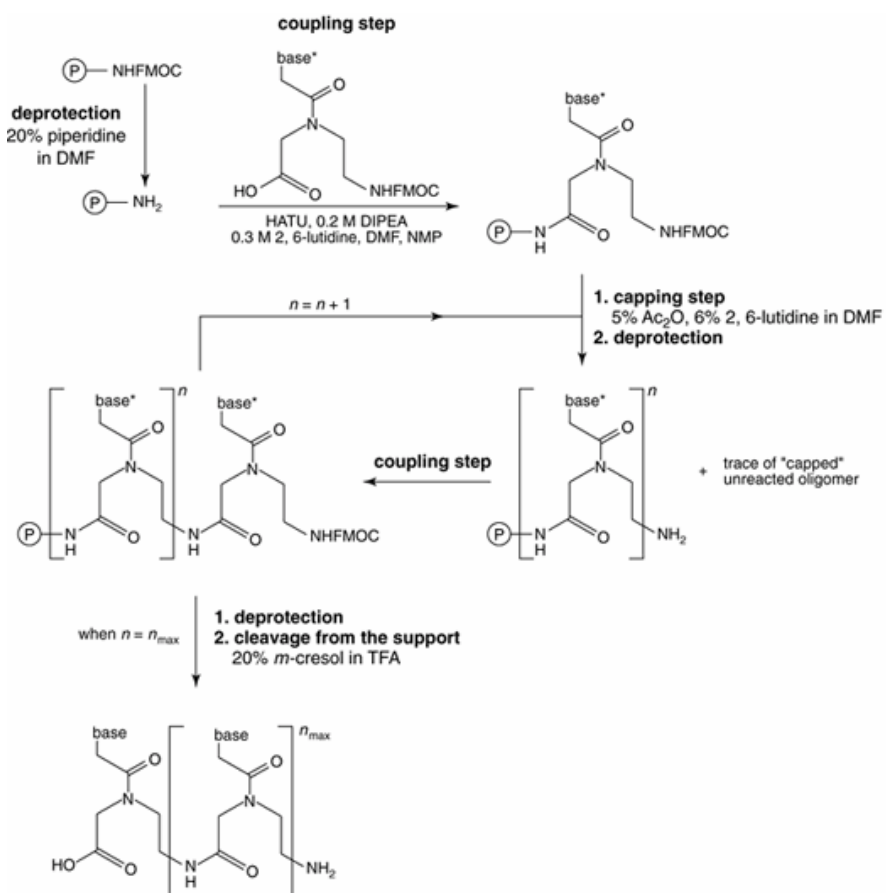


Figure 1-8. Automated PNA synthesis on the Expedite 8909 (Chemistries). PNA synthesis is a cyclic process involving activation and coupling of the PNA monomer to the resin bound oligonucleotide, capping of unreacted terminal amines, and deblocking of newly added N-terminal amine.

*From Braasch D.A., Nulf C., and Corey D.R. (2002) Current Protocols in Nucleic Acid Chemistry. Synthesis and Purification of Peptide Nucleic Acids.

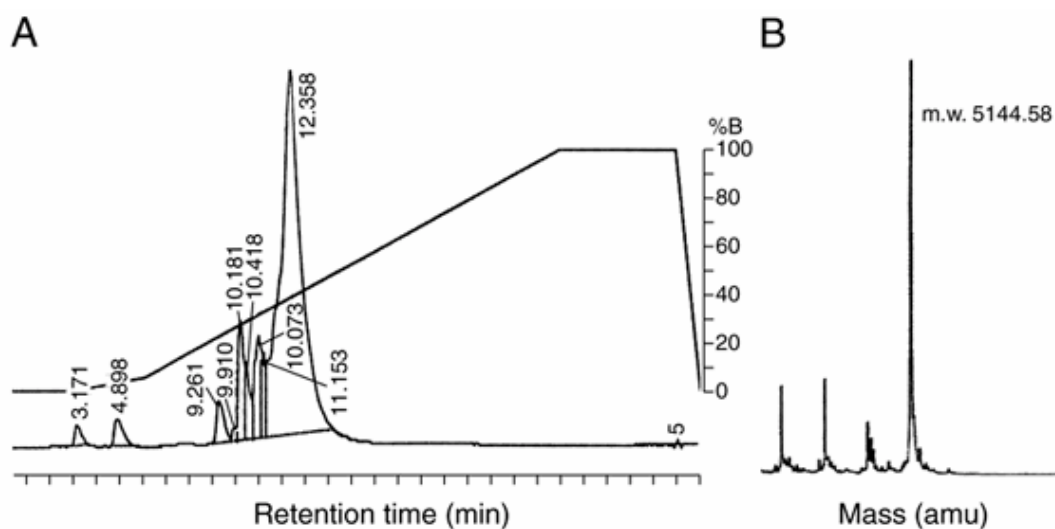


Figure 1-9. RP-HPLC and MALDI-TOF MS of PNA. A.) Analysis and purification of crude PNA products is done by RP-HPLC monitoring the flow-through by UV absorbance at $\lambda 260$. The more hydrophobic full length PNA will have a longer retention time than the truncated PNA products making purification simple. B.) The molecular weight of the PNA product is identified by MALDI-TOF MS. Truncated PNA products will have mass differences of a PNA monomer.

Matrix-assisted laser desorption/ionization time-of-flight mass spectroscopy (MALDI-TOF MS) is used to identify the correct molecular weight of the PNA (**Figure 1-9b. MALDI-TOF MS of PNAs**). Truncated PNA products from failed or incomplete synthesis will appear as peaks with molecular weight differences of the PNA monomer where coupling was inefficient. Knowing the identity of the incorrect products can be invaluable to troubleshooting instrumentation problems.

Correctly synthesized PNAs should also show a thermodynamically reversible hyperchromic/hypochromic effect at λ_{260} when hybridized to a complementary oligonucleotide (**Figure 1-10. Hyperchromic/Hypochromic effect of PNA:DNA hybridization**). Greater detail of this process can be found in Chapter 5 of this manuscript.

From a practical standpoint, PNAs are no more difficult to handle in the lab than DNA oligonucleotides provided that the user is aware of the aggregative properties of the oligonucleotide. PNAs are easily soluble in slightly acidic dH₂O (pH 5-6.5) at high concentration, but will aggregate over time, with longer PNAs (more hydrophobic) and purine-rich PNAs being more problematic. Basic solutions (pH 7.5+) can cause aggregation of the PNA molecules at high concentrations and should be avoided if possible. As a general rule, stock PNA solutions are heated to 70°C for 5 minutes the day of use to disrupt aggregated PNA oligomers.

Designing the PNA to include a positively charged amino acid on either end of the molecule during synthesis can enhance the solubility of a PNA. Incorporate a lysine at the C-terminus which not only gives the PNA a positive charge at neutral pH (ϵ -amine pK_a ~10) but also increases PNA synthesis yields (it is the first residue to be coupled to

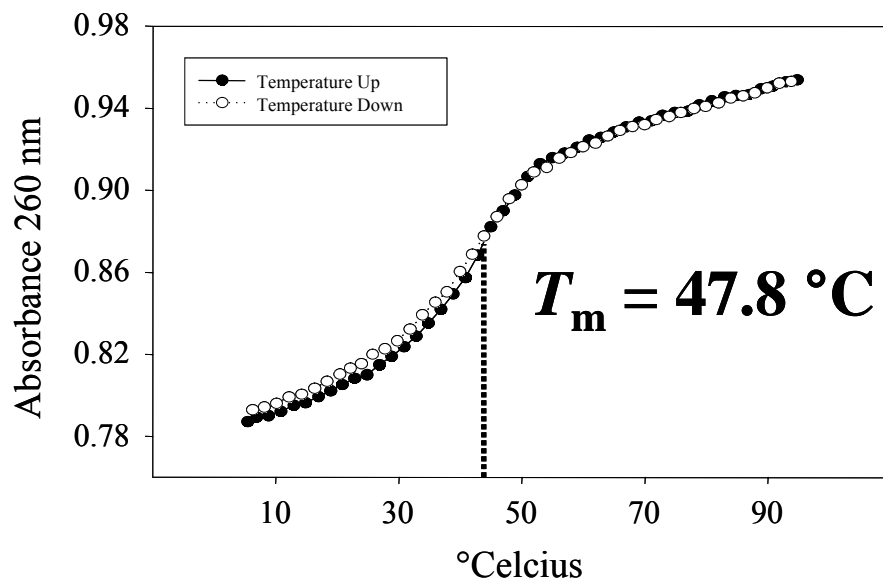


Figure 1-10. Hyperchromic/Hypochromic effect of PNA:DNA Hybridization. PNAs hybridizing to complementary DNA oligonucleotides should demonstrate a thermodynamically reversible sigmoidal UV absorbance profile across a range of temperatures. The melting temperature (T_m) of a PNA:DNA duplex is defined as the temperature at which 50% of the PNA is hybridized (or the point of transition in the profile). The T_m is a reflection of the affinity a PNA has for its complementary DNA.

the resin) and can also be used (at the ϵ -amine) to conjugate other molecules (fluorophores or biotin). There has also been reports that an increase in the number of positive charges on a PNA increased affinity for negatively charged complementary DNA (K. Kaihatsu, personal communication).

PNAs are a stable molecule and can withstand repeated freeze-thaws without affecting function. They are also resistant to nucleases and proteases (29), and are not known to degrade over time. PNAs are stable over a wide pH range (30). PNAs can be stored at -20°C in either a lyophilized form or as the concentrated solution. Working diluted PNA solutions can be stored at 4°C.

Current uses of PNAs

The synthesis and discovery of the unique biophysical properties of PNAs has attracted the attention of synthetic chemists, nucleic acid specialists and medicinal chemists for the development of gene therapeutic drugs and genetic diagnostics. Researchers have applied PNAs to a diverse number of applications. PNAs can be easily modified with fluorescent molecules and used as probes for *in situ* hybridization (FISH) (31, 32, 33) (**Figure 1-11. Fluorescence *in situ* hybridization (FISH) of telomeres with PNA-Cy3**) and identification of bacterial or viral contaminants in biological samples (34, 35). Miniaturized PNA biosensors have been developed that convert the basic hybridization event into an electrical event generating a signal proportional to the total number of hybridization events (36). PNAs have even been introduced into microarray technology (37, 38). In these cases, the PNA

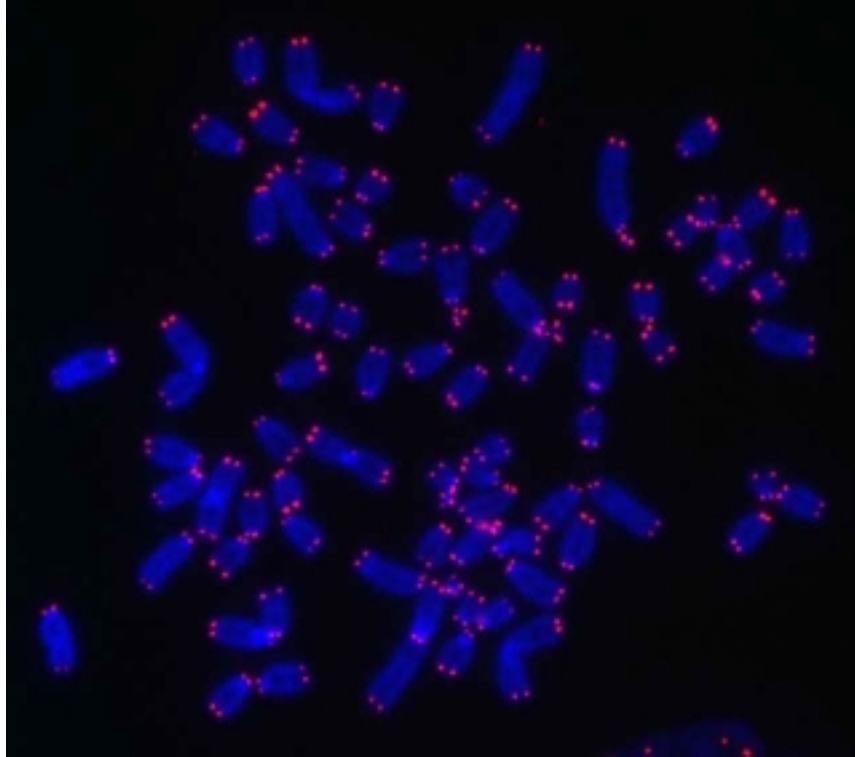


Figure 1-11. Fluorescence *in situ* hybridization (FISH) of telomeres with PNA-Cy3. Mouse chromosomes prepared by PNA-telomere hybridization procedure from PreB fetal liver cells. Chromosomes are stained with DAPI. Telomeres are visualized using PNA/CY3 probe.

*From: Chuang T.C., Moshir S., Garini Y., Chuang A.Y., Young I.T., Vermolen B., Doel Rv R., Mougey V., Perrin M., Braun M., Kerr P.D., Fest T., Boukamp P., Mai S. (2004) The three-dimensional organization of telomeres in the nucleus of mammalian cells. *BMC Biol.* 2(1):12.

probes yield greater signal-to-noise ratios and are more discriminatory to mismatched targets compared the to traditional DNA probes.

PNAs are also suited to PCR-based applications where PNA "clamps" prevent amplification of a specific sequence. This technique works when identifying oncogenic point mutations within tissue samples (39) Likewise, PNA light-up probes or "beacons" have been used to identify specific PCR products (40, 41).

PNA have also been used to sequence-specifically purify DNA or RNA from sample solutions (17, 18). In a slightly more complex technique, PNA "openers" have been employed to capture plasmid DNA (42) or fluorescently label plasmid DNA (43). Here, strand invasion by PNAs into duplex DNA creates a displaced single stranded DNA region that can be targeted by a functionalized oligonucleotide (biotinylated or fluorescently labeled). The advantage is that whole plasmids can be "tagged" and monitored without interfering with the biological function of the plasmid and without relying on the expression of the protein encoded within the plasmid.

While PNA oligomers themselves cannot be enzymatically altered with commonly used methylases or nucleases, they can be employed as tools in the lab by molecular biologists to prevent (44, 45, 46) or encourage (47) such enzymatic reactions from occurring to ssDNA or dsDNA bound by PNA. In a similar fashion, modification of DNA bases with potassium permanganate (KMnO₄) or diethylpyrocarbonate (DEPC) (aka. chemical probing) (48) can be blocked by hybridized PNAs. Using PNAs as molecular tools allows the scientist to expand the repertoire of reagents commonly used in the lab to modify nucleic acid sequences (49).

PNAs as antisense molecules

Antisense biotechnology is a potentially powerful tool for the generation of specific gene knock-downs. However, three major obstacles have stalled the progression of synthetic oligonucleotides for antisense applications:

1. Non-specific associations of the anionic ribose phosphate backbone with cellular proteins
2. Limited half-life of antisense oligonucleotides inside cells due to degradation by endogenous nucleases
3. Inability of oligonucleotides to readily cross cell membranes

Because endogenous nucleases recognize the phosphodiester units and bind with a charge-charge interaction, the first two biological barriers instigated exploration in chemical modification of the oligonucleotide backbone. PNAs were designed to include an uncharged amide backbone. The absence of the anionic backbone in PNAs demonstrated less non-specific binding to proteins and cellular debris than oligonucleotides with negatively charged linkages (**50, 51**). Less interaction with cellular proteins suggests decreased toxic effects from PNAs relative to anionic oligonucleotides that harbor the proinflammatory CpG motif (**52**). In addition, it was discovered that if PNAs were incubated in cell-free extracts or human serum, they were resistant to both nucleolytic and proteolytic hydrolysis (**29**). This suggests that PNAs could have greater biological stability than those oligonucleotides that are rapidly degraded by endogenous

nucleases. These two findings suggested that PNAs could be used as antisense agents *in vivo* (53, 54, 100).

RNase H, an endogenous enzyme that cleaves the RNA strand of an RNA:DNA duplex (57, 58), is thought to be an important enzyme for antisense mechanisms (59) and is often exploited by other chemically modified antisense oligonucleotides to reduce gene expression (60, 61, 62). Antisense PNAs bound to single stranded RNA do not activate RNase H (55, 56). PNAs function by sterically blocking protein-RNA interactions. There are a large number of functional antisense mechanisms to sterically knock-down gene expression including (63): steric blocking of translation initiation machinery at the extreme 5'-UTR of an RNA transcript (64), physically blocking ribosomal movement (65, 66), blocking splice sites to alter splicing mechanisms (67, 68), and inhibition of ribonucleoprotein activity (69, 70) (**Figure 1-12. Blocking of nucleic targets by antisense oligonucleotides**). Maintaining transcript integrity could be important for mRNA that have alternatively spliced isoforms or utilize different AUG start sites generating different proteins. Degradation of the transcript by siRNA or RNase H-based mechanisms may unintentionally decrease “off target” proteins (66).

Predicting which region to target within a given transcript for the best antisense effect is difficult. Unknown secondary structures within RNA may render a particular sequence inaccessible to an incoming oligonucleotide (71). In this regard, PNAs may be superior to other oligonucleotides because of enhanced strand invasion properties into duplex nucleic acids (72, 73, 74). However, several PNAs targeting different regions of a transcript would still have to be empirically tested to maximize inhibition (70).

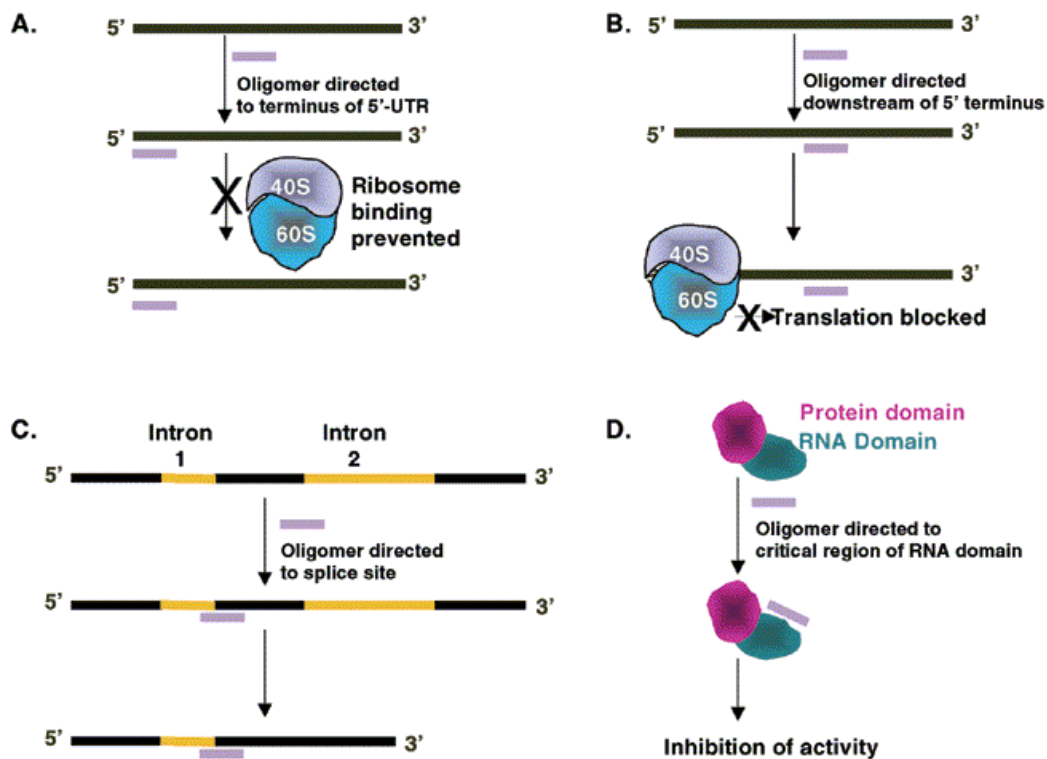


Figure 1-12. Blocking of nucleic targets by antisense oligonucleotides.

A.) Inhibition of gene expression by preventing ribosome binding.
 B.) Inhibition of gene expression by preventing translocation of the ribosome. C.) Alteration of splicing. D.) Inhibition of ribonucleoprotein activity.

*From Braasch D.A., Corey D.R. (2002) Novel Antisense and Peptide Nucleic Acid Strategies for Controlling Gene Expression *Biochemistry*. 41 (14), 4503–4510.

Delivery of PNAs into cells

Even though PNAs have many of the desired properties of an antisense or antigene "drugs", they still must overcome the biological barrier that hinders all synthetic antisense oligonucleotides: transportation across the cellular membrane (75, 76).

A number of earlier reports have demonstrated the antisense activity of PNA molecules when introduced into cells. Antisense PNAs that had been microinjected into cell nuclei demonstrated suppressed levels SV40 large T antigen from those cells constitutively expressing SV40 large T antigen (55, 77). Cells that had been transiently permeabilized with streptolysin-O (SLO) also demonstrated PNA uptake as confirmed by fluorescein labeling and fluorescent microscopy (78). Likewise, lysolecithin-permeabilized human prostatic cancer cells showed that PNAs readily entered the nuclei of cells and effectively inhibited transcription of unique androgen receptor (AR) and TATA-binding protein TBP (79). Introduction of antisense PNAs into E.Coli required using mutant strains with defective outer membrane lipopolysaccharide (LPS) layers or cell-wall-permeabilizing agents (80).

The need for a more practical and efficient method of delivering PNAs led some researchers to modify PNAs. Some scientists have taken advantage of the Fmoc chemistry used to synthesize PNAs to include peptides known to cross cell membranes (81, 82). These transducing peptides (10-16 amino acids) can be used as a 'transporter' to promote the delivery of PNAs across biological membranes by a receptor- and transporter-independent mechanism. For example, a PNA specific for the HIV TAR sequence was conjugated to a membrane-permeating peptide vector, transportan. *In*

vitro, the PNA-transportan conjugate retained its affinity for TAR similar to the unconjugated PNA. Yet, in tissue cultures the PNA-transportan conjugate was efficiently internalized into the cells when added to the culture medium while the unconjugated PNA was not (83). A number of other PNA-peptide conjugations have been used including pTat, a 14-amino acid fragment from the HIV protein Tat (84), and pAnt, a 17-residue fragment of the *Drosophila* protein Antennapedia (85). For PNA transportation into *E. coli*, peptide fragment KFFKFFKFFK was conjugated to a PNA targeting messenger RNA (mRNA) encoding the essential fatty acid biosynthesis protein Acp. In addition to maintaining target specificity (diminished cell growth), the PNA-KFFKFFKFFK conjugate demonstrated faster kinetics across both the outer and inner membranes of *E. Coli* relative to unconjugated PNA (86, 87). These studies that the PNA molecule can be modified with a peptide to increase cell permeability, yet still retain the hybridization properties of an unmodified PNA.

Slightly more complicated conjugations involved PNAs with lactose moieties that were specific for the asialoglycoprotein receptor (ASGP-R) on the surface of liver cells. Lactosylated PNAs that targeted the telomerase ribonucleoprotein showed rapid uptake into HepG2 (liver) cells and inhibited telomerase activity while unmodified PNAs did not (88). Similarly, cellular delivery systems based on conjugates of streptavidin and the OX26 monoclonal antibody directed to the transferrin receptor were used to transport biotinylated PNAs across the blood brain barrier. PNAs delivered in this fashion still retained antisense activity (89). PNAs conjugated with other ligands such as antibodies or steroids have also been used to increase the PNA delivery efficiency (90, 91).

Still another approach used by researchers is to use cationic lipids to deliver a 'carrier DNA' oligonucleotide that is hybridized to the antisense PNA (64, 92) (**Figure 1-13. Lipid-mediated cellular delivery of PNAs**). In this case, the cationic lipid associates with the anionic phosphodiester backbone of the hybridized carrier DNA:PNA duplex facilitates contact and uptake of the duplex at the cell membrane. Presumably, upon delivery into the cell, the carrier DNA oligonucleotide is degraded by nucleases, releasing the antisense PNA to find its target RNA (64). Morpholinos, another DNA oligonucleotide analog with a radically different and uncharged backbone, have had similar success in maintaining antisense activity when utilizing this cellular delivery system (93, 94). This delivery system for antisense PNAs is the most cumbersome in execution and requires the most dedication towards optimization of transfection conditions. However, the PNA does not have to be modified, it can be applied to almost any cell type, and EC₅₀ in the 50-150 nM range have been reported (95).

The inability of PNAs (and oligonucleotides in general) to cross membranes may explain the poor *in vivo* pharmacokinetics reported (96, 97). In rats, two hours post-intraperitoneal (i.p.) injection of PNA, very low levels of oligomer were detected in the kidneys, liver, heart, spleen (in decreasing order). At 24 hours post-i.p. almost 90% of the PNA had been recovered in the urine (98). However, modifying the PNA oligomer by glycosylation can increase PNA uptake into the liver 40x-fold (99).

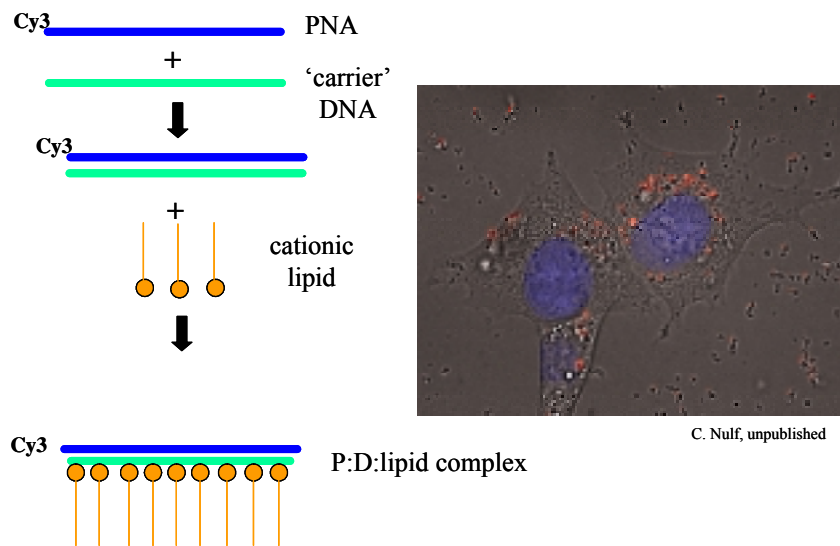


Figure 1-13. Lipid-mediated cellular delivery of PNAs. A.) Antisense PNAs are annealed to complementary “carrier” DNA oligonucleotide. The PNA:DNA duplex is complexed with a cationic lipid, which associates with the negative charges of the DNA oligonucleotide. The PNA:DNA:lipid complex solution is incubated on top of cell for delivery. B.) Fluorescence microscopy of live HepG2 cells transfected with PNA-Cy3 conjugate via carrier DNA and LipofectAMINE. The PNA-Cy3 (red) distributes predominately in punctate locations within the cytosol. As a counterstain, Hoechst (blue) localizes to the nucleus.

A detailed understanding of PNA antisense mechanism and pharmacology are essential for successful application and further improvement of its effectiveness. The numerous experimental "baby steps" to improving PNA efficacy *in vivo*, along with the multitude of chemical modifications to enhance nucleic acid recognition inside the cell, can only eventually lead to gene-specific medicinal therapeutics.

References for Chapter 1

- 1 Nielsen P.E., Egholm M., Berg R.H., Buchardt O. (1991) Sequence-selective recognition of DNA by strand displacement with a thymine-substituted polyamide. *Science*. 254(5037):1497-500.
- 2 Egholm M., Buchardt O., Nielsen P.E., Berg R.H. (1992) Peptide nucleic acids (PNA). Oligonucleotide analogs with an achiral peptide backbone. *J. Am. Chem. Soc.* 114: 1895-1897.
- 3 Egholm M., Buchardt O., Christensen L., Behrens C., Freier S.M., Driver D.A., Berg R.H., Kim S.K., Norden B., Nielsen P.E. (1993) PNA hybridizes to complementary oligonucleotides obeying the Watson-Crick hydrogen-bonding rules. *Nature*. 365(6446):566-8.
- 4 Egholm M., Behrens C., Christensen L., Berg R.H., Nielsen P.E., Buchardt O. (1993) Peptide nucleic acids containing adenine or guanine recognize thymine and cytosine in complementary DNA sequences. *J. Chem. Soc. Chem. Commun.*, 800-801.
- 5 Cherny D.Y., Belotserkovskii B.P., Frank-Kamenetskii M.D., Egholm M., Buchardt O., Berg R.H., Nielsen P.E. (1993) DNA unwinding upon strand-displacement binding of a thymine-substituted polyamide to double-stranded DNA. *Proceedings of the National Academy of Sciences of the United States of America*. 90(5):1667-70.
- 6 Nielsen P.E., Egholm M., Buchardt O. (1994) Evidence for (PNA)₂/DNA triplex structure upon binding of PNA to dsDNA by strand displacement. *Journal of Molecular Recognition*. 7(3):165-70.
- 7 Giesen U., Kleider W., Berding C., Geiger A., Orum H., Nielsen P.E. (1998) A formula for thermal stability (T_m) prediction of PNA/DNA duplexes. *Nucleic Acids Research*. 26(21):5004-6.
- 8 Betts L., Josey J.A., Veal J.M., Jordan S.R. (1995) A nucleic acid triple helix formed by a peptide nucleic acid-DNA complex. *Science*. 270(5243):1838-41.

- 9 Egholm M., Christensen L., Dueholm K.L., Buchardt O., Coull J., Nielsen P.E. (1995) Efficient pH independent sequence-specific DNA binding by pseudoisocytosine-containing bis-PNA. *Nucleic Acids Res.* 23(2):217-22.
- 10 Kaihatsu K., Shah R.H., Zhao X., Corey D.R.(2003) Extending recognition by peptide nucleic acids (PNAs): binding to duplex DNA and inhibition of transcription by tail-clamp PNA peptide conjugates. *Biochemistry.* 42(47):13996-4003.
- 11 Zhang X., Ishihara T., and Corey D.R. (2000) Strand invasion by mixed base PNAs and a PNA–peptide chimera. *Nucleic Acids Res.* 28 (17): 3332–3338.
- 12 Orum H., Nielsen P.E, Egholm M., Berg R.H., Buchardt O., Stanley C. (1993) Single base pair mutation analysis by PNA directed PCR clamping. *Nucleic Acids Research.* 21(23):5332-6.
- 13 Tomac S., Sarkar M., Ratilainen T., Wittung P., Nielsen P.E, Nordén B., Gräslund A. (1996) Ionic effects on the stability and conformation of peptide nucleic acid complexes. *Journal of the American Chemical Society.* 118: 5544-5552.
- 14 Jensen K.K., Ørum, H., Nielsen, P.E. and Nordén, B. (1997) Kinetics for Hybridization of Peptide Nucleic Acids (PNA) with DNA and RNA Studied with the BIAcore Technique. *Biochemistry.* 36, 5072-5077.
- 15 Wittung P., Nielsen P.E, Buchardt O., Egholm M., Norden B. (1994) DNA-like double helix formed by peptide nucleic acid. *Nature.* 368(6471):561-3.
- 16 Chen C., Wu B., Wei T., Egholm M., Strauss W.M. (2000) Unique chromosome identification and sequence-specific structural analysis with short PNA oligomers. *Mammalian Genome.* 11(5):384-91.

- 17 Orum H., Nielsen P.E., Jorgensen M., Larsson C., Stanley C., Koch T. (1995) Sequence specific purification of nucleic acids by PNA-controlled hybrid selection. *Biotechniques*. 19(3):472-80.
- 18 Chandler D.P., Stults J.R., Anderson K.K., Cebula S., Schuck B.L., Brockman F.J. (2000) Affinity capture and recovery of DNA at femtomolar concentrations with peptide nucleic acid probes. *Anal Biochem*. 283:241-249.
- 19 Chandler D.P., Stults J.R., Cebula S., Schuck B.L., Weaver D.W., Anderson K.K., Egholm M., Brockman F.J. (2000) Affinity purification of DNA and RNA from environmental samples with peptide nucleic peptide nucleic acid clamps. *Appl. Environ. Microbiol.* 66:3438 3445.
- 20 Eriksson M., Nielsen P.E. (1996) PNA-nucleic acid complexes. structure, stability and dynamics. *Quarterly Reviews of Biophysics*. 29: 369-394.
- 21 Brown S.C., Thomson S.A., Veal J.M., Davis D.G. (1994) NMR solution structure of a peptide nucleic acid complexed with RNA. *Science*. 265(5173):777-80.
- 22 Leijon M., Graslund A., Nielsen P.E., Buchardt O., Norden B., Kristensen S.M., Eriksson M. (1994) Structural characterization of PNA-DNA duplexes by NMR. Evidence for DNA in a B-like conformation. *Biochemistry*. 33(33):9820-5.
- 23 Eriksson M., Nielsen P.E. (1996) Solution structure of a peptide nucleic acid-DNA duplex. *Nature Structural Biology*. 3(5):410-3.
- 24 Rasmussen H., Kastrup J.S., Nielsen J.N., Nielsen J.M., Nielsen P.E. (1997) Crystal structure of a peptide nucleic acid (PNA) duplex at 1.7 Å resolution. *Nat. Struct. Biol.* 4(2):98-101.
- 25 Christensen L., Fitzpatrick R., Gildea B., Petersen K.H., Hansen H.F., Koch T., Egholm M., Buchardt O., Nielsen P.E., Coull J., Berg R.H. (1995) Solid-phase synthesis of peptide nucleic acids. *J. Pept. Sci.* 1, 175-183.

- 26 Casale R., Jensen I.S., Egholm M. (1999) Synthesis of PNA oligomers by Fmoc chemistry. *In: Peptide nucleic acids: protocols and applications.* (Eds: P. E. Nielsen, M. Egholm) Horizon Scientific Press, Wymondham, United Kingdom, 39-50.

- 27 Stein C.A., Cheng Y-A. (1997) Antisense inhibition of gene expression. *In Principles and Practice of Oncology*, ed. V.T. DeVita, S.A. Rosenberg, S. Hellman, pp.3059-74. New York: Lippincott.

- 28 Braasch D.A., Nulf C.J., and Corey D.R. (2002) *Current Protocols in Nucleic Acid Chemistry. Unit 4.11 Synthesis and Purification of Peptide Nucleic Acids.* pp.14.11.11-14.11.18, John Wiley & Sons, New York

- 29 Demidov V.V., Potaman V.N., Frank-Kamenetskii M.D., Egholm M., Buchard O., Sonnichsen S.H. and Nielsen P.E. (1994) Stability of peptide nucleic acids in human serum and cellular extracts. *Biochem. Pharmacol.*, 48, 1310–1313.

- 30 Eriksson M., Christensen L., Schmidt J., Haaima G., Orgel L., Nielsen P.E.(1998) Sequence dependent N-terminal rearrangement and degradation of peptide nucleic acid (PNA) in aqueous solution. *Nouv. J. Chim.* 22:1055-9.

- 31 Hultdin M., Gronlund E., Norrback K., Eriksson-Lindstrom E., Just T., Roos G. (1998) Telomere analysis by fluorescence in situ hybridization and flow cytometry. *Nucleic Acids Res.* 26(16):3651-6.

- 32 Rufer N., Dragowska W., Thornbury G., Roosnek E., Lansdorp P.M. (1998) Telomere length dynamics in human lymphocyte subpopulations measured by flow cytometry. *Nat. Biotechnol.* 16(8):743-7.

- 33 Chuang T.C., Moshir S., Garini Y., Chuang A.Y., Young I.T., Vermolen B., Doel Rv R., Mougey V., Perrin M., Braun M., Kerr P.D., Fest T., Boukamp P., Mai S. (2004) The three-dimensional organization of telomeres in the nucleus of mammalian cells. *BMC Biol.* 2(1):12.
- 34 Drobniewski F.A., More P.G., Harris G.S. (2000) Differentiation of Mycobacterium tuberculosis complex and nontuberculous mycobacterial liquid cultures by using peptide nucleic acid fluorescence In situ hybridization probes. *J. Clin. Microbiol.* 38(1):444-7.
- 35 Perry-O'Keefe H., Rigby S., Oliveira K., Sorensen D., Stender H., Coull J., Hyldig-Nielsen J.J. (2001) Identification of indicator microorganisms using a standardized PNA FISH method. *J. Microbiol. Methods.* 47(3):281-92.
- 36 Wang J., Nielsen P.E., Jiang M., Cai X., Fernandes J.R., Grant D.H., Ozsoz M., Beglieter A., Mowat M. (1997) Mismatch-sensitive hybridization detection by peptide nucleic acids immobilized on a quartz crystal microbalance. *Anal. Chem.* 69(24):5200-2.
- 37 Brandt O., Feldner J., Stephan A., Schroder M., Schnolzer M., Arlinghaus H.F., Hoheisel J.D., Jacob A. (2003) PNA microarrays for hybridisation of unlabelled DNA samples. *Nucleic Acids Res.* 31(19):e119.
- 38 Jain K.K. (2000) Applications of biochip and microarray systems in pharmacogenomics. *Pharmacogenomics.* 1(3):289-307.
- 39 Behn M., Schuermann M. (1998) Sensitive detection of p53 gene mutations by a 'mutant enriched' PCR-SSCP technique. *Nucleic Acids Res.* 26(5):1356-8.
- 40 Kuhn H., Demidov V.V., Gildea B.D., Fiandaca M.J., Coull J.C., Frank-Kamenetskii M.D. (2001) PNA beacons for duplex DNA. *Antisense Nucleic Acid Drug Dev.* 11(4):265-70.

- 41 Petersen K., Vogel U., Rockenbauer E., Nielsen K.V., Kolvraa S., Bolund L., Nexø B. (2004) Short PNA molecular beacons for real-time PCR allelic discrimination of single nucleotide polymorphisms. *Mol. Cell Probes*. 18(2):117-22.
- 42 Demidov V.V., Bukanov N.O., Frank-Kamenetskii M.D. Duplex DNA capture. (2000) *Current Issues in Molecular Biology*. 2(1):31-5.
- 43 Demidov V.V., Kuhn H., Lavrentieva-Smolina I.V., Frank-Kamenetskii M.D. (2001) Peptide nucleic acid-assisted topological labeling of duplex dna. *Methods*. 23(2):123-31.
- 44 Nielsen P.E., Egholm M., Berg R.H., Buchardt O. (1993) Sequence specific inhibition of DNA restriction enzyme cleavage by PNA. *Nucleic Acids Res*. 21: 197-200.
- 45 Veselkov A.G., Demidov V.V., Frank-Kamenetskii M.D., Nielsen P.E (1996) PNA as a rare genome-cutter. *Nature* (London). 379: 214.
- 46 Protozanova E., Demidov V.V., Nielsen P.E., Frank-Kamenetskii M.D. (2003) Pseudocomplementary PNAs as selective modifiers of protein activity on duplex DNA: the case of type II restriction enzymes. *Nucleic Acids Research*. 31(14):3929-35.
- 47 Demidov V.V., Frank-Kamenetskii M.D., Egholm M., Buchardt O., Nielsen P.E. (1993) Sequence selective double strand DNA cleavage by peptide nucleic acid (PNA) targeting using nuclease S1. *Nucleic Acids Res*. 21: 2103-2107.
- 48 Haaima G., Hansen H.F., Christensen L., Dahl O., Nielsen P.E. (1997) Increased DNA binding and sequence discrimination of PNA oligomers containing 2,6-diaminopurine. *Nucleic Acids Res*. 25(22):4639-43.

- 49 Nielsen P.E., Ørum H. Peptide nucleic acid (PNA) as new biomolecular tools. (1995) *In Molecular Biology: Current Innovations and Future Trends*. Edited by Griffin H. Horizon Scientific Press, UK;73-86.
- 50 Mischianti C., Borgatti M., Bianchi N., Rutigliano C., Tomassetti M., Feriotto G. and Gambari R. (1999) Interaction of the human NF-kappaB p52 transcription factor with DNA-PNA hybrids mimicking the NF-kappaB binding sites of the human immunodeficiency virus type 1 promoter. *J. Biol. Chem.* 274, 33114–33122.
- 51 Hamilton S.E., Iyer M., Norton J.C. and Corey D.R. (1996) Specific and nonspecific inhibition of RNA synthesis by DNA, PNA and phosphorothioate promoter analog duplexes. *Bioorg. Med. Chem. Lett.* 6, 2897–2900.
- 52 Yuan X., Ma Z., Zhou W., Niidome T., Alber S., Huang L., Watkins S., Li S. (2003) Lipid-mediated delivery of peptide nucleic acids to pulmonary endothelium. *Biochem. Biophys. Res. Commun.* 302(1):6-11.
- 53 Nielsen P.E. (2000) Antisense peptide nucleic acids. *Curr. Opin. Mol. Ther.* 2(3):282-7.
- 54 Nielsen P.E. (2000) Peptide nucleic acids: on the road to new gene therapeutic drugs. *Pharmacol. Toxicol.* 86(1):3-7.
- 55 Hanvey J.C., Peffer N.C., Bisi J.E., Thomson S.A., Cadilla R., Josey J.A., Ricca D.J., Hassman C.F., Bonham M.A., Au K.G., Carter S.G., Bruckenstein D.A., Boyd A.L., Noble S.A., Babiss L.E. (1992) Antisense and antigene properties of peptide nucleic acids. *Science*. 258,1481-1485.
- 56 Knudsen H., Nielsen P.E. (1996) Antisense properties of duplex- and triplex-forming PNAs. *Nucleic Acids Res.* 24, 494-500.

- 57 Dash P., Lotan I., Knapp M., Kandel E.R., Goelet P. (1987) Selective elimination of mRNAs in vivo: complementary oligodeoxynucleotides promote RNA degradation by an RNase H-like activity. *Proceedings of the National Academy of Sciences of the United States of America*. 84(22):7896-900.
- 58 Cazenave C., Loreau N., Thuong N.T., Toulme J.J., Helene C. (1987) Enzymatic amplification of translation inhibition of rabbit beta-globin mRNA mediated by anti-messenger oligodeoxynucleotides covalently linked to intercalating agents. *Nucleic Acids Research*. 15(12):4717-36.
- 59 Monia B.P., Lesnik E.A., Gonzalez C., Lima W.F., McGee D., Guinosso C.J., Kawasaki A.M., Cook P.D., Freier S.M. (1993) Evaluation of 2'-modified oligonucleotides containing 2'-deoxy gaps as antisense inhibitors of gene expression. *J. Biol. Chem.* 5;268(19):14514-22.
- 60 Robbins I., Mitta G., Vichier-Guerre S., Sobol R., Ubysz A., Rayner B., Lebleu B. (1998) Selective mRNA degradation by antisense oligonucleotide-2,5A chimeras: involvement of RNase H and RNase L. *Biochimie*. 80(8-9):711-20.
- 61 Rait V.K., Shaw B.R. (1999) Boranophosphates support the RNase H cleavage of polyribonucleotides. *Antisense Nucleic Acid Drug Dev.* (1):53-60.
- 62 Veal G.J., Agrawal S., Byrn R.A. (1998) Sequence-specific RNase H cleavage of gag mRNA from HIV-1 infected cells by an antisense oligonucleotide in vitro. *Nucleic Acids Res.* 26(24):5670-5.
- 63 Braasch D.A., Corey D.R. (2002) Novel antisense and peptide nucleic acid strategies for controlling gene expression. *Biochemistry*. 41(14):4503-10.
- 64 Doyle D.F., Braasch D.A., Simmons C.G., Janowski B.A., Corey D.R. (2001) Inhibition of gene expression inside cells by peptide nucleic acids: effect of mRNA target sequence, mismatched bases, and PNA length. *Biochemistry*. 40(1):53-64.

- 65 Senamaud-Beaufort C., Leforestier E., Saison-Behmoaras T.E. (2003) Short pyrimidine stretches containing mixed base PNAs are versatile tools to induce translation elongation arrest and truncated protein synthesis. *Oligonucleotides*. 13(6):465-78.
- 66 Liu Y., Braasch D.A., Nulf C.J., Corey D.R.(2004) Efficient and isoform-selective inhibition of cellular gene expression by peptide nucleic acids. *Biochemistry*. 43(7):1921-7.
- 67 Kole R., Vacek M., Williams T. (2004) Modification of alternative splicing by antisense therapeutics. *Oligonucleotides*. 14(1):65-74.
- 68 Siwkowski A.M., Malik L., Esau C.C., Maier M.A., Wancewicz E.V., Albertshofer K., Monia B.P., Bennett C.F., Eldrup A.B. (2004) Identification and functional validation of PNAs that inhibit murine CD40 expression by redirection of splicing. *Nucleic Acids Res*. 32(9):2695-706.
- 69 Herbert B., Pitts A.E., Baker S.I., Hamilton S.E., Wright W.E., Shay J.W., Corey D.R. (1999) Inhibition of human telomerase in immortal human cells leads to progressive telomere shortening and cell death. *Proc. Natl. Acad. Sci. U S A*. 96(25):14276-81.
- 70 Hamilton S.E., Pitts A.E., Katipally R.R., Jia X., Rutter J.P., Davies B.A., Shay J.W., Wright W.E., Corey D.R. (1997) Identification of determinants for inhibitor binding within the RNA active site of human telomerase using PNA scanning. *Biochemistry*. 36(39):11873-80.
- 71 Sohail M., Southern E.M. (2000) Hybridization of antisense reagents to RNA. *Curr. Opin. Mol. Ther.* 2(3):264-71.
- 72 Armitage B. (2003) The impact of nucleic acid secondary structure on PNA hybridization. *Drug Discovery Today*. 8(5):222-8.

- 73 Dias N., Senamaud-Beaufort C., Forestier El E., Auvin C., Helene C., Ester Saison-Behmoaras T. (2002) RNA hairpin invasion and ribosome elongation arrest by mixed base PNA oligomer. *J. Mol. Biol.* 320(3):489-501.
- 74 Kushon S.A., Jordan J.P., Seifert J.L., Nielsen H., Nielsen P.E., Armitage B.A. (2001) Effect of secondary structure on the thermodynamics and kinetics of PNA hybridization to DNA hairpins. *J. Am. Chem. Soc.* 123(44):10805-13.
- 75 Stein C.A. and Cheng Y.C. (1993) Antisense oligonucleotides as therapeutic agents – is the bullet really magical? *Science.* 261, 1004–1012.
- 76 Gray G.D., Basu S. & Wickström E. (1997) Transformed and immortalized cellular uptake of oligodeoxynucleoside phosphorothioates, 3'-alkylamino oligodeoxynucleotides, 2'-O-methyl oligoribonucleotides, oligodeoxynucleoside methylphosphonates, and peptide nucleic acids. *Biochem. Pharmacol.* 53, 1465-1476.
- 77 Bonham M.A., Brown S., Boyd A.L., Brown P.H., Bruckenstein D.A., Hanvey J.C., Thomson S.A., Pipe A., Hassman F., Bisi J.E., Froehler B.C., Mattuecchi M.D., Wagner R.W., Noble S.A., Babiss L.E. (1995) An assessment of the antisense properties of RNase H-competent and steric-blocking oligomers. *Nucleic Acids Res.* 23(7):1197-203.
- 78 Faruqi A.F., Egholm M., Glazer P.M. (1998) Peptide nucleic acid-targeted mutagenesis of a chromosomal gene in mouse cells. *Proc. Nat. Acad. Sci. U S A.* 95(4):1398-403.
- 79 Boffa L.C., Morris P.L., Carpaneto E.M., Louissaint M., Allfrey V.G. (1996) Invasion of the CAG triplet repeats by a complementary peptide nucleic acid inhibits transcription of the androgen receptor and TATA-binding protein genes and correlates with refolding of an active nucleosome containing a unique AR gene sequence. *J. Biol. Chem.* 271(22):13228-33.

- 80 Good L., Sandberg R., Larsson O., Nielsen P.E., Wahlestedt C. (2000) Antisense PNA effects in Escherichia coli are limited by the outer-membrane LPS layer. *Microbiology*. 146 (Pt 10):2665-70.
- 81 Awasthi S.K., Nielsen P.E. (2002) Synthesis of PNA-Peptide Conjugates, Kap. II, 3 In: *Peptide Nucleic Acids. Methods and Protocols* (Ed.: Nielsen, P.E.). Humana Press.
- 82 Mayfield L., Katipally R.R., Simmons C.G., and Corey D.R. (1998) Solid Phase synthesis of peptide nucleic acid (PNA)-peptide conjugates." Tam J. P. (Ed.) *Peptides: Chemistry Structure and Biology (Proceedings of the Fifteenth American Peptide Symposium) ESCOM*, Leiden, The Netherlands.
- 83 Kaushik N., Basu A., Palumbo P., Myers R.L., Pandey V.N. (2002) Anti-TAR polyamide nucleotide analog conjugated with a membrane-permeating peptide inhibits human immunodeficiency virus type 1 production. *J. Virol.* 76(8):3881-91.
- 84 Koppelhus U., Awasthi S.K., Zachar V., Holst H.U., Ebbesen P., Nielsen P.E. (2002) Cell-dependent differential cellular uptake of PNA, peptides, and PNA-peptide conjugates. *Antisense Nucleic Acid Drug Dev.* 12(2):51-63.
- 85 Pooga M., Soomets U., Hallbrink M., Valkna A., Saar K., Rezaei K., Kahl U., Hao J.X., Xu X.J., Wiesenfeld-Hallin Z., Hokfelt T., Bartfai T., Langel U. (1998) Cell penetrating PNA constructs regulate galanin receptor levels and modify pain transmission in vivo. *Nat. Biotechnol.* 16,857-861.
- 86 Good L., Awasthi S.K., Dryselius R., Larsson O., Nielsen P.E. (2001) Bactericidal antisense effects of peptide-PNA conjugates. *Nat. Biotechnol.* 19(4):360-4.
- 87 Eriksson M., Nielsen P.E., Good L. (2002) Cell permeabilization and uptake of antisense peptide-peptide nucleic acid (PNA) into Escherichia coli. *J. Biol. Chem.* 277(9):7144-7.

- 88 Zhang X., Simmons C.G., Corey D.R. (2001) Liver cell specific targeting of peptide nucleic acid oligomers. *Bioorg. Med. Chem. Lett.* 11(10):1269-72.
- 89 Boado R.J., Tsukamoto H., Pardridge W.M. (1998) Drug delivery of antisense molecules to the brain for treatment of Alzheimer's disease and cerebral AIDS. *J. Pharm. Sci.* 87(11):1308-15.
- 90 Penichet M.L., Kang Y.S., Pardridge W.M., Morrison S.L., Shin S.U. (1999) An antibody-avidin fusion protein specific for the transferrin receptor serves as a delivery vehicle for effective brain targeting: initial applications in anti-HIV antisense drug delivery to the brain. *J. Immunol.* 163:4421-6.
- 91 Rebuffat A.G., Nawrocki A.R., Nielsen P.E., Bernasconi A.G., Bernal-Mendez E., Frey B.M., Frey F.J. (2002) Gene delivery by a steroid-peptide nucleic acid conjugate. *FASEB J.* 16:1426-8.
- 92 Hamilton S.E., Simmons C.G., Kathiriya I.S., Corey D.R. (1999) Cellular delivery of peptide nucleic acids and inhibition of human telomerase. *Chem. Biol.* 6(6):343-51.
- 93 Gebiski B.L., Mann C.J., Fletcher S., and Wilton S.D. (2003) Morpholino antisense oligonucleotide induced dystrophin exon 23 skipping in mdx mouse muscle. *Human Molecular Genetics*. Vol. 12, No. 15, 1801-1811.
- 94 Morcos P.A. (2001) Achieving Efficient Delivery of Morpholino Oligos in Cultured Cells. *Genesis*. 30:94-102.
- 95 Nulf C.J., Corey D.R. (2004) Intracellular Inhibition of Hepatitis C Virus (HCV) Internal Ribosomal Entry Site (IRES)-Dependent Translation by Peptide Nucleic Acids (PNAs) and Locked Nucleic Acids (LNAs). *Nucleic Acids Research*. In Press.

- 96 Agrawal S., Temsamani J., Galbraith W., Tang J. (1995) Pharmacokinetics of antisense oligonucleotides. *Clin. Pharmacokinet.* 28(1):7-16.
- 97 Crooke S.T., Graham M.J., Zuckerman J.E., Brooks D., Conklin B.S., Cummins L.L., Greig M.J., Guinosso C.J., Kornbrust D., Manoharan M., Sasmor H.M., Schleich T., Tivel K.L., Griffey R.H. (1996) Pharmacokinetic properties of several novel oligonucleotide analogs in mice. *J. Pharmacol. Exp. Ther.* 277(2):923-37.
- 98 McMahon B.M., Mays D., Lipsky J., Stewart J.A., Fauq A., Richelson E. (2002) Pharmacokinetics and tissue distribution of a peptide nucleic acid after intravenous administration. *Antisense Nucleic Acid Drug Dev.* 12(2):65-70.
- 99 Hamzavi R., Dolle F., Tavitian B., Dahl O., Nielsen P.E. (2003) Modulation of the pharmacokinetic properties of PNA: preparation of galactosyl, mannosyl, fucosyl, N-acetylgalactosaminy, and N-acetylglucosaminy derivatives of aminoethylglycine peptide nucleic acid monomers and their incorporation into PNA oligomers. *Bioconjug. Chem.* 14(5):941-54.
- 100 Larsen H.J., Bentin T, Nielsen P.E. (1999) Antisense properties of peptide nucleic acid. *Biochim. Biophys. Acta.* 1489(1):159-66.

CHAPTER 2 - DNA ASSEMBLY BY BIS-PEPTIDE NUCLEIC ACIDS (bisPNAs)

	<u>Page</u>
Introduction	50
DNA in nano-biotechnology	50
PNA potentials in nano-biotechnology	54
Rational design of novel bisPNAs	56
Chemical synthesis and analysis of PNA and bisPNA molecules	56
Models of dual DNA oligonucleotide hybridization	
Melting temperature (T_m) analysis of exact complement and overhanging DNA oligonucleotides to bisPNAs	58
Assembly of short, complementary oligonucleotides by bisPNA	62
Assembly of oligonucleotides that project beyond the bisPNA	62
DNA assembly by bisPNAs connected by spacers of differing lengths	64
Reasons for inefficient assembly of oligonucleotides that project inward	69
Applications of PNAs for the assembly of DNA structures	72
BisPNAs strand-invasion into duplex DNA	75
Uses of bisPNA to strand invade at two individual duplex DNA locations	78
Conclusions	80
References for Chapter 2	84

Introduction

Nanotechnology involves assembly of small molecules into complex architectures for higher function (1). The goal of nanotechnology is to control the precise location of each atom (or element) in a three dimensional space. Current conventional "top-down" processes of small-scale devices (i.e. miniturizing processes such as photolithography) are limited to about 200-100 nm accuracy. "Bottom-up" technologies based on the self-assembly of molecular building blocks (5-10 nm) to form larger functional elements are being explored as potential ways to fabricate nanometer-size devices (2).

DNA in nano-biotechnology

The DNA molecule is an ideal medium for applications in nanotechnology and has shown great potential in fabrication and construction of nanostructures and devices for several reasons. First, the simple self-assembly of DNA molecules using the canonical Watson–Crick base-pairing rules of adenine to thymine and guanine to cytosine is ideal for organizing biomolecules in a controllable, highly predictable fashion. Atomical, chemical, structural and biophysical properties of traditional single-stranded and double-stranded DNA molecules (ssDNA, and A-form and B-form dsDNA) as well as unusual DNA topologies and motifs (Z-form DNA, four-stranded quadruplexes, pseudoknots) are well documented in the literature (**Figure 2-1. Chemical and physical dimensions of duplex DNA**). A number of controllable variables influencing these properties are also well documented. For example, high temperatures break hydrogen bonds between base-pairs, the presence of cations can stabilize annealed nucleic acids, and certain nucleotide sequences can create "bends" in duplex DNA.

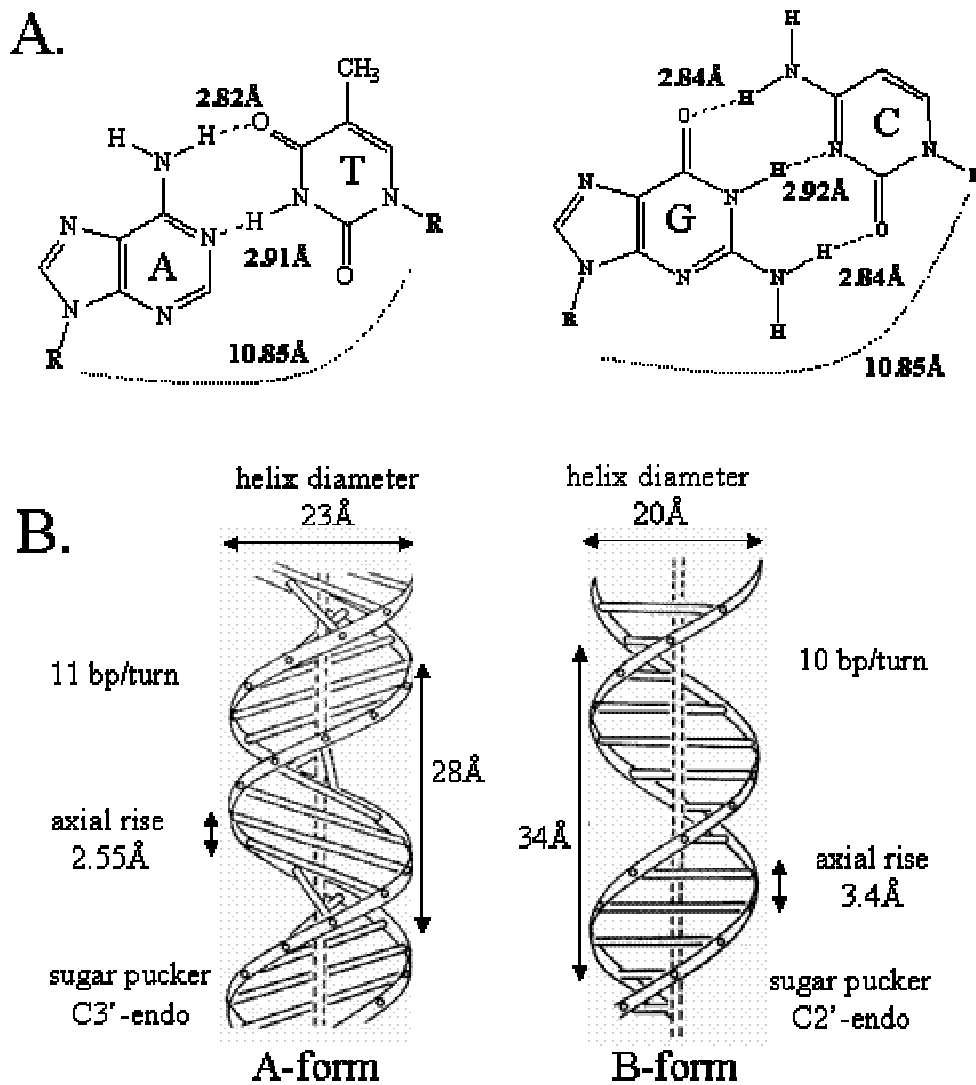


Figure 2-1. Chemical and physical dimensions of duplex DNA. A.) Hydrogen Bond Lengths between base pairs and distance between backbones B.) Parameters of helical DNA, A-form and B-form. Data is from X-ray crystallographic data. Each of these physical parameters can be easily controlled by changing ionic buffers, temperature, and nucleotide sequences.

Second, DNA/RNA synthesis is a robust chemistry. Any sequence can be synthesized at oligonucleotide lengths suited for building nanostructures for minimal costs. Likewise, simple modifications to the oligonucleotide can be introduced for added functions, such as biotin, linker groups, or fluorescence molecules.

Third, DNA can be manipulated and modified by a large battery of enzymes that include DNA ligases, restriction endonucleases, kinases, and exonucleases. Likewise, nucleobases can be modified by chemical means. For instance, dimethylsulfate (DMS) alkylates guanines at ring position N7 while chloroacetaldehyde (CAA) reacts predominantly toward cytosines and adenines.

In addition, basic protocols for manipulating, analyzing, and handling DNA are well documented. UV absorbance spectroscopy, gel electrophoresis, and biochemical assays are common, easy-to-use tools for studying DNA structure and topology. Nuclear magnetic resonance (NMR), circular dichromism (CD), and x-ray crystallography are also available for many laboratories.

Numerous reports using oligonucleotides to build nanostructures include DNA matrices based on subunits of fixed Holliday junctions (**3**), streptavidin–DNA fragment nanoparticle networks (**4**) and DNA dendrimer formations for drug delivery (**5**; **for reviews see 6, 7, 8 9**). Likewise, several "mechanical tools" based on the ssDNA have been described, such as the "molecular tweezers" (**10**). Here, the hybridization a partial complementary ssDNA brings together the ends of a longer ssDNA (**Figure 2-2a. DNA Molecular "Tweezers"**).

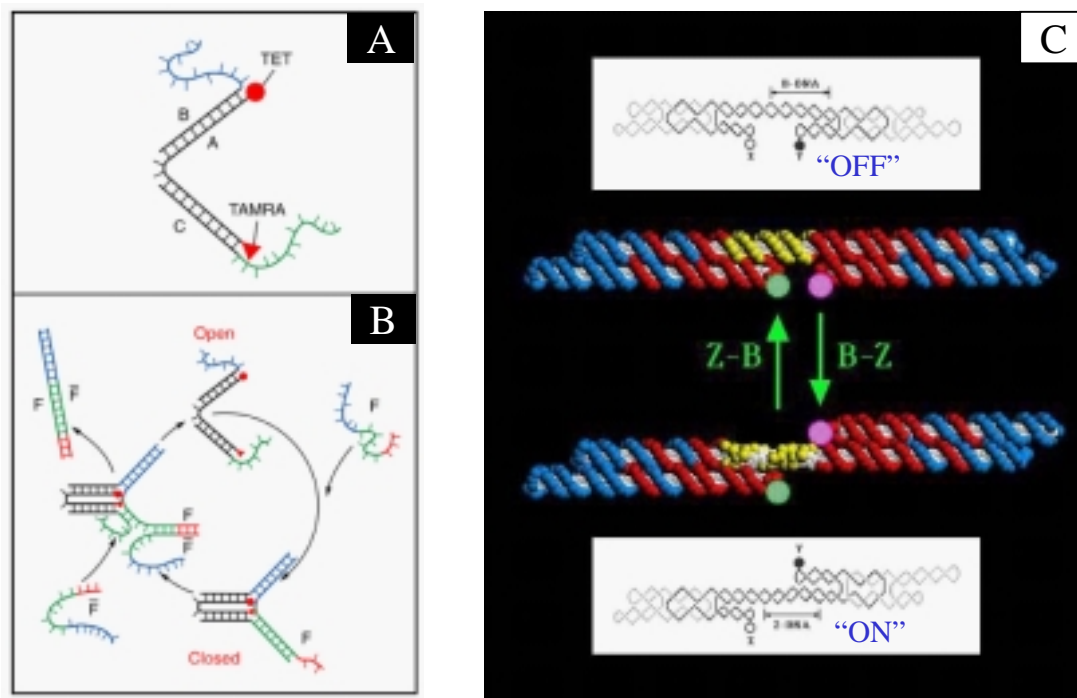


Figure 2-2. DNA Molecular “Tweezers” and “Switches” A.) Molecular “tweezer” structure formed by hybridization of oligonucleotide strands A, B and C B.) Closing and opening the molecular tweezers. Fuel strand F hybridizes with the dangling ends of strands B and C (shown in blue and green) to pull the tweezers closed. Hybridization with the overhang section of F (red) allows strand F to remove F from the tweezers forming a double-stranded waste product F F and allowing the tweezers to open. C.) B to Z transition of dsDNA topology due to a change in ionic conditions results in movement of the fluorescent molecule (X) and quencher molecule (Y) away from one another.

*From: Yurke B., Turberfield A.J., Mills A.P. Jr, Simmel F.C., Neumann J.L. (2000) A DNA-fuelled molecular machine made of DNA. *Nature*. 406(6796):605-8

Mao C., Sun W., Shen Z., Seeman N.C. (1999) A nanomechanical device based on the B-Z transition of DNA. *Nature*. 397(6715):144-6.

"Molecular switches" have also been described whereby a change in the ionic conditions of the buffer changes the helicity and topology of the DNA strands. Using fluorescence resonance energy transfer spectroscopy, which measures the relative proximity of two dye molecules attached to the free ends of the DNA molecules, altering the buffer conditions induces a DNA helicity change to cause an atomic displacement of 20-60 Å between the quencher molecule and the fluorescent molecule (11, 12) (**Figure 2-2b. DNA Molecular "Switches"**). In this case, a "molecular switch" is turned from "OFF" to "ON".

PNA potentials in nano-biotechnology

PNAs are a promising connector for the assembly of DNA-based nanostructures. PNAs have an exceptional ability to hybridize to sequences within duplex DNA by strand invasion suggesting that PNA molecules should also be superior agent for binding to single-stranded DNA at regions that contains intramolecular structure. High affinity binding by PNAs has already been used for nanostructure assembly, with applications for labeling of DNA (13, 14) and strand invasion into DNA hairpins and tetraloop motifs (15; **for reviews see 16 and 17**).

The following chapter describes the synthesis and characterization of bisPNAs, two PNA sequences with a tethering spacer region (**Figure 2-3. The bisPNA design**). Each half of the bisPNA was designed to target individual DNA oligonucleotides. Several bisPNAs of varying length and amino acid additions within the spacer region were synthesized. I characterized the ability of bisPNAs to assemble DNA and observed

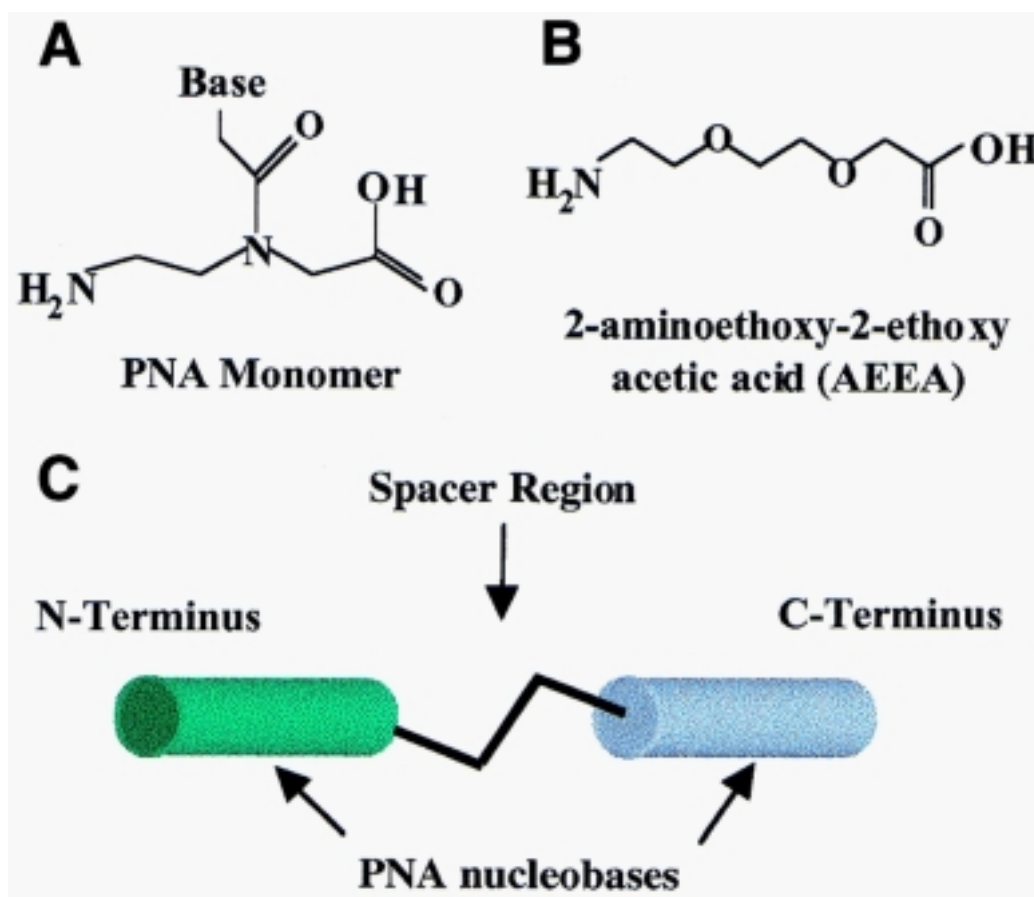


Figure 2-3. The bisPNA design. A.) Chemical structure of the PNA monomer (unprotected). B.) Chemistry of 2-aminoethoxy-2-ethoxy acetic acid (AEEA). As a tethering (linker) molecule, it is approximately 11Å long, flexible, has rotational freedom along the axis, water soluble, and compatible with PNA synthesis. C.) Design of the bisPNA molecule. Two different 12-mer PNAs sequences are tethered with linker molecules (and amino acids) in the spacer region.

that the capacity of a bisPNA molecule to hybridize to two oligonucleotides is primarily dependent on the arrangement of the DNA oligonucleotides being assembled. These results suggest that bisPNA molecules with simple chemical modifications can be used in generating DNA:bisPNA:DNA ‘units’ for nanotechnology and DNA nanostructure assembly, but that proper orientation of the assembled DNA oligonucleotides is essential.

Rational design of novel bisPNAs

I designed bisPNA molecules containing two PNA strands linked by spacer regions of varied lengths (see **Figure 2-3c**). Previous reports have demonstrated that polypyrimidine bisPNAs can form four-stranded complexes capable of invading duplex DNA (**18**). The PNA sequences used in our studies, however, contained mixed purine and pyrimidine sequences because they were designed to bind and assemble two different single-stranded DNA oligonucleotides.

To test the effects of linker length and amino acid substitution within the spacer region between the two PNA strands, I varied the number of AEEA linker molecules (see **Figure 2-3b. and Table 2-1. BisPNA sequences, expected and observed masses**) and number and identity of amino acids. Each AEEA molecule is approximately 11 Å in length, compatible with PNA synthesis, water soluble, highly flexible and rotational about the axis. Amino acids were included in some of the spacer regions to increase the distance between the PNA sequences and to test the effect of amino acid charge and steric bulk on the ability of the bisPNA to assemble both DNA oligonucleotides.

bisPNA	Sequence (N→C)	Mass (Da) (found/calculated)	T_m^* (°C)
PNA 1	tcttcacctaga -lys	3332.70/3332.60	50.4
PNA 2	gatacatatttg -lys	3412.19/3411.62	47.8
AEEA ₁	tcttcacctaga -(aeea) ₁ -gatacatatttg -lys	6738.01/6744.42	52.7/48.3
AEEA ₃	tcttcacctaga -(aeea) ₃ -gatacatatttg -lys	7032.80/7034.82	49.5/45.6
AEEA ₆	tcttcacctaga -(aeea) ₆ -gatacatatttg -lys	7476.20/7470.42	49.1/46.3
AEEA _{6asp5}	tcttcacctaga -(aeea-asp) ₅ (aeea)-gatacatatttg -lys	8023.45/8028.92	48.4/46.7
AEEA _{6lys5}	tcttcacctaga -(aeea-lys) ₅ (aeea)-gatacatatttg -lys	8092.93/8093.42	49.1/47.8
AEEA _{6phe5}	tcttcacctaga -(aeea-phe) ₅ (aeea)-gatacatatttg -lys	8495.29/8496.35	50.3/50.5

Table 2-1. BisPNA sequences, expected and observed masses, and melting temperature values (T_m) for hybridization to oligonucleotide complements. Differences in the bisPNA molecules include the number of AEEA molecules in the spacer region and the inclusion of amino acids between the AEEA molecules. The distances between the PNA sequences (in the spacer region) are approximately 11Å, 33Å, 66Å, and 85Å for the bisPNAs with amino acids in the spacer region. 12-mer PNAs corresponding to each half of the bisPNA were used for comparison. Each bisPNA and PNA has a C-terminal lysine residue.

*For bisPNAs, the temperature on the right is the T_m of the N-terminal half of the bisPNA (analogous to PNA 1), while the temperature on the left is the T_m of the C-terminal half of the bisPNA (analogous to PNA 2).

Chemical synthesis and analysis of PNA and bisPNA molecules

The automated synthesis of bisPNA molecules involving at least 25 couplings required additional precautions to ensure complete synthesis of the molecule. Typically, when a PNA sequence contains three or more consecutive purines or pyrimidines synthesis efficiency decreases. To minimize this problem I repeated coupling steps for addition of the third consecutive base and any that followed. I found that the spacer molecule AEEA was difficult to couple efficiently, so each of these couplings was repeated prior to addition of the next molecule. Repeated coupling was also done for each amino acid. With these precautions, automated synthesis of bisPNAs with extensive spacer regions was routine. I analyzed and purified bisPNAs by C₁₈ RP-HPLC. Full-length PNAs were retained on the C₁₈ column longer than truncated products from failed syntheses. The desired structures were confirmed by mass spectrometry (see **Table 2-1**). Both HPLC and mass spectral analysis routinely indicated that the main product was the desired one.

Models of dual DNA oligonucleotide hybridization

I designed DNA oligonucleotides to hybridize to bisPNAs in four different arrangements (**Figure 2-4. Models of bisPNA hybridized to DNA oligonucleotides**). The oligonucleotides were either exactly complementary to the PNA strands or longer, so that overhanging single-stranded regions were created. The longer oligonucleotides could project outwards (DNA-1_{outward} and DNA-2_{outward}), project partially outwards and partially inwards (DNA-1_{mid} and DNA-2_{mid}) or project inwards (DNA-1_{inward} and DNA-2_{inward})

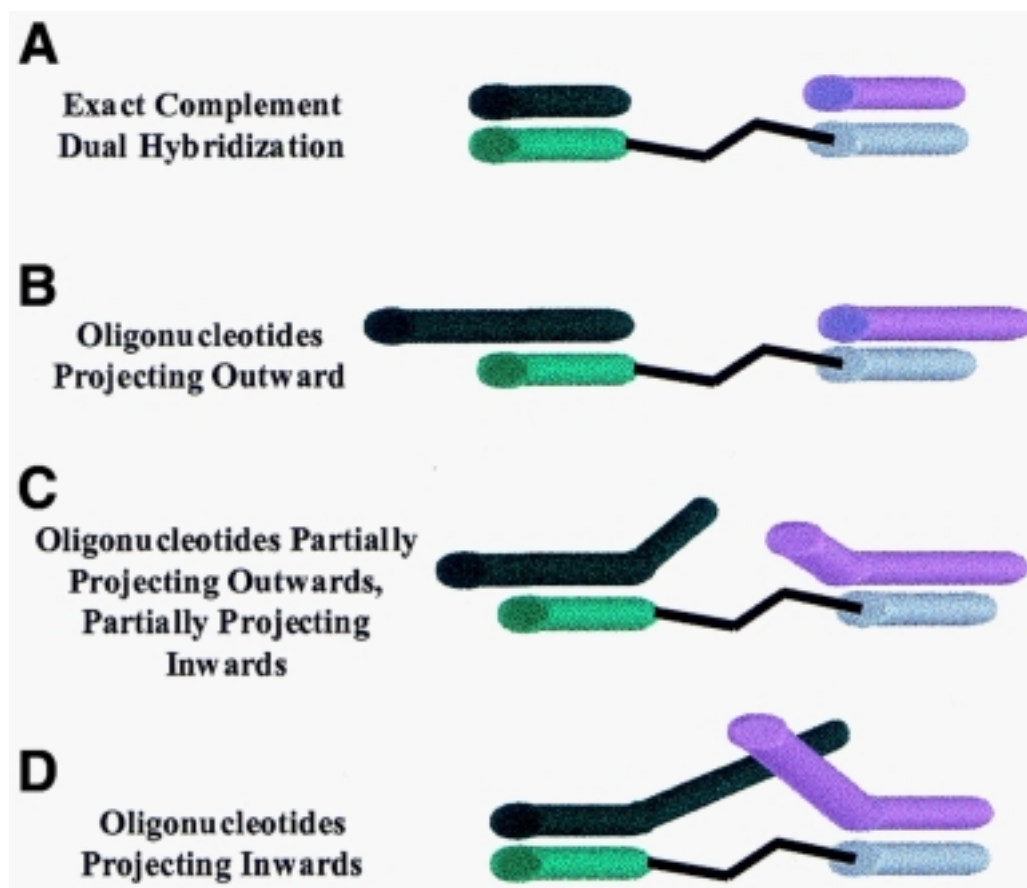


Figure 2-4. Models of bisPNA hybridized to DNA oligonucleotides. A.) DNA oligonucleotides that are exactly complementary to the PNA and do not have overhanging regions. B.) DNA oligonucleotides that have overhanging regions projecting outwards. C.) DNA oligonucleotides that have overhanging regions partially projecting inwards and partially projecting outwards. D.) DNA oligonucleotides that have overhanging regions projecting inwards.

relative to the bisPNA. Except for the target sequence, each base of the DNA oligonucleotide was randomized to minimize secondary structure and DNA:DNA interactions. I studied the ability of PNAs to assemble DNA oligonucleotides with overhanging bases because such overhangs can be used to bind additional nucleic acids and permit complex structures to assemble.

Melting temperature (T_m) analysis of exact complement and overhanging DNA oligonucleotides to bisPNAs

I determined the melting temperature (T_m) values of the bisPNAs and complementary DNA oligonucleotides to characterize their potential for stable and selective hybridization (**Table 2-2. DNA oligonucleotides, T_m Analysis with bisPNA-AEEA₃ and differences in T_m between exact complements and overhanging oligonucleotides**). Both the thermal profile and the T_m values for hybridization of bisPNAs with exactly complementary oligonucleotides were nearly the same as that of the individual 12 base PNAs corresponding to each half of the bisPNA. The length of the spacer region also does not affect the thermal profile of the reversible hyperchromic effect (data not shown). This similarity in T_m values demonstrates that neither the molecules that make up the spacer region nor the unbound half of the bisPNA molecule significantly affects the temperature dependence of hybridization of the PNA and DNA oligonucleotides that lack an overhanging region. As I describe below, the interactions of bisPNAs with DNA oligonucleotides that do contain overhanging regions increase the T_m values in some cases.

	Name	Sequence (5' → 3')	T_m (°C)	ΔT_m (°C)
Exact complements	DNA-1 _{exact}	tctaggtgaaga	49.5	-
	DNA-2 _{exact}	caaatatgtatc	45.6	-
Projecting outward	DNA-1 _{outward}	tctaggtgaaga(n) ₃₈	49.3	-0.2
	DNA-2 _{outward}	(n) ₂₈ caaatatgtatc	48.1	2.5
Partial inward/partial outward	DNA-1 _{mid}	(n) ₁₉ tctaggtgaaga(n) ₁₉	54	4.5
	DNA-2 _{mid}	(n) ₁₄ caaatatgtatc(n) ₁₄	52.8	6.2
Projecting inward	DNA-1 _{inward}	(n) ₃₈ tctaggtgaaga	54.4	4.9
	DNA-2 _{inward}	caaatatgtatc(n) ₂₈	51.9	5.4

Table 2-2. DNA oligonucleotides, T_m Analysis with bisPNA-AEEA₃ and differences in T_m between exact complements and overhanging oligonucleotides. “n” represents a randomized nucleotide.

Assembly of short, complementary oligonucleotides by bisPNA

I analyzed the hybridization of bisPNAs to DNA oligonucleotides by non-denaturing polyacrylamide gel electrophoresis. In all of the experiments described below, I established the mobility of labeled DNA alone, the mobility of labeled DNA bound to one PNA strand, and the mobility of a mixture of labeled and unlabeled DNA oligonucleotides directed to each half of the bisPNA. ³²P-labeled and unlabeled oligonucleotides were added to bisPNAs in a tris buffer and the temperature was ramped from 95°C to 4°C before electrophoresis.

A bisPNA containing three AEEA linkers (PNA-AEEA₃) readily assembled short complementary DNA oligonucleotides, DNA-1_{exact} and DNA-2_{exact}. Surprisingly, when bisPNA-AEEA₃ hybridized to both 12-mer DNA oligonucleotides migration was faster than a single hybridized bisPNA-AEEA₃ (**Figure 2-5. Non-denaturing polyacrylamide gel electrophoresis of bisPNA-AEEA₃ with exact complement DNA oligonucleotides**). The faster mobility of the DNA:bisPNA:DNA was not observed with the longer DNA oligonucleotides (see below). The increased mobility of the larger complex may be due to the dual hybridized bisPNA-AEEA₃ having twice the negative charge (from the second oligonucleotide phosphate backbone) and to formation of a more compact structure than the single hybridized bisPNA.

Assembly of oligonucleotides that project beyond the bisPNA

I next tested the ability of bisPNA-AEEA₃ to hybridize longer DNA oligonucleotides that extended past one or both PNA termini (see **Figure 2-4b, c, d**). Characterizing assembly of these longer oligonucleotides is important because the

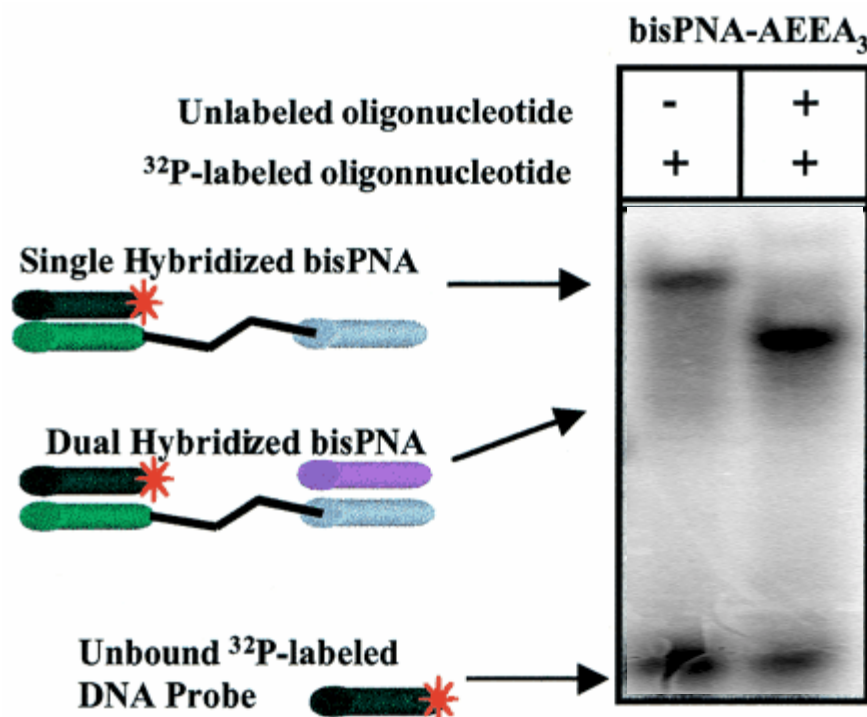


Figure 2-5. Non-denaturing polyacrylamide gel electrophoresis of bisPNA-AEEA₃ with exact complement DNA oligonucleotides. Non-denaturing polyacrylamide gel electrophoresis of bisPNA-AEEA₃ with ³²P-labeled DNA-1_{exact} and unlabeled DNA-2_{exact}. Left lane, bisPNA-AEEA₃ and ³²P-labeled DNA-1_{exact} are present in a 1:1 ratio (150:150 nM). Right lane, bisPNA-AEEA₃ and ³²P-labeled DNA-1_{exact} and unlabeled DNA-2_{exact} are present in a 1:1:3.3 ratio (150:150:500 nM). Hybridization of bisPNA by two exact complement 12-mer DNA oligonucleotides results in a faster moving band than a hybridization of a single DNA oligonucleotide.

extended DNA sequences provide the potential for additional base pairing necessary for formation of higher order structures. When bisPNA was incubated with DNA oligonucleotides designed to project outwards I observed that the bisPNA readily assembled both DNA strands with similar results regardless of which DNA strand was labeled with ^{32}P (**Figure 2-6. Comparison of each half of bisPNA-AEEA₃ for hybridization to one or two outward projecting DNA oligonucleotides**). The efficiency of hybridization was not affected by increasing the concentration of the unlabeled strands.

In contrast to the ability of bisPNAs to successfully assemble short DNA oligonucleotides or DNA oligonucleotides with overhangs that project outwards (**Figure 2-7. Comparison of bisPNA-AEEA₃ hybridization to DNA oligonucleotides that project outwards, partially project inwards, and project inwards, lane 2**), assembly of DNA oligonucleotides that project inwards upon hybridization was less apparent (**Figure 2-7, lanes 4 and 6**). In an attempt to improve binding of inward facing oligonucleotides, I varied several of the annealing conditions including extending the annealing time (up to 3 hours) buffers ($\text{Na}_2\text{H}_2\text{PO}_4$, 0.1 M), but our attempts to bind two DNA oligonucleotides with inward projecting overhanging sequences invariably yielded only a small fraction of bisPNA bound to both DNA strands.

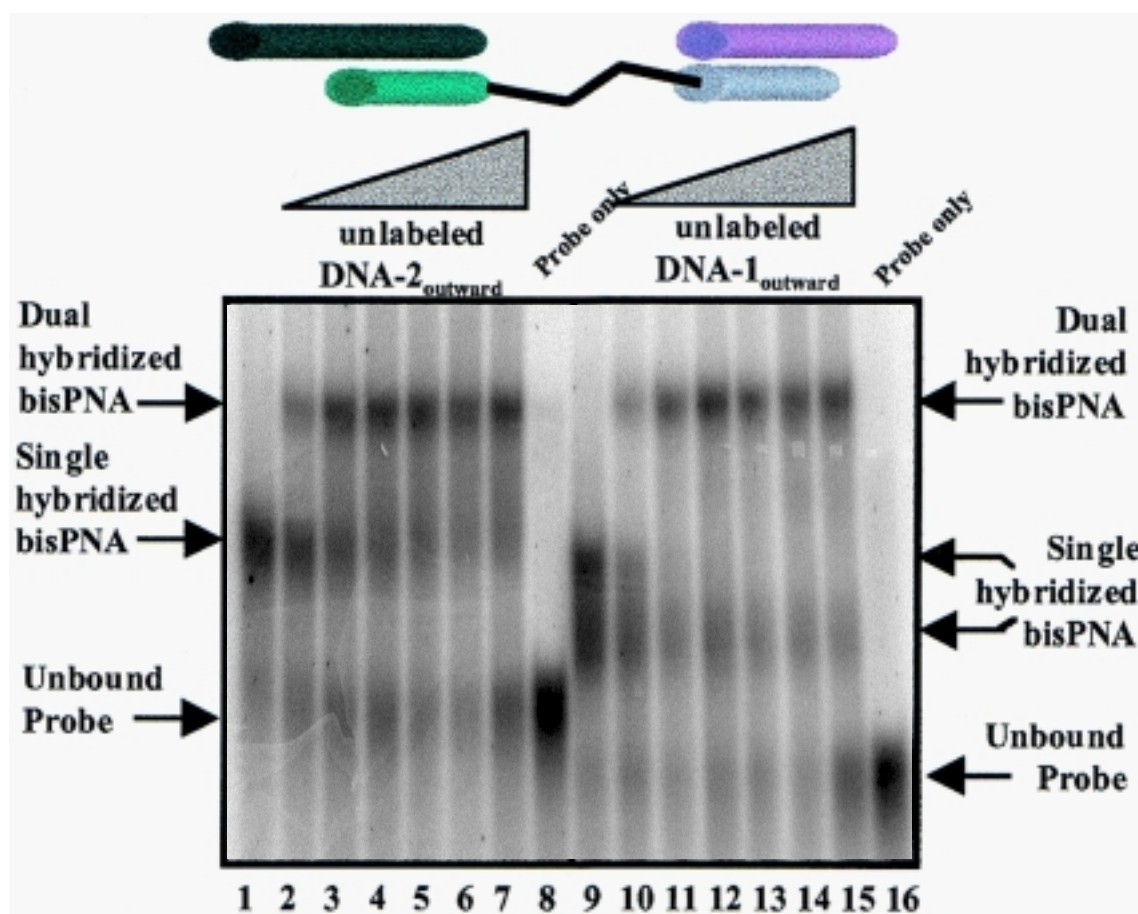


Figure 2-6. Comparison of each half of bisPNA-AEEA₃ for hybridization to one or two outward projecting DNA oligonucleotides. Comparison of each half of bisPNA-AEEA₃ for hybridization to one or two outward projecting DNA oligonucleotides. Lanes 1–7 show hybridization of a 1:1 (150:150 nM) ratio of bisPNA-AEEA₃ and ³²P-labeled DNA-1_{outward}. For lanes 2–7, unlabeled DNA-2_{outward} was added in increasing concentrations (equivalents relative to bisPNA): 0.33, 1.66, 3.33, 16.6, 33.3 and 166 equiv. Lane 8 is ³²P-labeled DNA-1_{outward} only. Lanes 9–15 show hybridization of a 1:1 ratio (150:150 nM) of bisPNA-AEEA₃ and ³²P-labeled DNA-2_{outward}. For lanes 10–15, unlabeled DNA-1_{outward} was added in increasing concentrations (equivalents relative to bisPNA): 0.33, 1.66, 3.33, 16.6, 33.3 and 166 equiv. Lane 16 is ³²P-labeled DNA-2_{outward} only.

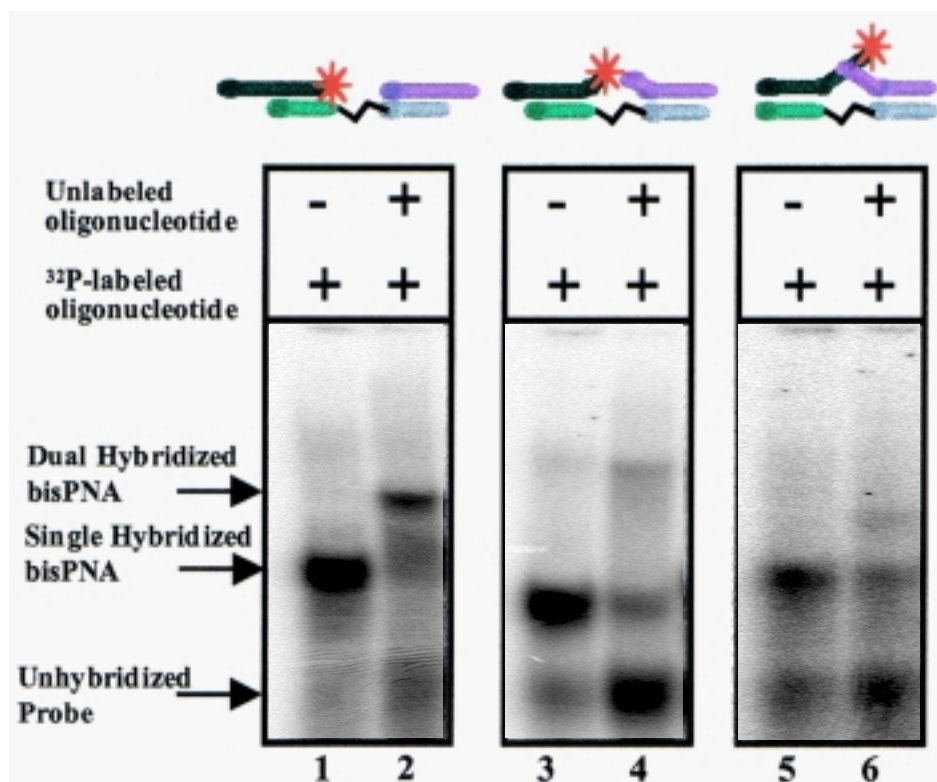


Figure 2-7. Comparison of bisPNA-AEEA₃ hybridization to DNA oligonucleotides that project outwards, partially project inwards, and project inwards. Comparison of bisPNA-AEEA₃ hybridization to DNA oligonucleotides that project outwards, partially project inwards and project inwards. Lane 1, bisPNA-AEEA₃ and ^{32}P -labeled DNA-1_{outward} at 1:1 ratios (150:150 nM). Lane 2, bisPNA-AEEA₃ and ^{32}P -labeled DNA-1_{outward} and unlabeled DNA-2_{outward} at 1:1:33 ratios (150:150:5000 nM). Lane 3, bisPNA-AEEA₃ and ^{32}P -labeled DNA-1_{mid} at 1:1 ratios (150:150 nM). Lane 4, bisPNA-AEEA₃ and ^{32}P -labeled DNA-1_{mid} and unlabeled DNA-2_{mid} at 1:1:33 ratios (150:150:5000 nM). Lane 5, bisPNA-AEEA₃ and ^{32}P -labeled DNA-1_{inward} at 1:1 ratios (150:150 nM). Lane 6, bisPNA-AEEA₃ and ^{32}P -labeled DNA-1_{inward} and unlabeled DNA-2_{inward} at 1:1:33 ratios (150:150:5000 nM).

DNA assembly by bisPNAs connected by spacers of differing lengths

Inefficient assembly of the inward facing DNA oligonucleotides suggested that the first oligonucleotide bound to the bisPNA blocked binding of the second. One solution for overcoming this obstacle was to increase the length of the spacer region between the two PNA strands. In theory, this would position the PNA strands farther apart, making them less susceptible to intramolecular interactions that might block hybridization.

To investigate the effect of changing the spacer region on PNA assembly I compared bisPNAs with one, three or six AEEA linkers (bisPNAs AEEA₁, AEEA₃ and AEEA₆, **see Table 2-4**). Spacer regions also alternated five amino acids (aspartic acid, lysine or phenylalanine) within six AEEA molecules (AEEA₆asp₅, AEEA₆lys₅ or AEEA₆phe₅). Aspartic acid, lysine and phenylalanine were selected based on their varied electrostatic and steric properties, allowing the effects of substantial chemical alteration to be investigated. In all cases I observed hybridization by DNA oligonucleotides that projected outwards (**Figure 2-8a. Comparison of oligonucleotide assembly by bisPNAs that contain spacers with varying numbers of AEEA spacers and amino acids**). Hybridization by bisPNA-AEEA₆lys₅ was the least efficient, suggesting that electrostatic interactions between lysine and DNA may be blocking hybridization of the second DNA strand.

BisPNA hybridization to partially inward projecting DNA oligonucleotides did not occur as readily as to outward projecting DNA oligonucleotides (**Figure 2-8b.**). The DNA oligonucleotides containing a short region projecting inward were assembled by the two bisPNAs with the linker regions containing aspartic acid or phenylalanine (**Figure 2-**

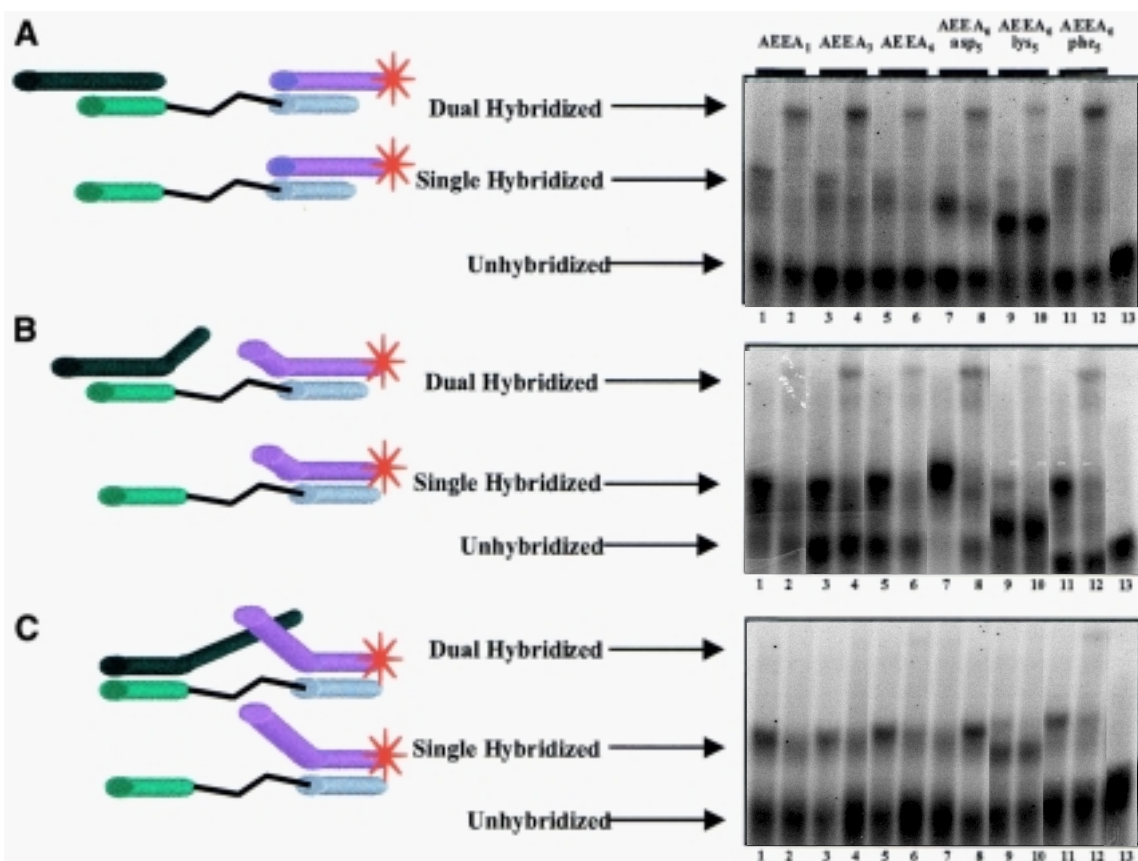


Figure 2-8. Comparison of oligonucleotide assembly by bisPNAs that contain spacers with varying numbers of AEEA spacers and amino acids. The DNA oligonucleotides project outwards, partially inwards and inwards. A.) bisPNA hybridization to DNA oligonucleotides that project outwards. B.) bisPNA hybridization to DNA oligonucleotides that project partially inwards. C.) bisPNA hybridization to DNA oligonucleotides that project inward. Lanes 1 and 2 represent bisPNA-AEEA₁, lane 3 and 4 represent bisPNA-AEEA₃, lanes 5 and 6 represent bisPNA-AEEA₆, lanes 7 and 8 represent bisPNA-AEEA₆asp₅, lanes 9 and 10 represent bisPNA-AEEA₆lys₅ and lanes 11 and 12 represent bisPNA-AEEA₆phe₅. For each hybridization reaction, bisPNA and ³²P-labeled DNA oligonucleotide are at a 1:1 ratio (150:150 nM). Even numbered lanes include an additional 10 equiv. of unlabeled oligonucleotide (1500 nM). Lane 13 is ³²P-labeled DNA oligonucleotide only.

8b, lanes 8 and 12) but not by bisPNA-AEEA₆lys₅ that contained lysine residues (**Figure 2-8b, lanes 2 and 10**). In contrast, DNA oligonucleotides with long regions that projected inward exhibited virtually no assembly by bisPNAs regardless of the length or chemical properties of the linker (**Figure 2-8c.**). These same results were observed under a variety of annealing conditions.

In this study I have focused on making increasingly flexible linkers. It is possible that rigid linkers with defined geometries might be able to hold the two strands of the PNAs far apart and allow more efficient assembly of complex DNA oligonucleotides. Shi and Bergstrom have described the synthesis of such linkers and have used them to bridge two single-stranded DNA oligonucleotides for nanostructure assembly (19).

Reasons for inefficient assembly of oligonucleotides that project inward

One reason for the inefficient assembly of DNA oligonucleotides containing inward overhanging regions is that once the DNA is bound to the complementary PNA strand, the inward facing overhanging region may associate with the second PNA strand through non-Watson–Crick interactions (**Figure 2-9a. Non-specific interactions of bisPNA and DNA oligonucleotides**). Normally such interactions would be weak, but in this case they may be more important because they would be effectively intramolecular. If this type of non-specific association were to occur, it would be reflected in elevated T_m values for the inward facing DNA oligonucleotides relative to DNA oligonucleotides that are direct complements or that contain regions that are outward facing. Support for the belief that non-specific PNA-DNA contacts can be important is provided by Raney and

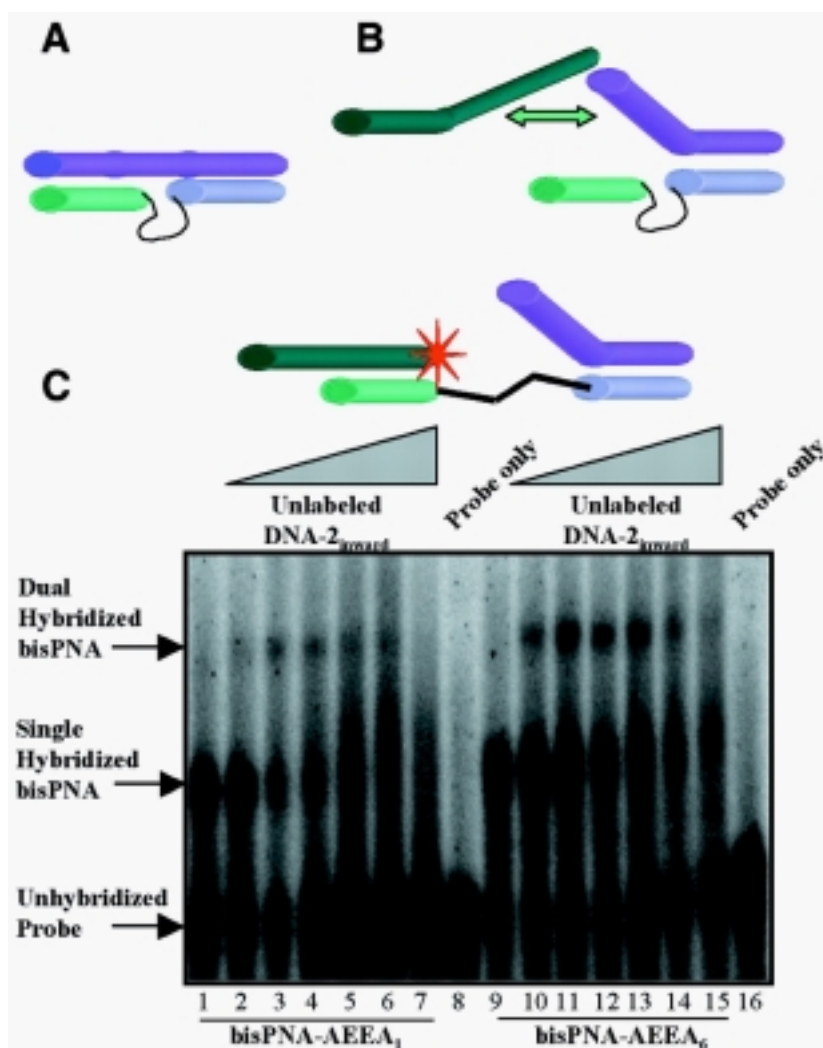


Figure 2-9. Non-specific interactions of bisPNA and DNA oligonucleotides. A.) Interference with dual hybridization by an inward facing oligonucleotide that makes Watson-Crick base pairs with a complementary PNA strand, and forms non-Watson-Crick interactions with the non-complementary PNA strand. B.) Interference with dual hybridization by steric conflicts between two inward facing oligomers. The explanations for the inefficient dual hybridization portrayed in (A) and (B) are not mutually exclusive. C.) Comparison of bisPNA-AEEA₁ (11 Å spacer region) and bisPNA-AEEA₆ (66 Å spacer region) for their ability to hybridize to both an inward projecting and an outward projecting DNA oligonucleotide. Lanes 1–7, bisPNA-AEEA₁ and ³²P-labeled DNA-1_{outward} in 1:1 ratios (150:150 nM). For lanes 2–7, unlabeled DNA-2_{inward} was added in increasing equivalents (relative to bisPNA-AEEA₁): 0.33, 1.66, 3.33, 16.6, 33.3 and 166 equiv. Lane 8 is ³²P-labeled DNA-1_{outward} only. Lanes 9–15, bisPNA-AEEA₆ and ³²P-labeled DNA-1_{outward} in 1:1 ratios (150:150 nM). For lanes 10–15, unlabeled DNA-2_{inward} was added in increasing equivalents (relative to bisPNA-AEEA₆: 0.33, 1.66, 3.33, 16.6, 33.3 and 166 equiv. Lane 16 is ³²P-labeled DNA-1_{outward} only.

co-workers, who noted that PNAs have a high propensity for interactions with single-stranded DNA that promote non-sequence-specific aggregation (20).

DNA oligonucleotides with overhanging regions that projected outwards (DNA-1_{outward} and DNA-2_{outward}) had melting temperatures nearly equal to that of short 12-mer DNA oligonucleotides (**Table 2-2**). However, the DNA oligonucleotides that projected inwards or partially inwards had slightly higher T_m values relative to the exact complement DNA oligonucleotides, increasing by 4.5–6.2°C. These data are consistent with the suggestion that non-Watson-Crick interactions between PNA and DNA oligonucleotides can form and may contribute to the inability of the second DNA oligonucleotide to efficiently bind PNA.

Another explanation for inefficient assembly of DNA oligonucleotides that project inwards is that the two overhanging regions physically interfere with one another and block dual hybridization (**Figure 2-9b.**). If this steric conflict were preventing hybridization, it should be possible for PNAs to assemble a DNA oligonucleotide with an inward projecting region and a DNA strand that is exactly complementary or that contains an overhanging region that projects outward. To test this hypothesis I hybridized both inward projecting and outward projecting DNA oligonucleotides to bisPNA-AEEA₁ or bisPNA-AEEA₆.

In contrast to the inability of two inward projecting oligonucleotides to hybridize simultaneously (**Figure 2-8c.**), I observed that bisPNA-AEEA₁ and bisPNA-AEEA₆ were able to assemble an inward and an outward projecting oligonucleotide (**Figure 2-9c.**). Assembly by bisPNA-AEEA₁ (**Figure 2-9c, lanes 1–7**) was not as efficient as was assembly by bisPNA-AEEA₆ (**Figure 2-9c, lanes 9–15**), suggesting that longer spacers

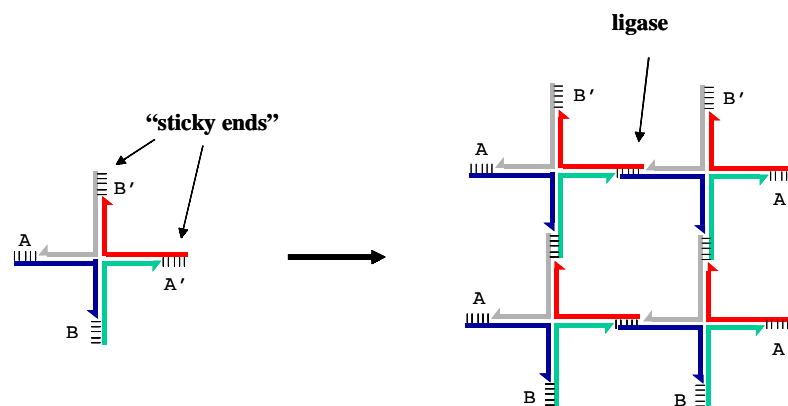
can promote assembly. The finding that an inward and an outward facing DNA can be assembled supports the conclusion that conflicts between overhanging strands were one factor contributing to the lack of dual hybridization by two inward projecting DNA oligonucleotides. It is likely that assembly is complicated by both steric conflicts between the overhanging regions and non-sequence-specific interactions with the second PNA strand.

Applications of bisPNAs for the assembly of DNA structures

PNAs may have many applications in the field of nanotechnology and one of the purposes of this study was to determine the rules guiding use of PNAs for the assembly of DNA structures. There have been recent reports of the use of DNA oligonucleotides to assemble nanostructures, most of which describe systems that could use PNAs as a facilitator for construction. Seeman and co-workers constructed 2- and 3-dimensional DNA arrays based on the DNA branched junction motif and ‘sticky ends’ to ligate individual ‘units’ together (21). BisPNAs could be used similarly, with the tether molecules forming the corners between the PNA:DNA duplexes on either side in a 2-dimensional arrangement. Furthermore, trisPNAs can be synthesized (C.J. Nulf, unpublished results), capable of hybridizing to three DNA oligonucleotides and forming the vertices of a 3-dimensional cube (**Figure 2-10. "DNA motifs" and "bisPNA motifs" for supramolecular oligonucleotide assembly.**)

PNAs could also be used for joining the ends to generate circular oligonucleotides or concatamers. Circular DNA oligonucleotides have unique functions and interesting hybridization properties (22). They have been synthesized by ligating two ends of a linear

“DNA Motif” – fixed Holliday junctions using four DNA oligonucleotides*



“bisPNA Motif” – tethered PNAs hybridized to the ends of DNA oligonucleotides

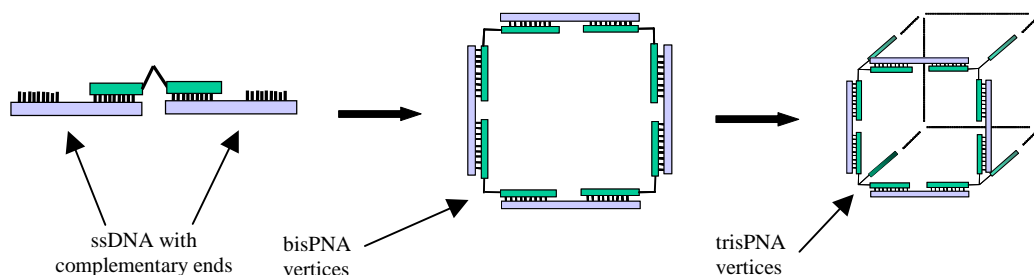


Figure 2-10. DNA motifs and PNA motifs for supramolecular oligonucleotide assembly. The “DNA motif” is four single-stranded oligonucleotides with specificity for one another*. The oligonucleotide sequences are based on fixed Holliday Junction sequences. Complementary “sticky ends” anneal one DNA motif with another, which subsequently can be ligated together for stability. Similar, bisPNAs can assemble two longer single-stranded oligonucleotides facing outwards. Complementary ends of the oligonucleotides can be specific for each other, generating polygonal 2-D arrays. 3-dimensional supramolecular assemblies could be generated if trisPNAs were connecting 3 outward projecting oligonucleotides with complementary ends.

*From: Seeman N.C. (1998) DNA nanotechnology: novel DNA constructions. *Annu. Rev. Biophys. Biomol. Struct.* 27, 225–248.

oligonucleotide after bringing the two ends together with a connecting oligonucleotide (23). The bisPNAs used in our studies could be used to stably join DNA ends without the need for ligation and the resultant circular constructs could be used to build higher order structures.

A third possible application of PNAs in nanotechnology is the development of electrical-sensitive nanoprobe. Recently, Mirkin and co-workers have functionalized gold nanoparticles with DNA oligonucleotides that create conductivity changes associated with target–probe binding events (24). Similarly, Josephson and co-workers have determined by magnetic resonance imaging that monodispersed oligonucleotide-modified magnetic nanoparticles exhibit a decrease in relaxation time of adjacent water molecules when hybridized to a complementary oligonucleotide-modified magnetic nanoparticle (25). The superior hybridization properties of PNAs might make them ideal for these applications, and their neutrality might be useful for the probing and optimization of electrical sensors.

Importantly, all of the applications discussed above involve hybridization to the terminal ends of DNA oligonucleotides, an ability that our studies indicate is possessed by bisPNAs. Other applications, especially those that require assembly within living cells, may be more challenging. PNAs can efficiently invade duplex DNA (14, 15, 16) but the assembly of two duplex DNAs is likely to be complicated because of the problems that I have uncovered with joining inward overhanging sequences.

Another interesting biological application would be the use of PNAs to bridge RNA sequences to alter splicing or expression. This tactic would also require that bisPNAs doubly bind RNA overhanging sequences, but since this hybridization would be

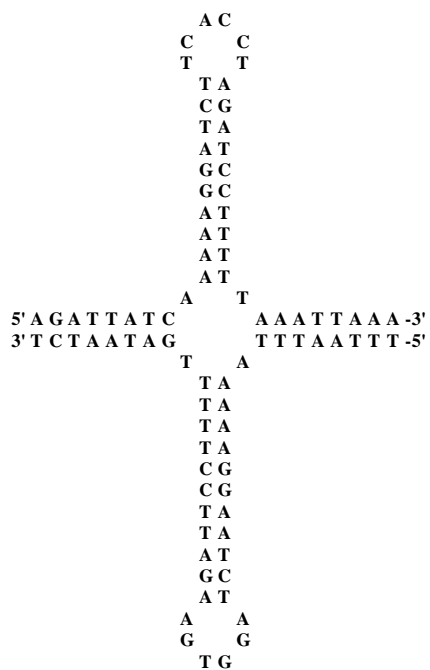
intramolecular (i.e. the PNA strands would bind to different sites on the same RNA), it might occur more readily than the intermolecular assembly attempted in our studies.

BisPNAs strand invasion into duplex DNA

PNAs have demonstrated the ability to strand invade supercoiled plasmid DNA at regions containing inverted repeat sequences that can form hairpin or cruciform structures (26). DNA hairpin structures within conformationally strained supercoiled DNA have been suggested to 'breathe' from duplex regions to single stranded regions (27) making the DNA accessible to PNA targeting. While I could not demonstrate that a single bisPNA could assemble two supercoiled plasmids by strand invading at individual target sites within each plasmid (data not shown), I could demonstrate that each half of the bisPNA strand invades at the intended DNA target site without interference of the other half of the bisPNA.

As a model for bisPNA strand invasion, the DNA sequences I targeted are within cruciform hairpin regions of plasmid pUC19 (**Figure 2-11. Strand-invasion target sites: Cruciform structure of plasmid pUC19**). These two sites were previously shown to be accessible to PNA hybridization so long as the plasmid was supercoiled (28). Strand invasion was demonstrated using a modified T7 sequencing assay (26) (**Figure 2-12. Detection of PNA strand-invasion into supercoiled plasmid DNA: T7 Sequenase Assay**). A hybridizing PNA displaces a looped plasmid DNA sequence (the P-loop) accessible to a DNA sequencing primer under the specific annealing temperature of 25°C (Note: a DNA-peptide conjugate primer was used in these assays to increase the rate of

Target #1
pUC19 (1531-1573)



Target #2
pUC19(2542-2587)

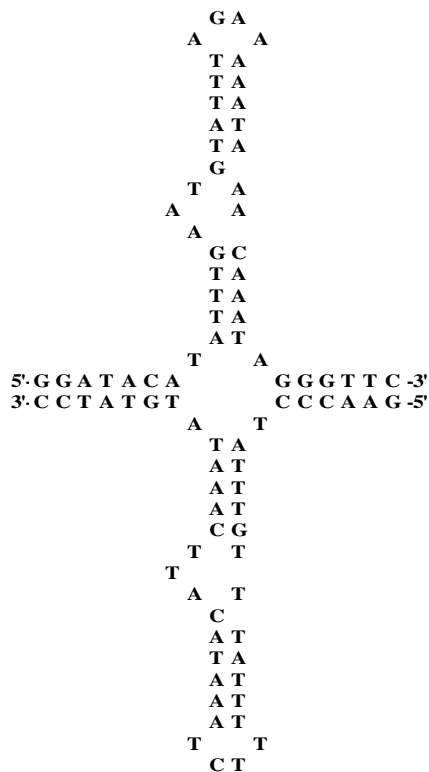
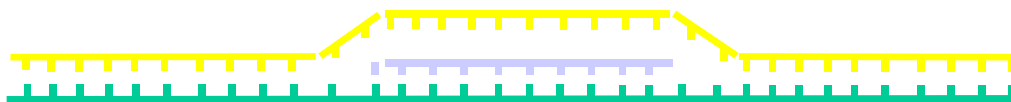
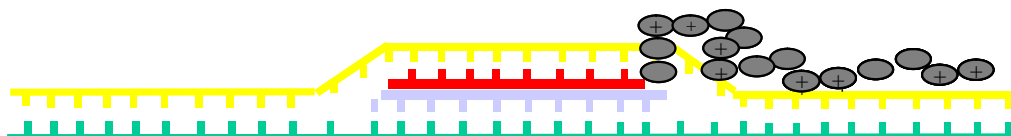


Figure 2-11. Strand-invasion target sites: Cruciform structure of supercoiled pUC19. BisPNAs target the ‘bottom’ of the hairpin, while primer-peptide conjugates are specific for the ‘top’ of the hairpin. Primer-peptide conjugates only anneal to target sequences at 25°C if a bisPNA is hybridized to its target site first.

Step 1. Mix bisPNA and plasmid DNA at 37°C to form bisPNA:plasmid complex (P-loop).

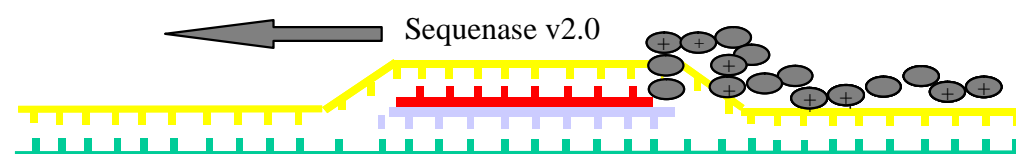


Step 2. Cool bisPNA:plasmid complex to 25°C, a temperature that is not permissive for binding of unaided DNA primer.



Step 3. Add DNA primer to form bisPNA:plasmid:primer complex.

Step 4. Add modified T7 DNA polymerase and elongate primer using sequencing procedure with dNTPs, ^{35}S -ATP, and ddNTPs.



Step 5. Analyze elongation products by denaturing 6% polyacrylamide gel to verify sequence-specificity of PNA strand invasion.

Figure 2-12. Detection of PNA strand-invasion into supercoiled plasmid DNA: T7 Sequenase Assay. Plasmid DNA is represented in green and yellow. Strand invading PNA (or bisPNA) is represented in purple. DNA-peptide conjugate is represented as red. DNA primer-peptide will not anneal to P-loop at 25°C if the PNA is not bound first. Elongation products determine sequence specificity of PNA hybridization while the radioactive intensity (of the sum of all products) determines efficiency of PNA hybridization.

the annealing reaction of the primer). Addition of T7 polymerase and other sequencing reagents (dNTPs, [³⁵S]-dATP, and dideoxynTPs) generates extension products from the annealed DNA sequencing primer which can be resolved by denaturing polyacrylamide gel electrophoresis. The intensity of the radioactive signal (the sum of the elongation products) is directly proportional to the efficiency of PNA hybridization to the hairpin cruciform structure within the supercoiled plasmid. The absence of strand invading PNA does not allow the DNA primer to bind at 25°C, and subsequent polymerase extension products are not observed.

A bisPNA with two different PNA sequences on either sides of the spacer molecule, bisPNA-AEEA₃, revealed sequencing products when two different DNA sequencing primers (in two different reactions) were annealed to plasmid DNA (**Figure 2-13. T7 Sequenase Assay demonstrating strand-invasion of bisPNA-AEEA₃ into dsDNA**). Conditions where no bisPNA was incubated with supercoiled plasmid DNA did not yield sequencing product when the DNA sequencing primer was added at 25°C, a non-permissive temperature for DNA primer hybridization. These efficiency of binding by bisPNA-AEEA₃ is similar to previous results seen with 12-mer PNAs (28). These results suggest that a bisPNA molecule still retains the ability to strand invade supercoiled duplex DNA without interference of the unhybridizing half of the bisPNA. However, the bisPNA has the added capacity to target two different dsDNA strands sequence-specifically.

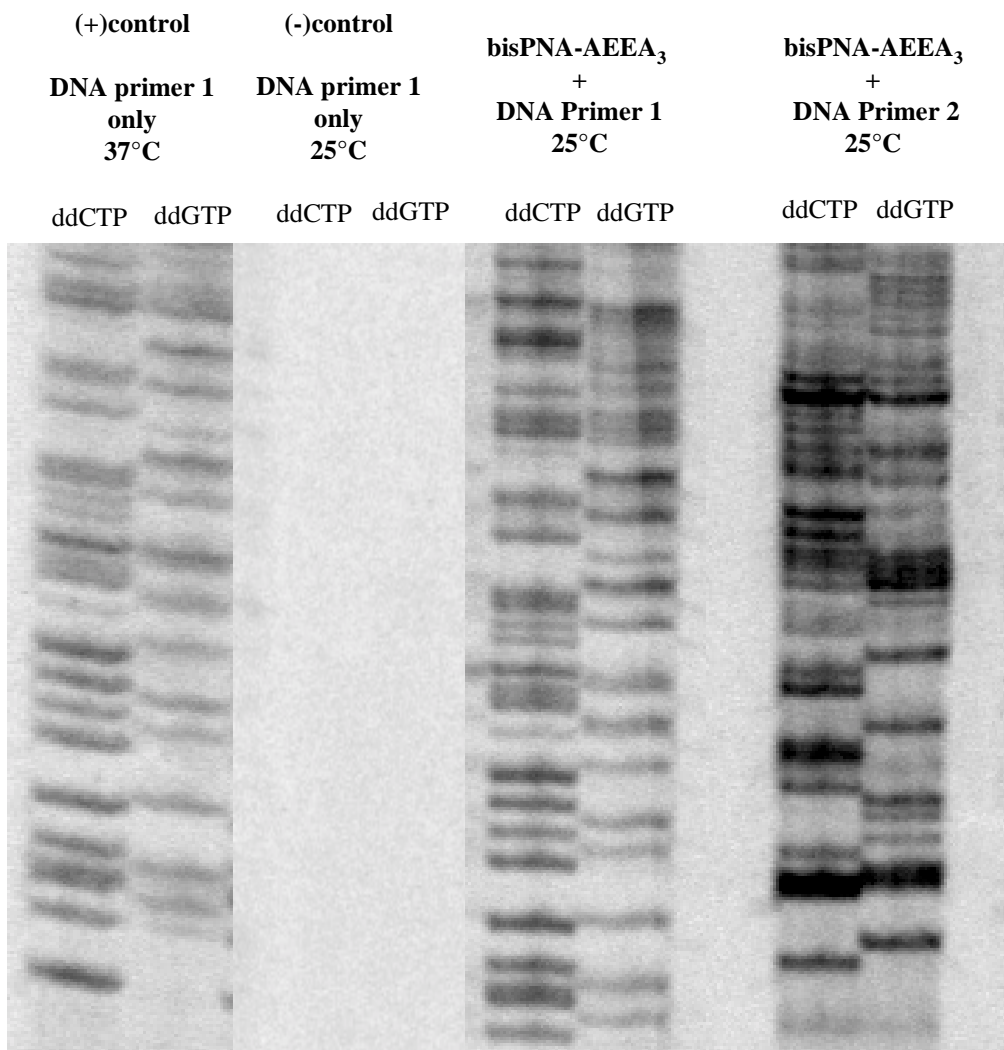


Figure 2-13. T7 Sequenase Assay demonstrating strand-invasion of bisPNA-AEEA₃ into dsDNA. Supercoiled pUC19 was mixed with bisPNA-AEEA₃ at 37°C for 60 minutes. At 25°C, a DNA primer was annealed to the single-stranded P-loop created by the hybridized bisPNA. Sequencing reagents were added (dNTPs, [³⁵S]-dATP, dideoxynTPs) allowing for polymerase extension. Denaturing polyacrylamide gel electrophoresis and autoradiography reveals sequencing products. In the absence of bisPNA hybridization, DNA primers do not anneal to plasmid DNA target at 25°C (the negative control), but will anneal to target at 37°C yielding sequencing products (the positive control). DNA primer 1 and DNA primer 2 are specific for hybridizing to the P-loops created by strand-invasion of the N-terminal half and the C-terminal half of the bisPNA, respectively. DNA primer 2 does not give elongation products if incubated at 25°C to supercoiled pUC19 in the absence of bisPNA hybridization (data not shown). For simplicity, only ddGTP and ddCTP lanes are analyzed.

Uses of bisPNA to strand invade at two individual duplex DNA locations

When targeting duplex DNA within cells, it may be useful to have a single oligomer capable of hybridizing to two different sequences. For example, disease-associated mutated mitochondrial DNA (mtDNA) and wild-type mtDNA co-exist within the same cell. Taylor *et al.* demonstrated that linked-oligonucleotides were able to hybridize simultaneously to two mtDNA sites, bridging a short intervening mtDNA sequence that is only present in mutant mtDNA. Cooperative hybridization increased binding affinity of the linked-oligonucleotides. Furthermore, the bridging oligonucleotides were capable of partially inhibiting replication of the mutant mtDNA *in vitro* (29) **(Figure 2-14. Schematic representation to show how a bridging oligonucleotide can be used to target deleted mtDNA molecules).**

Rogers *et al.* also used bifunctional PNA-DNA conjugates as a strategy to promote site-directed recombination (31). In their experiments a bisPNA was coupled to a 40-nt donor DNA fragment homologous to an adjacent region in the target gene. A strand invading PNA into duplex DNA would localize the DNA fragment next to the plasmid and encourage recombination between the DNA fragment and the plasmid. The PNA-DNA conjugate was found to mediate site-directed recombination with a plasmid substrate in human cell-free extracts, resulting in correction of a mutation in a reporter gene at a frequency at least 60-fold above background (30, 31) **(Figure 2-15. Schematic of a tethered DNA fragment being targeted to chromosomal DNA to encourage recombination).**

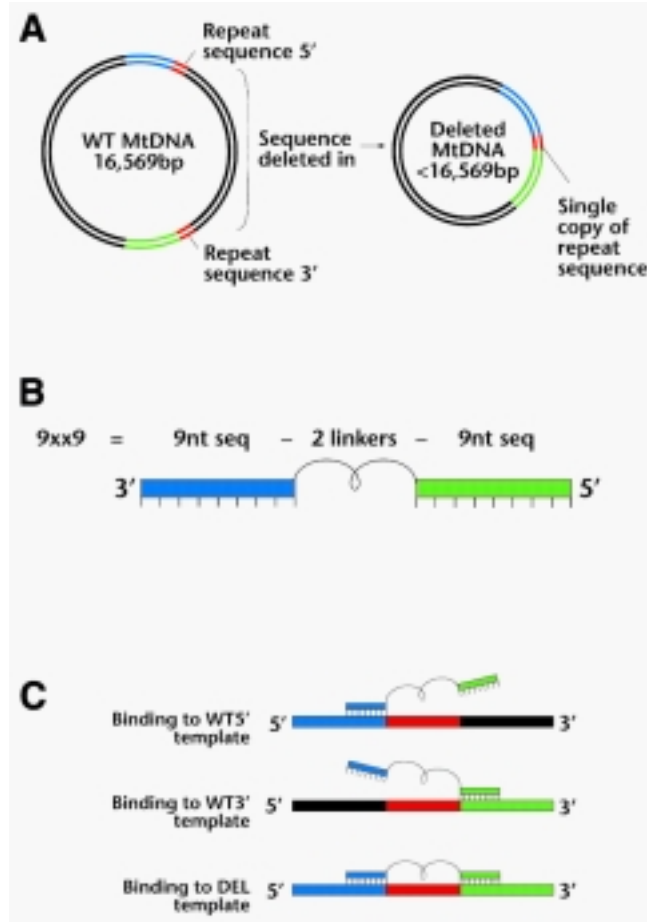


Figure 2-14. Schematic of a bridging oligonucleotide targeting deleted mtDNA molecules. A.) Wild-type mtDNA has many repeated sequences between the two target sites. Mutant (disease-associated) mtDNA has only a single copy of the repeated sequence. B.) The bridging oligomers contain two 9-mers specific for the target sequences on either side of the repeated sequences. The two 9-mers are joined together via two polyoxyethylene linker molecules. C.) Each half of the bridging oligomers can bind to the wild-type templates (WT5' or WT3') individually, but both 9-mer sequences can bind to the mutant deleted template cooperatively. Cooperative hybridization potentially increases the binding affinity of the bridging oligomers for the deleted templates. Consequently, these bridging oligomers will selectively target the deletion breakpoint in the single-stranded mtDNA replication intermediate of the deleted molecule, inhibiting replication.

*From: Taylor R.W., Wardell T.M., Connolly B.A., Turnbull D.M., Lightowlers R.N. (2001) Linked oligodeoxynucleotides show binding cooperativity and can selectively impair replication of deleted mitochondrial DNA templates. *Nucleic Acids Res.* 29(16):3404-12.

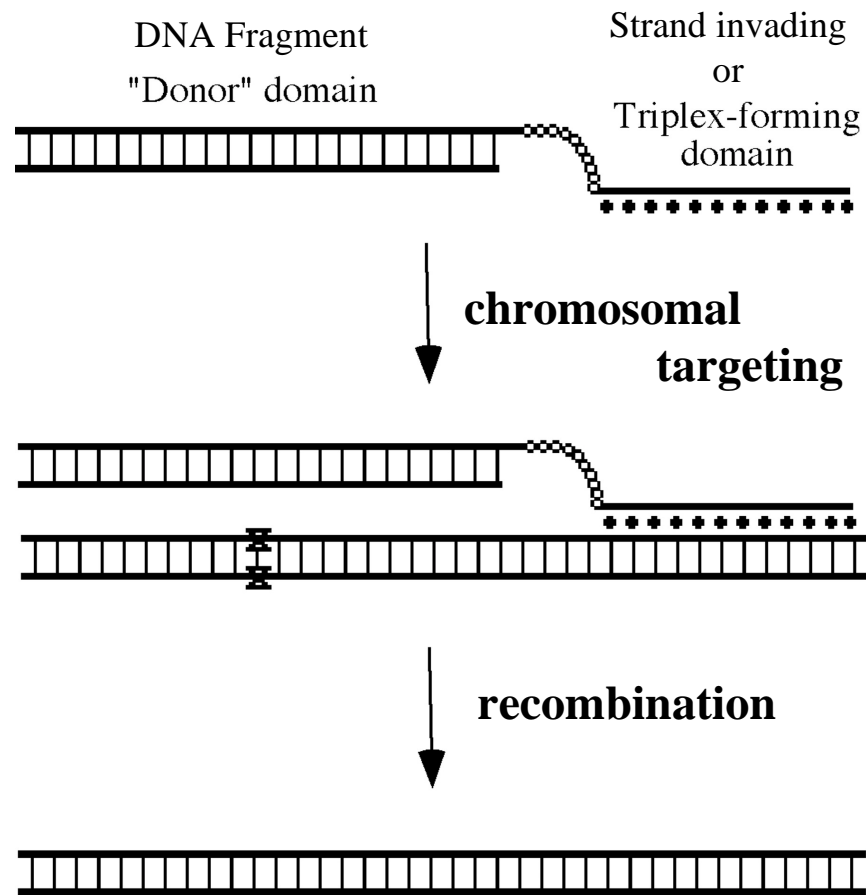


Figure 2-15. Schematic of a tethered DNA fragment being targeted to chromosomal DNA to encourage recombination. One half of the bis-oligonucleotide is complementary for a chromosomal sequence while the other half of the bis-oligonucleotide is tethered to a DNA fragment. X, the base pair to be changed.

*From: Chan P.P., Lin M., Faruqi A.F., Powell J., Seidman M.M., Glazer P.M.(1999) Targeted correction of an episomal gene in mammalian cells by a short DNA fragment tethered to a triplex-forming oligonucleotide. *J. Biol. Chem.* 274(17):11541-8.

Conclusions

I showed here that bisPNAs can be used to assemble DNA oligonucleotides, but that this assembly depends on the relative geometries of the DNAs being assembled. Assembly occurs readily when the DNAs are exactly complementary to the PNA strands or contain overhanging regions that project outwards. Steric conflicts between the DNA oligonucleotides and non-Watson-Crick association between DNA and PNA complicate assembly of DNA oligonucleotides that contain regions that project inwards. Since most applications of DNA for nanostructure assembly use oligonucleotides that project outwards from a central connection, our results indicate that the bisPNAs can be used for nanotechnology applications and that their favorable characteristics may lead to improved assemblies.

I also demonstrated the capacity of the novel bisPNA molecule to strand-invade duplex DNA at two different locations. The bifunctional hybridization ability could be beneficial for new drug therapies targeting disease-associated mutant DNA sequences. Bifunctional oligomers could also increase homologous recombination events for gene therapy applications.

References for Chapter 2

- 1 Feynman R.P. (1961) There is plenty of room at the bottom. In Gilbert H.D. (ed.), *Miniaturization*. Reinhold, New York, NY, pp. 282–296.
- 2 Whitesides G.M., Mathias J.P., Seto C.T. (1991) Molecular self-assembly and nanochemistry: a chemical strategy for the synthesis of nanostructures. *Science*. 254(5036):1312-9.
- 3 Winfree E., Liu F., Wenzler L.A. and Seeman N.C. (1998) Design and self-assembly of two-dimensional DNA crystals. *Nature*. 394, 539–544.
- 4 Niemeyer C.M., Adler M., Gao S. and Chi L.F. (2001) Nanostructured DNA-protein aggregates consisting of covalent oligonucleotide-streptavidin conjugates. *Bioconjugate Chem.* 12, 364–371.
- 5 Wang Y., Boros P., Liu J., Qin L., Bai Y., Bielinska A.U., Kukowska-Latallo J.F., Baker J.R. and Bromberg J.S. (2000) DNA/dendrimer complexes mediate gene transfer into murine cardiac transplants ex vivo. *Mol. Ther.* 2, 602–608.
- 6 Seeman N.C. (1998) DNA nanotechnology: novel DNA constructions. *Annu. Rev. Biophys. Biomol. Struct.* 27, 225–248.
- 7 Seeman N.C. (1998) Nucleic acid nanostructures and topology. *Angew. Chem. Int. Ed.* 37, 3220–3238.
- 8 Seeman N.C. (1999) DNA engineering and its application to nanotechnology. *Trends Biotechnol.* 17, 437–443.

- 9 Niemeyer C.M. (2001) Nanoparticles, proteins and nucleic acids: biotechnology meets materials science. *Angew. Chem. Int. Ed.* 40, 4128–4158.
- 10 Yurke B., Turberfield A.J., Mills A.P. Jr, Simmel F.C., Neumann J.L. (2000) A DNA-fuelled molecular machine made of DNA. *Nature*. 406(6796):605-8.
- 11 Simmel F.C., Yurke B., Sanyal R.J. (2002) Operation kinetics of a DNA-based molecular switch. *J. Nanosci. Nanotechnol.* 2(3-4):383-90.
- 12 Mao C., Sun W., Shen Z., Seeman N.C. (1999) A nanomechanical device based on the B-Z transition of DNA. *Nature*. 397(6715):144-6.
- 13 Zelphati O., Liang X., Hobart P. and Felgner P.L. (1999) Gene chemistry: functionally and conformationally intact fluorescent plasmid DNA. *Hum. Gene Ther.* 10, 15–24.
- 14 Demidov V.V., Kuhn H., Lavrentieva-Smolina I.V. and Frank-Kamenetskii M.D. (2001) Peptide nucleic acid-assisted topological labeling of duplex DNA. *Methods*. 23, 123–131.
- 15 Datta B. and Armitage B.A. (2001) Hybridization of PNA to structured DNA targets: quaduplex invasion and the overhang effect. *J. Am. Chem. Soc.* 123, 9612–9619.
- 16 Demidov V.V., Bukanov N.O. and Frank-Kamenetskii M.D. (2001) Duplex DNA capture. *Curr. Issues Mol. Biol.* 2, 31–35.
- 17 Nielsen P.E. (2001) Peptide nucleic acid: a versatile tool in genetic diagnostics and molecular biology. *Curr. Opin. Biotechnol.* 12, 16–20.

- 18 Hansen G.I., Bentin T., Larsen H.J. and Nielsen P.E. (2001) Structural isomers of bis-PNA bound to a target in duplex DNA. *J. Mol. Biol.* 307, 67–74.
- 19 Shi J.F. and Bergstrom D.E. (1997) Assembly of novel DNA cycles with rigid tetrahedral linkers. *Angew. Chem. Int. Ed.* 36, 111–113.
- 20 Tackett A.J., Corey D.R. and Raney K.D. (2002) Non-Watson–Crick interactions between PNA and DNA inhibit the ATPase activity of bacteriophage T4Dda helicase. *Nucleic Acids Res.* 30, 950–957.
- 21 Qi J., Li X.J., Yang X.P. and Seeman N.C. (1996) Ligation of triangles built from bulged 3-arm DNA branched junctions. *J. Am. Chem. Soc.* 118, 6121–6130.
- 22 Kool E.T. (1996) Circular oligonucleotides—new concepts in oligonucleotide design. *Annu. Rev. Biophys. Biomol. Struct.* 25, 1–28.
- 23 Wang S. and Kool E.T. (1994) Circular RNA oligonucleotides. Synthesis, nucleic acid binding properties and a comparison with circular DNAs. *Nucleic Acids Res.* 22, 2326–2333.
- 24 Park S.J., Taton T.A. and Mirkin C.A. (2002) Array-based electrical detection of DNA with nanoparticle probes. *Science.* 295, 1503–1506.
- 25 Perez J.M., O’Loughin T., Simeone F.J., Weissleder R. and Josephson L. (2002) DNA-based magnetic nanoparticle assembly acts as a magnetic relaxation nanoswitch allowing screening of DNA-cleaving agents. *J. Am. Chem. Soc.* 124, 2856–2857.

- 26 Smulevitch S.V., Simmons C.G., Norton J.C., Wise T.W., Corey D.R. (1996) Enhancement of strand invasion by oligonucleotides through manipulation of backbone charge. *Nat Biotechnol.* 14(13):1700-4.
- 27 Bentin T. and Nielsen P.E. (1996) Enhanced peptide nucleic acid binding to supercoiled DNA: possible implications for DNA "breathing" dynamics. *Biochemistry.* 35, 8863–8869.
- 28 Zhang X., Ishihara T., Corey D.R. (2000) Strand invasion by mixed base PNAs and a PNA-peptide chimera. *Nucleic Acids Res.* 28(17):3332-8.
- 29 Taylor R.W., Wardell T.M., Connolly B.A., Turnbull D.M., Lightowlers R.N. (2001) Linked oligodeoxynucleotides show binding cooperativity and can selectively impair replication of deleted mitochondrial DNA templates. *Nucleic Acids Res.* 29(16):3404-12.
- 30 Chan P.P., Lin M., Faruqi A.F., Powell J., Seidman M.M., Glazer P.M. (1999) Targeted correction of an episomal gene in mammalian cells by a short DNA fragment tethered to a triplex-forming oligonucleotide. *J. Biol. Chem.* 274(17):11541-8.
- 31 Rogers F.A., Vasquez K.M., Egholm M., Glazer P.M. (2002) Site-directed recombination via bifunctional PNA-DNA conjugates. *Proc. Natl. Acad. Sci. U.S.A.* 99(26):16695-700.

**CHAPTER 3 - INTRACELLULAR INHIBITION OF HEPATITIS C VIRUS
(HCV) INTERNAL RIBOSOMAL ENTRY SITE (IRES)-DEPENDENT
TRANSLATION BY PEPTIDE NUCLEIC ACIDS (PNAs) AND
CHIMERIC LOCKED NUCLEIC ACIDS (LNAs)**

	<u>Page</u>
Background and relevance	89
Design of PNAs and chimeric LNAs to target sequences within the HCV IRES	95
Cellular delivery of PNA and chimeric LNA oligonucleotides	100
Fluorescent microscopy of PNAs transfected into CV-1 cells	100
Analysis of lipid-mediated delivery of LNAs by flow cytometry	103
Inhibition of IRES-dependent translation by PNAs	103
Carrier DNA does not appear to influence IRES-dependent translation inhibition by antisense PNAs	108
Effect of PNA length on inhibition of gene expression	110
PNA length and mechanisms of antisense inhibition	111
Inhibition of IRES-dependent translation by chimeric LNAs	113
Factors governing the potencies of anti-IRES PNAs and LNAs	115
IRES Sequences as targets for PNAs and chimeric LNAs	116
Future Directions	118
References for Chapter 3	120

Background and relevance

Currently, there are about 200 million people worldwide who are infected with the Hepatitis C virus (HCV). In the United States, 2.7 million people have chronic hepatitis C (1) and the incidence of new symptomatic infections has been estimated to be 25,000/year (2). There is no vaccine available and recombinant interferon-alpha (rIFN- α) as a therapeutic treatment is effective in only a portion of the infected population (3). Lack of an adequate animal model and difficulty in generating virions from a tissue culture system has limited studies involving the molecular biology of HCV (4).

HCV has a positive, single-stranded RNA genome consisting of roughly 9600 nucleotides (5) (**Figure 3-1. Lifecycle of HCV**). The genome has highly conserved 5'- and 3'-noncoding regions and an open reading frame coding for a polyprotein of approximately 3000 amino acids. The polyprotein is co- and post-translationally cleaved into multiple viral proteins by both host and viral proteases. These viral proteins make up both the structural proteins necessary for virion formation and the non-structural proteins necessary for viral genome translation and replication.

The antiviral response of an HCV infected host cell is to shut down global 7^mG-cap-dependent translation (6). HCV evades this immune response by using an internal ribosomal entry site (IRES) within the 5'-UTR. (7, 8) (**Figure. 3-2 The RNA secondary structure of the HCV 5'UTR/IRES**). IRES' form a well-defined and highly conserved RNA structure adjacent to AUG start sites and recruit host ribosomal subunits for cap-independent translation (9, 10). HCV IRES binds eIF-3 and 40S ribosomal subunits in the absence of other cellular factors (11, 12) and deletion and point mutations within the

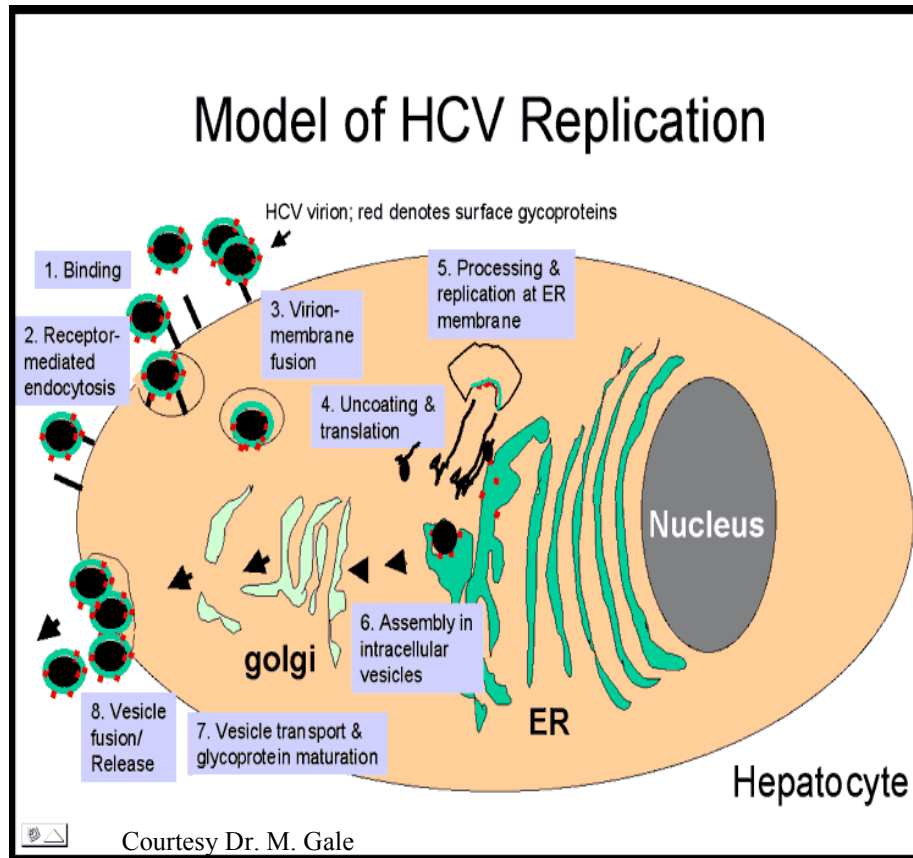


Figure 3-1. Lifecycle of HCV. Upon infection, the HCV genome is released into the cytosol. Translation and replication occurs in the cytosol without the genome entering the nucleus. The genome is a positive-stranded (+) RNA molecule approximately 9.6kb. Codes for a single polypeptide of approximately 3000 amino acids, which is subsequently cleaved by viral and host proteases. There is no 7mG cap. The 5'UTR (approx. 340 nt.) contains a highly conserved tertiary structure important for viral translation called the Internal Ribosomal Entry Site (IRES).

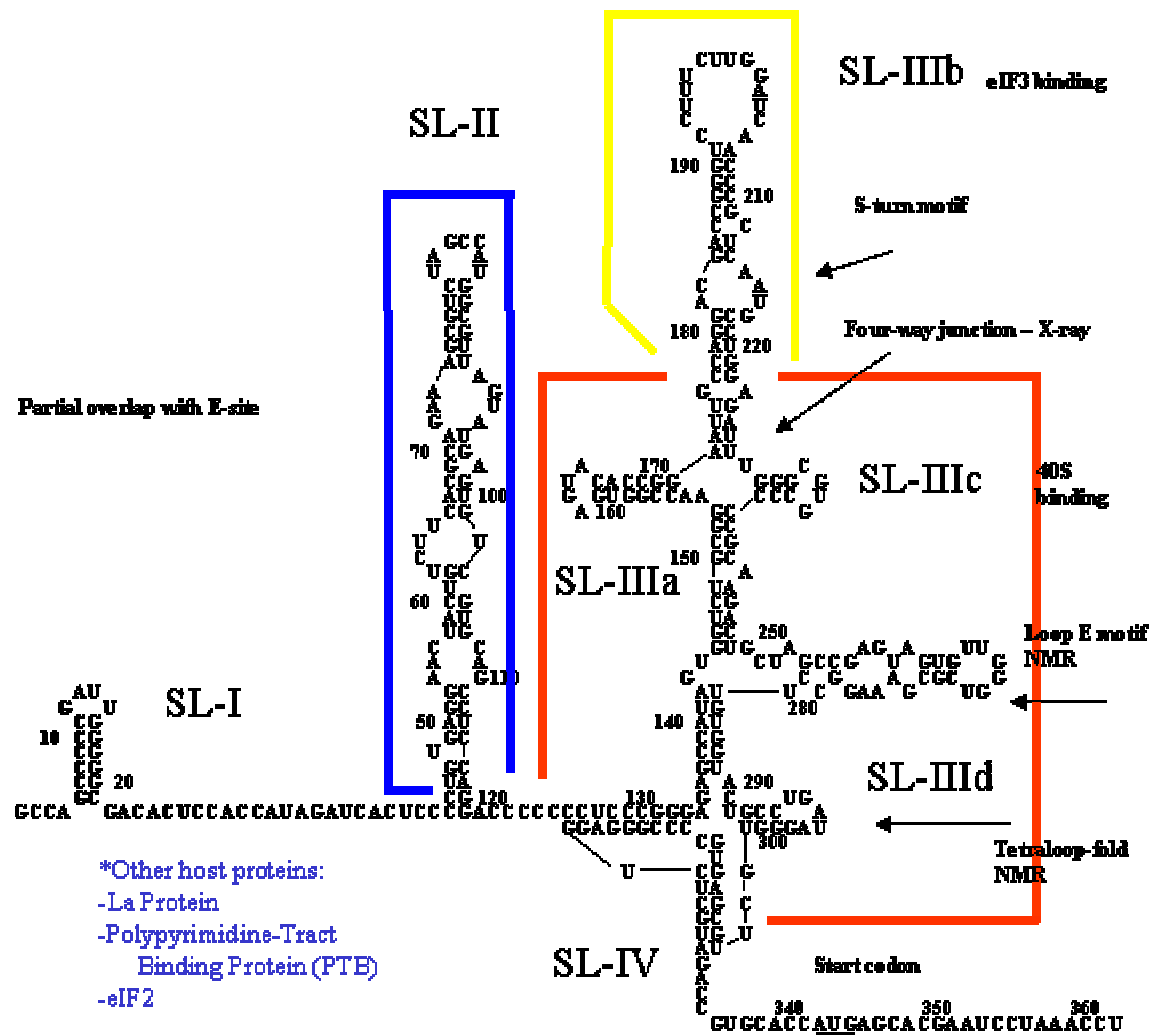
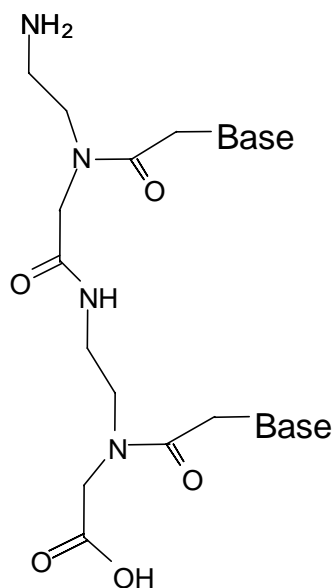


Figure 3-2. The RNA secondary structure of the HCV 5'UTR/TRES. The highly conserved sequence recruits a minimal number of translation factors to initiate translation (7mG-Cap-independent translation). Point mutations and deletion mutations that distort the tertiary structure cause decreases in translation efficiency from the AUG start site (nt. 342). NMR and x-ray crystallographic studies have identified RNA regions that bind the 40S ribosomal subunit, eIF3, and other host factors necessary for translation initiation. Other interesting RNA structures include a ion-dependent dynamic 4-way junction and pseudoknot motif.

*From: Samow P. (2003) Viral internal ribosome entry site elements: novel ribosome-RNA complexes and roles in viral pathogenesis. *J. Virol.* 77(5):2801-6.

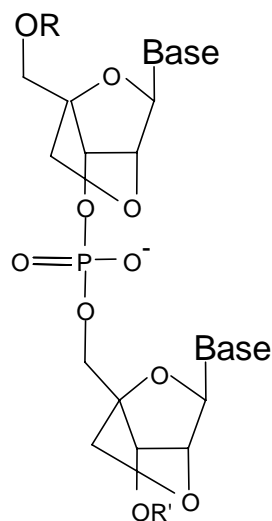
HCV IRES cause substantial decreases in viral translation (13). The importance of the IRES for translation of HCV suggests that it may be an excellent target for oligonucleotide-based therapeutics (14, 15, 16, 17, 18). However, to be active, oligonucleotides must demonstrate an ability to invade structured RNA and block protein binding.

Although HCV is an RNA virus that mutates its genome under selective pressure, the 5'-UTR/IRES sequence is highly conserved relative to the coding region of the genome (19, 20, 21). Therefore, several studies have investigated use of antisense oligonucleotides to target the HCV IRES. Hanecak and colleagues reported that oligonucleotides with phosphorothioate and 2'-modifications could inhibit HCV IRES-dependent translation (22). More recently, cationic phosphoramidate α -oligonucleotides were also shown to be effective (23). In cell free studies, Toulme and colleagues have demonstrated that antisense oligonucleotides compete for binding with the 40S ribosomal subunit (24), and Jang and colleagues have used antisense oligonucleotides to help identify other proteins involved in IRES recognition (25). I hypothesized that oligonucleotides capable of enhanced recognition of sequences embedded within nucleic acid structure might be superior agents for IRES recognition. Two such agents are peptide nucleic acids (PNAs) (26) and locked nucleic acids (LNAs) (27, 28) (**Figure 3-3. Comparisons of PNAs and LNAs**).



Peptide Nucleic Acid (PNA)

2-aminoethyl glycine backbone
 Fmoc-based chemistries (compatible with
 peptide synthesis)
 Charge neutral
 Increased nuclease resistance
 Increased affinity
 Strand-invasion of duplex nucleic acids



Locked Nucleic Acid (LNA)

Phosphodiester backbone
 Phosphoramidate chemistries (compatible
 with DNA/RNA synthesis)
 2'-O-4' methylene bridge fixes 3'-endo
 conformation of the furanose ring
 Increased nuclease resistance
 High affinity for target

Figure 3-3. Comparisons of PNAs with LNAs. Chimeric LNAs were obtained from Proligo LLC.

PNAs can be effective antisense agents inside cultured mammalian cells (29, 30) but the ability of PNA to invade highly structured RNA sequences inside cells has not been well established. The previous reports by Doyle (29) and Braasch (31, 32) outlined a simple method for delivering PNAs into cells by first annealing the PNA to a ‘carrier’ DNA oligonucleotide and then incubating the PNA:DNA duplex with a commercially available cationic lipid. Some basic ‘rules’ for maximal efficiency of PNA translation inhibition were described (see **figure 1-13. Lipid-mediated cellular delivery of PNAs**).

Locked nucleic acid (LNA) bases contain a bridging methylene carbon between the 2' and 4' positions of the ribose ring, fixing the sugar into the 3'-endo conformation (27, 28, 32). This constraint “preorganizes” the oligonucleotide backbone and can increase T_m values by as much as 10°C per LNA base substitution (33). LNA bases are introduced by standard DNA/RNA synthesis protocols, allowing the binding properties of chimeric oligonucleotides to be “fine-tuned” for recognition of specific targets. LNAs are resistant to cellular nucleases (34) but do not activate RNase H (34). However, chimeric LNA-DNA “gapmers” containing a stretch of at least seven DNA bases can recruit RNase H for degradation of targeted RNA transcripts (35). LNAs have been demonstrated to be active antisense agents inside cultured mammalian cells (32, 36, 37) and can also block the association of HIV TAT protein with its RNA target TAR (38). Like PNAs, limited information is available on the ability of LNAs to target RNA secondary structure in cells.

Here I show that PNA and chimeric LNA oligonucleotides that are complementary to HCV IRES can inhibit IRES-dependent gene expression inside cells.

Design of PNAs and chimeric LNAs to target sequences within the HCV IRES

I synthesized PNA and obtained chimeric LNA oligonucleotides (**Tables 3-1 and 3-2**) to test the hypothesis that chemically modified oligonucleotides could be effective inhibitors of IRES-mediated gene expression inside cells. The IRES sequence controlling expression of HCV was chosen as a target because it has been well characterized and because inhibitory oligonucleotides could become lead compounds for therapeutic development (**18**).

The binding of PNAs to RNA inside cells does not cause degradation of RNA because PNA:RNA hybrids are not substrates for RNase H (**39**). To allow direct comparison of the inhibitory effects of LNAs and PNAs, the chimeric LNAs used in these studies (with the exception of L9) were mixtures of LNA and DNA bases and were designed to have three or fewer consecutive DNA bases. Such designs have been demonstrated to have little or no ability to recruit RNase H upon binding to RNA (**35**). The exception, L9, contained seven contiguous bases and would be expected to activate RNase H (**35**). L9 was targeted to the coding region of reporter luciferase mRNA and had previously been shown to be a potent inhibitor of expression (**32**). Each of the PNAs and chimeric LNAs was 17 nucleotides in length (unless otherwise stated). Also, each PNA was synthesized with a single lysine residue at the C-terminus giving an additional positive charge (of the ϵ -amine) at physiological pH. The chimeric LNAs are of the same sequences as the PNAs.

Name	Sequence (N- to C-termini)	Mass Expected/Found	T _m °C	Target IRES sequence
P1	GAGTGATCTATGGTGGGA	4868 / 4871	78.1	26-42
P2	ACGCCATGGCTAGACGC	4743 / 4748	80.1	75-91
P3	GTTGATCCAAGAAAGGA	4830 / 4827	73.7	191-207
P3-19	GTTGATCCAAGAAAGGACC	5332 / 5335	82.5	191-209
P3-21	GTTGATCCAAGAAAGGACCCG	5876 / 5879	87.9	191-211
P4	GCGGGGGCACGCCAAA	4793 / 4795	88.6	226-242
P5	TTTCGCGACCCAACACT	4653 / 4650	80.8	260-276
P5-scrambled	CATCATCGATCCTAGCC	4653 / 4650	73.7	control
P5-sense	AGTGTTGGGTCGCGAAA	4853 / 4826	80.1	control
P6-15	ACGAGACCTCCCGGG	4201 / 4202	83.3	315-329
P6	TACGAGACCTCCCGGGG	4759 / 4764	85.1	314-330
P6-19	CTACGAGACCTCCCGGGGC	5261 / 5261	87.9	313-331
P6-21	TCTACGAGACCTCCCGGGGCA	5803 / 5800	90.0	312-332
P7	GTGCTCATGGTGCACGG	4805 / 4810	83.0	333-349
P8	TGTCGTTGCGGGGCGCA	4781 / 4780	90.0	F-luc

Table 3-1. PNA sequences, expected and found masses, T_m s, and location of target. PNAs are listed from N- to C- termini. All PNAs contain a C-terminal lysine. T_m values are for hybridization to exactly complementary sequences. F-luc: a sequence within the coding region for Firefly luciferase.

Name	Sequence (5' → 3')	T_m °C	Target IRES Sequences
L3	GTTGATCCAAGAAAGGA	75.3	191-207
L4	GCGGGGGCACGCCAAA	91.6	226-242
L8-sense	AGTGTTGGGTCGCGAAA	82.8	control
L6	TACGAGACCTCCCGGGG	91.8	314-330
L7	GTGCTCATGGTGCACGG	82.6	333-349
L9*	GTCGTTGCGGGCGC	81.0	coding region

Table 3-2. Chimeric LNA sequences, T_m s, and target HCV IRES sequences. Bases in bold are LNA while unbolded bases are DNA. T_m data is from chimeric LNA:DNA duplex formation. Chimeric LNA L9 targets the coding region of Firefly luciferase and can activate RNase H.

Chimeric LNAs and PNAs were designed to be complementary to sites that had been identified to form critical interactions with proteins during translation (**Figure 3-4. PNA and Chimeric LNA target sites within the HCV 5'UTR/IRES**). PNA P1 is complementary to a sequence involved in long-range RNA-RNA interactions within the HCV IRES core (nucleotides 428-442) (**40, 41**). PNA P2 targets a single stranded apical domain previously determined to be important for IRES-mediated translation (**8**). PNA P3 and chimeric LNA L3 are complementary to the single-stranded apical domain of SL-IIIb which is known to bind p120, a subunit of eIF3 (**12, 42**). PNA P4 and chimeric LNA L4 were designed to bind to the partially single-stranded region surrounding the SL-IIIabc four-way junction and disrupt the ion-dependent tertiary folding necessary to bind eIF3 (**43**). PNA P5 targets SL-IIId, covering RNA bases G266, G267, G268 which are believed to come in contact with the 40S ribosomal subunit (**44**). PNA P6 and chimeric LNA L6 are specific for a conserved RNA pseudoknot (**45**). PNA P7 and chimeric LNA L7 target the AUG translation start site downstream from the IRES and is adjacent to the target site of a phosphorothioate oligonucleotide that is currently being tested in Phase II clinical trials for the treatment of HCV (**46**). PNA P8 and chimeric LNA L9 target a sequence within the coding region of Firefly luciferase. PNA P5-sense and chimeric LNA L8-sense are sense strand oligonucleotides and are used as negative controls.

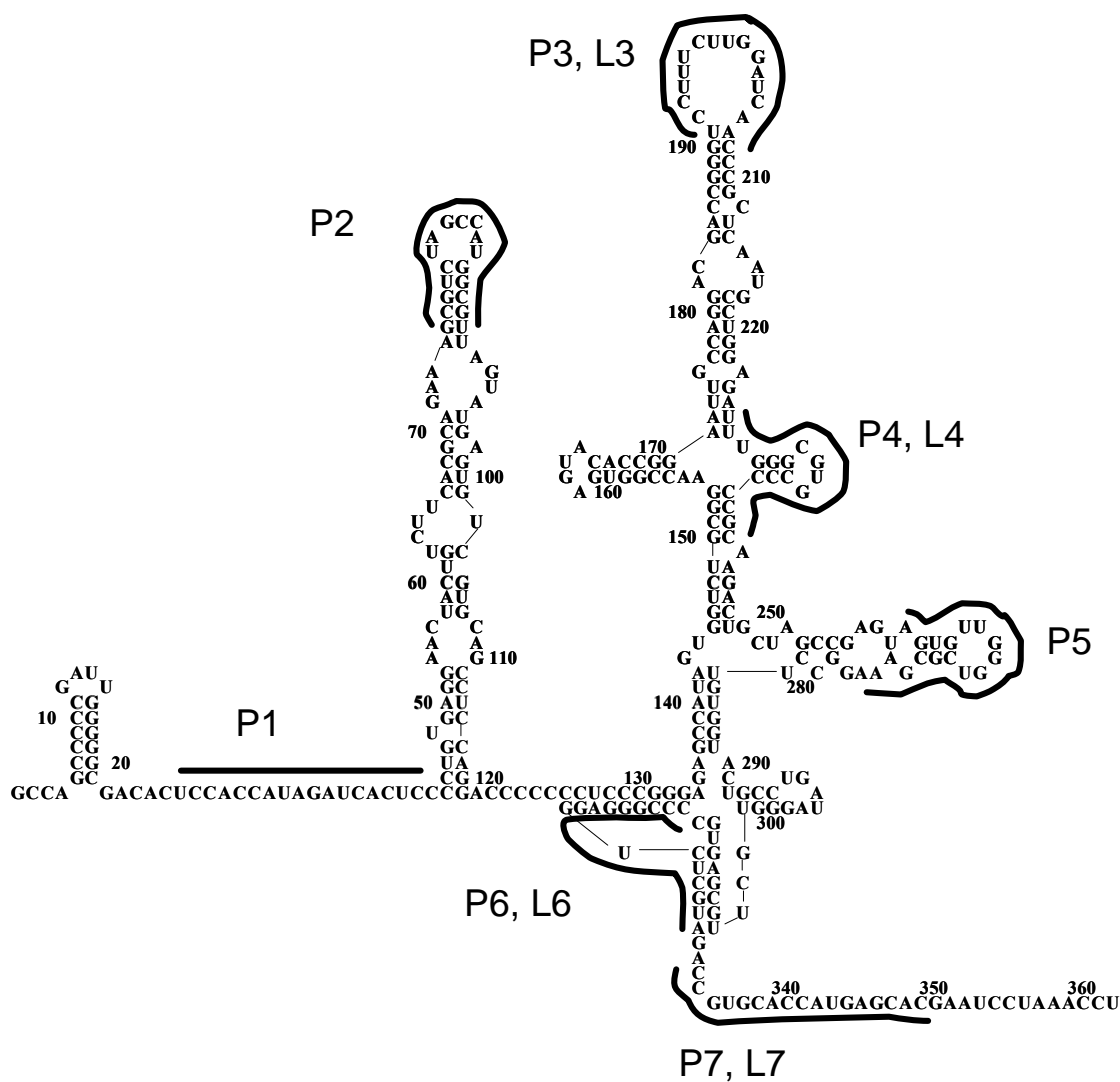


Figure 3-4. PNA and chimeric LNA target sites within the HCV 5'UTR/IRES. The dark lines represent PNA and chimeric LNA binding sites. Control PNAs include P5-sc (a scrambled PNA), P5-sense (a sense-strand PNA, complementary to P5) and P8 (targeting downstream of the AUG start site within the coding region of Firefly luciferase). Control chimeric LNAs include L8-sense (a sense-strand LNA) and L9 (RNase H activating "gapmer" targeting the coding region of Firefly luciferase).

Cellular delivery of PNA and chimeric LNA oligonucleotides

PNAs have an uncharged backbone and cannot be delivered into cells by standard lipid-mediated transfection protocols. To facilitate the efficient uptake of PNAs by cultured cells I annealed PNAs to ‘carrier’ DNA oligonucleotides and mixed the PNA:DNA duplex with a cationic lipid (**29, 30**) (see **figure 1-13**). The lipid binds to the anionic carrier DNA and allows it to associate with the cell membrane for uptake. The hybridized antisense PNA is then transported into the cell as cargo. Once the PNA:DNA duplex inside the cell it is believed that nucleases destroy the carrier DNA allowing the PNA to search for complementary RNA transcripts. Chimeric LNA oligonucleotides have a negatively charged phosphodiester backbone and were delivered into cells using standard lipid-mediated transfection protocols. The same amount of lipid was used for both PNA:DNA solutions and chimeric LNA solutions (i.e. lipid:charged oligonucleotide ratios were the same).

Fluorescent microscopy of PNAs transfected into CV-1 cells

To be active, antisense PNAs must efficiently enter the cytoplasm of cells. Previously, others in the lab had used fluorescence microscopy to indicate that PNAs delivered as PNA:DNA:Lipid complexes diffused throughout the entire cell (**29**). However, these experiments employed fixed cells, a technique that has since been shown to give inaccurate results (**47**). To remedy this, I performed confocal fluorescent microscopy on live unfixed CV-1 cells that had been transfected with PNA-Cy3:DNA:LipofectAMINE complexes. I found a punctate distribution of PNA-Cy3 throughout the cytosol with very little PNA-Cy3 fluorescence in the nucleus

(counterstained with Hoechst) (**Figure 3-5. Confocal fluorescence microscopy of live cells, Panel B**). Several recent reports of intracellular distribution of fluorescently labeled oligonucleotides in live cells have described a similar punctate staining pattern within the cytosol (48).

The cytosolic compartments are presumed to be endosomes filled with PNA-Cy3 taken up from the extracellular milieu which later fuse with lysosomes. To determine if transfected PNAs traffic to lysosomal compartments, a lysosomal-specific counterstain (LysoTracker, specific for vesicles with low pH) was added to the cells just prior to imaging. At a 24-hour time point post-transfection some of the PNA-filled endosomes co-localized with lysosomes while others remained as separate entities (**Figure 3-5. Confocal fluorescence microscopy of live cells, Panels C and D**). Transfection of PNA Cy3:DNA:lipid did not result in a diffuse cytoplasmic distribution of PNA Cy3 at earlier time points (2 hours) suggesting that the cationic lipid does not fuse with the cell membrane releasing the PNA:DNA into the cytosol, but rather is taken up into endosomes as a PNA:DNA:lipid complex (data not shown). The endosomal compartmentalization is not a function of either the Cy3 fluorophore or the PNA oligomer because other fluorophore-PNA conjugates demonstrate the same punctate cellular distribution, as does a transfected LNA-Cy3 oligonucleotide (data not shown) (32). Also, PNA cellular distribution is not a function of the cell line since HeLa, HepG2 (liver carcinoma), and RCF-26 (Huh-7-derivative, liver carcinoma) also give the same results (data not shown).

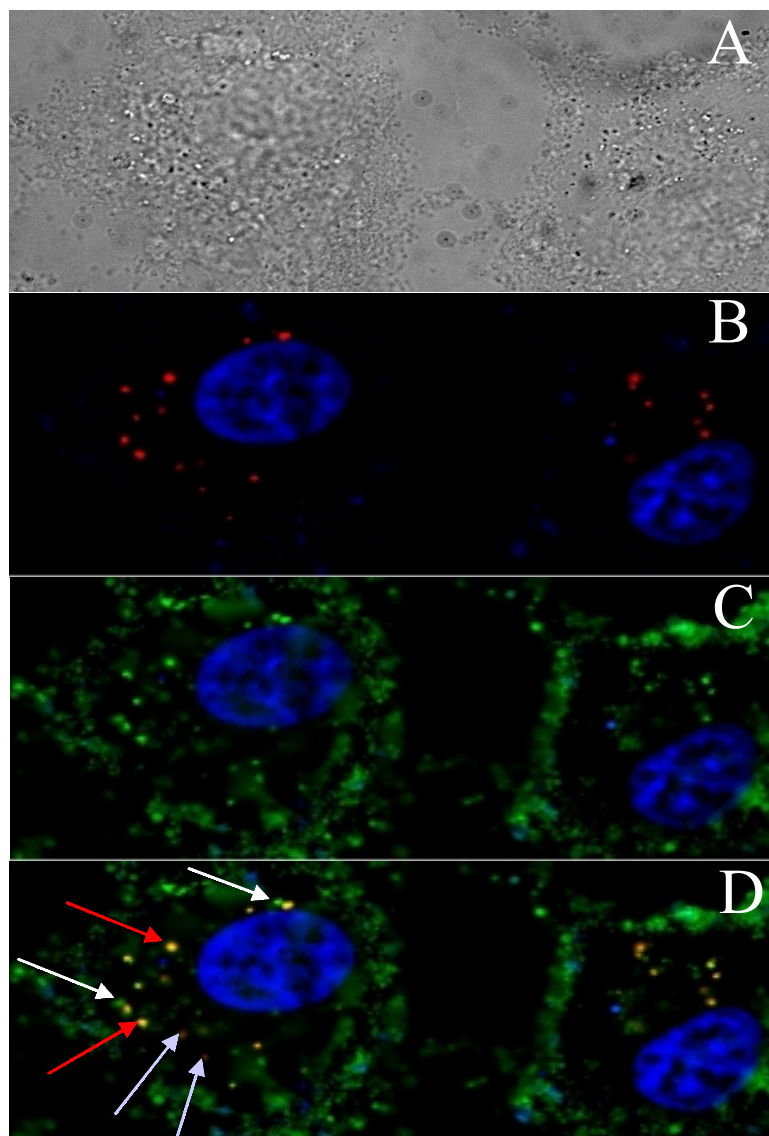


Figure 3-5. Confocal fluorescence microscopy of live cells. CV-1 cells were transfected with 200nM PNA Cy3:DNA:Lipid and imaged at a 24 hour time-point. Thirty minutes prior to imaging, cells were counterstained with Hoechst and LysoTracker and washed 3 times with OptiMEM. Images have been deconvoluted with Slidebook 4.0 imaging software. (A) Differential interference contrast (DIC) image (B) Fluorescent image using UV filter and Cy3 filter (C) Fluorescent image using the UV and FITC filter (D) Overlay of panels B and C. Images were deconvoluted with Slidebook 4.0 software. Purple arrows point to vesicles with PNA-Cy3. White arrows point to lysosomes (low pH vesicles). Red arrows point to co-localization of lysosomes and PNA-Cy3.

It is important to note that data obtained from fluorescence microscopy is subject to interpretation and that alternative scientific techniques should be used to corroborate the findings. Additional experiments are currently being explored.

Analysis of lipid-mediated delivery of LNAs by flow cytometry

Chimeric LNAs have a negatively charged backbone, thus can be delivered intracellularly with a cationic lipid without the need of a carrier DNA. By FACS analysis, lipid-mediated transfections of LNAs showed high efficiencies of cellular delivery (**Figure 3-6. FACS analysis of lipid-mediated transfection of LNA-Cy3 into CV-1 cells**). Also, like other oligonucleotides, LNAs do not readily cross cellular membranes without the assistance of a transfection agent.

Consistent with previous results (**56, 57**), flow cytometry indicated that fluorophore-labeled PNA and LNA oligomers were entering greater than 80% of cells.

Inhibition of IRES-dependent translation by PNAs

To investigate recognition of HCV IRES by PNAs, I introduced several PNAs into CV-1 (monkey kidney) cells. CV-1 cells were used because these cells were previously determined to be easily to transfect with PNA:DNA:lipid complexes and vectors (**29**). Several hours later, I introduced the bicistronic transcript expressing plasmid, pRL-HL (**49**) (**Figure 3-7. The HCV Bicistronic Expression Vector**). This plasmid encodes both Renilla luciferase (the internal control gene) and Firefly luciferase (the experimental gene) within a single mRNA transcript driven by a CMV promoter. Translation of Renilla luciferase occurs using a 7^mG-Cap-dependent process and should

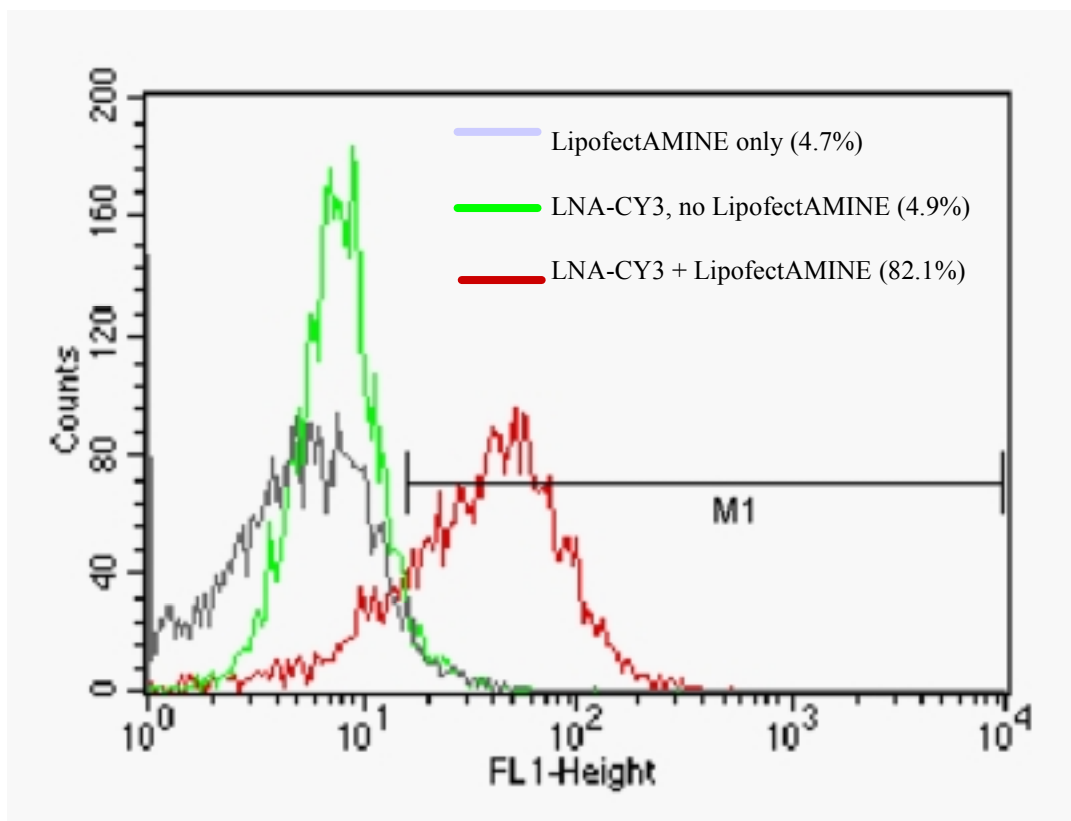


Figure 3-6. FACS analysis of lipid-mediated transfection of LNA-Cy3 into CV-1 cells. The protocol followed is exactly the same as for lipid-mediated transfection of PNA, but without the carrier DNA.

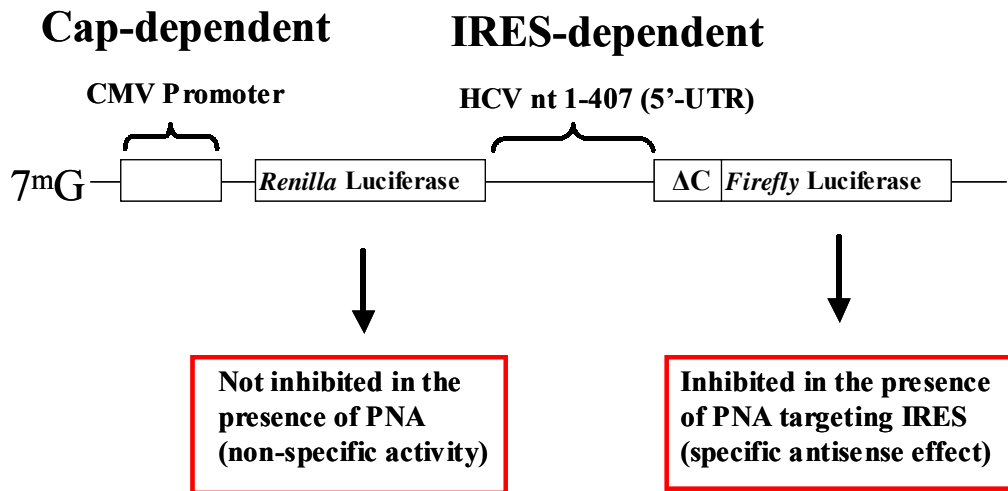


Figure 3-7. The HCV Bicistronic Expression Vector. This plasmid expresses a single bicistronic mRNA transcript. The HCV IRES sequence (nt 1-407) is positioned in between Renilla luciferase and Firefly luciferase. The mRNA can be translated by two different mechanisms. In a cap-dependent fashion Renilla luciferase is expressed (internal control). In an IRES-dependent fashion, Firefly luciferase is expressed. Antisense PNAs and chimeric LNAs targeting the HCV-IRES should inhibit expression of Firefly luciferase without inhibiting Renilla luciferase expression.

*From: Honda M., Kaneko S., Matsushita E., Kobayashi K., Abell G.A., Lemon S.M. (2000) Cell cycle regulation of hepatitis C virus internal ribosomal entry site-directed translation. *Gastroenterology*. 118(1):152-62.

not be affected by addition of antisense PNA. By contrast, translation of Firefly luciferase is under control of the HCV IRES. Firefly luciferase activity should be inhibited if the PNAs bound to their IRES target sequences and if binding is adequate to block protein association or distort RNA secondary structure.

Transfection procedures can reduce gene expression relative to untreated controls regardless of the complementarity of an oligomer for its target because oligomer:lipid complexes can cause cell population growth rates to decrease. This is especially true at higher concentrations of lipid and oligomer. To control for this non-selective inhibition, data was determined as the Firefly luciferase activities relative to Renilla luciferase activities, normalized to cells treated with lipid only (% Relative Firefly luciferase activity.)

I observed varying levels of dose-dependent inhibition of Firefly luciferase by PNAs P2 - P7 (**Figure 3-8. Antisense PNAs targeting the HCV IRES inhibit relative luciferase activities**). PNA P1 did not demonstrate inhibition of translation since the RNA-RNA interaction in which this region is involved is not present in the pRL-HL bicistronic transcript. Most importantly, negative control PNA P5-sense (a sense-strand PNA complementary to PNA P5) does not demonstrate inhibition of IRES-dependent translation. Therefore, the inhibition of translation is not due to a cellular response of the PNA:DNA:lipid transfection. Moreover, the carrier DNA for PNA P5-sense is complementary to the HCV IRES and could potentially cause sequence-specific translation inhibition. Lack of translation inhibition by this control PNA means that the carrier DNA oligonucleotides used for lipid-mediated transfections of PNAs is not the

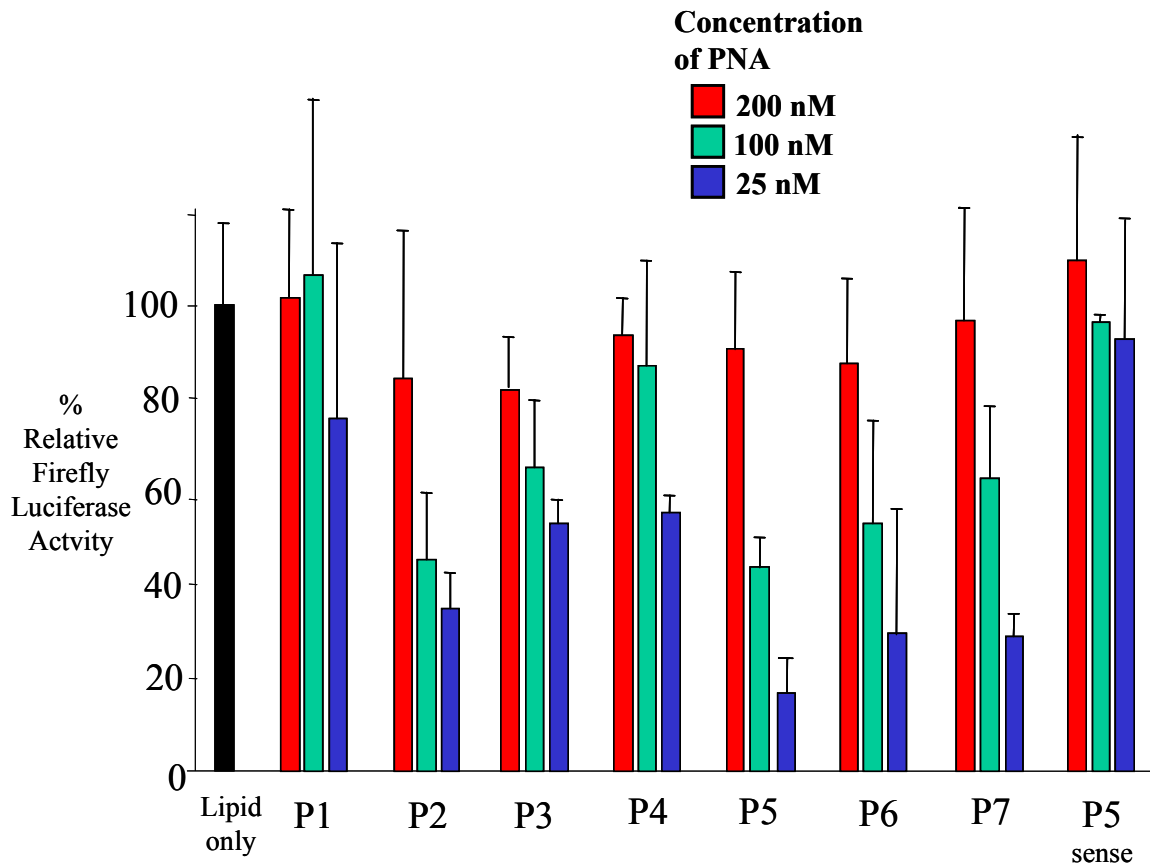


Figure 3-8. Antisense PNAs Targeting the HCV IRES inhibit relative luciferase activity. Varying degrees of translation inhibition is seen for each antisense PNA (P1-P7). Negative control P5-sense (complementary to P5) does not inhibit translation, suggesting that neither the PNA chemistry nor the carrier DNA is responsible for translation inhibition of Firefly luciferase. The % Relative Firefly Luciferase Activity is the ratio of Firefly:Renilla expression, normalized to lipid only control. Data is derived from at least three experiments.

cause of IRES-dependent translation inhibition. Similarly, negative control PNA P5-sc (scrambled) also did not inhibit relative Firefly luciferase activity (data not shown). These results suggest that the HCV IRES is susceptible to binding by antisense PNAs at a wide range of target sequences.

Carrier DNA does not appear to influence IRES-dependent translation inhibition by antisense PNAs

The differences in PNA inhibition of the results above could possibly be due to differences in affinities of the carrier DNA to the PNA. It has been suggested that PNA:DNA duplexes with high melting temperatures (over 75°C) could prevent release of the antisense PNA within the cell thereby reducing its effectiveness at finding complementary transcripts (Doyle 2001). To address this possible problem, antisense PNAs were annealed to different carrier DNA with lower T_m s and transfected into CV-1 cells. The carrier DNA oligonucleotides were either 11-base complements or 11-base complements with poly T tails (17-bases total) for comparison against the exact complement 17-base carrier DNA (**Table 3-3. Effects of carrier DNA on PNA inhibition**). In no PNA:DNA combination tested did the lower affinity carrier DNA enhance the efficiency of the antisense PNA in inhibiting translation from the IRES. The 17-mer fully complement carrier DNA worked best for inhibitory effects of antisense PNAs regardless of the T_m . This is contrary to what was seen previously in our lab which concluded that PNA:DNA duplexes must have T_m s above 65°C for stability during transfections but below 75°C for PNA release within the cytosol (**29**).

Name	Sequence	T_m	% expression*
P1	K-AGGTGGTATCTAGTGAG		
D1comp	TCCACCATAGATCACTC	78	76
D1-5	ATAGATCACTCTTTTTT	52	95
D1-6	ATAGATCACTC	51	75
P2	K-CGCAGATCGGTACCGCA		
D2comp	GCGTCTAGCCATGGCGT	80	35
D2-5	AGCCATGGCGTTTTTTT	61	53
D2-6	AGCCATGGCGT	60	71
P3	K-AGGAAAGAACCTAGTTG		
D3comp	TCCTTTCTTGGATCAAC	74	53
D3-5	CTTGGATCAACTTTTTT	58	54
D3-6	CTTGGATCAAC	54	55
P4	K-AAACCCGCACGGGGGCG		
D4comp	TTTGGGCGTGCCCCGC	89	55
D4-5	CGTGCCCCGCTTTTTT	78	78
D4-6	CGTGCCCCGC	79	64
P5	K-TCACAACCCAGCGCTTT		
D5comp	AGTGTTGGGTCGCGAAA	81	17
D5-5	GGGTCGCGAAATTTTTT	69	42
D5-6	GGGTCGCGAAA	65	64
P6	K-GGGGCCCTCCAGAGCAT		
D6comp	CCCCGGGAGGTCTCGTA	85	30
D6-5	GAGGTCTCGTATTTTTT	75	50
D6-6	GAGGTCTCGTA	78	70
P7	K-GGCACGTGGTACTCGTG		
D7comp	CCGTGCACCATGAGCAC	83	29
D7-5	ACCATGAGCACTTTTTT	64	40
D7-6	ACCATGAGCAC	61	59

Table 3-3. Effects of carrier DNA on PNA inhibition.

PNAs sequences are in purple, listed from C-terminal to N-terminal. Carrier DNA sequences are listed 5' to 3'.

*The % Relative Firefly expression (Firefly:Renilla, normalized to lipid only control) given is for transfection of 200 nM PNA:DNA.

A possible explanation for the results seen here may be the formation of intra- or intermolecular aggregation of unhybridized PNA sequences within a PNA:DNA duplex (i.e PNA overhangs). PNAs have a propensity to aggregate over time. While it is believed that PNA:DNA duplexes would be more soluble in aqueous solutions due to the charged DNA backbone, it is unknown as to whether PNA:DNA duplexes aggregate over time in transfection media or inside cells. Aggregation would limit the ability of PNAs to find complementary RNA targets and inhibit translation.

Another possible explanation may be the unequal formation of PNA:DNA duplexes during annealing. Solutions of PNA:DNA duplexes are made by mixing equimolar amounts of PNA and carrier DNA and ramping the temperature from 95°C to 4°C. While it is assumed that 100% of the PNAs and DNA oligonucleotides anneal during the temperature drop (giving equimolar PNA:DNA duplexes), this may not necessarily be true. The quality of the PNA synthesis and the quality of DNA synthesis will determine what fraction of PNAs will duplex with carrier DNA. PNAs that do not hybridize to a carrier DNA will not be intracellularly delivered with lipid, thus reducing the effective concentration of PNA for antisense activity.

Effect of PNA length on inhibition of gene expression

In a previous study, others had shown that antisense inhibition of expression of human caveolin-1 required that PNAs be at least 19 bases long (30). In our current study, however, I observed that 17-base PNAs were effective inhibitors of IRES-mediated expression. To investigate this discrepancy, I synthesized PNAs of varied length that

were analogous in sequence to PNAs P3 (specific for the apical loop of SL-IIIb) or P6 (specific for the pseudoknot region). PNAs of varying length were transfected with the same 17-mer carrier DNA to minimize transfection differences. I observed that PNAs P6-15mer or P6-17mer were as effective as longer PNAs P6-19mer or P6-21mer for inhibition of HCV IRES-mediated expression of luciferase (**Figure 3-9. Effect of PNA length on IRES-dependent translation of firefly luciferase**). Similarly, 17-base PNA P3 was approximately as potent an inhibitor as the longer analogs PNAs P3-19mer and P3-21mer.

PNA length and mechanisms of antisense inhibition

Our observation that 15- or 17-base PNAs are effective inhibitors of expression stands in striking contrast to our results with PNAs targeted to mRNA encoding human caveolin-1, which showed little inhibition by 15- or 17-base PNAs. The PNAs in the caveolin study were targeted to sequences within the coding region of the mRNA and, to function, were required to block ribosome movement. The anti-HCV IRES PNAs, by contrast, probably function by preventing proteins from binding to the RNA. One explanation for the effectiveness of our anti HCV-IRES PNAs is that blocking protein binding may be less demanding than the need to block progress of a ribosome that has already begun translation.

This hypothesis is consistent with a previous study from our laboratory of antisense inhibition by 15-base PNAs (29). It was observed previously that a 15-base PNA directed to the extreme 5'-end of transcript mRNA could efficiently block

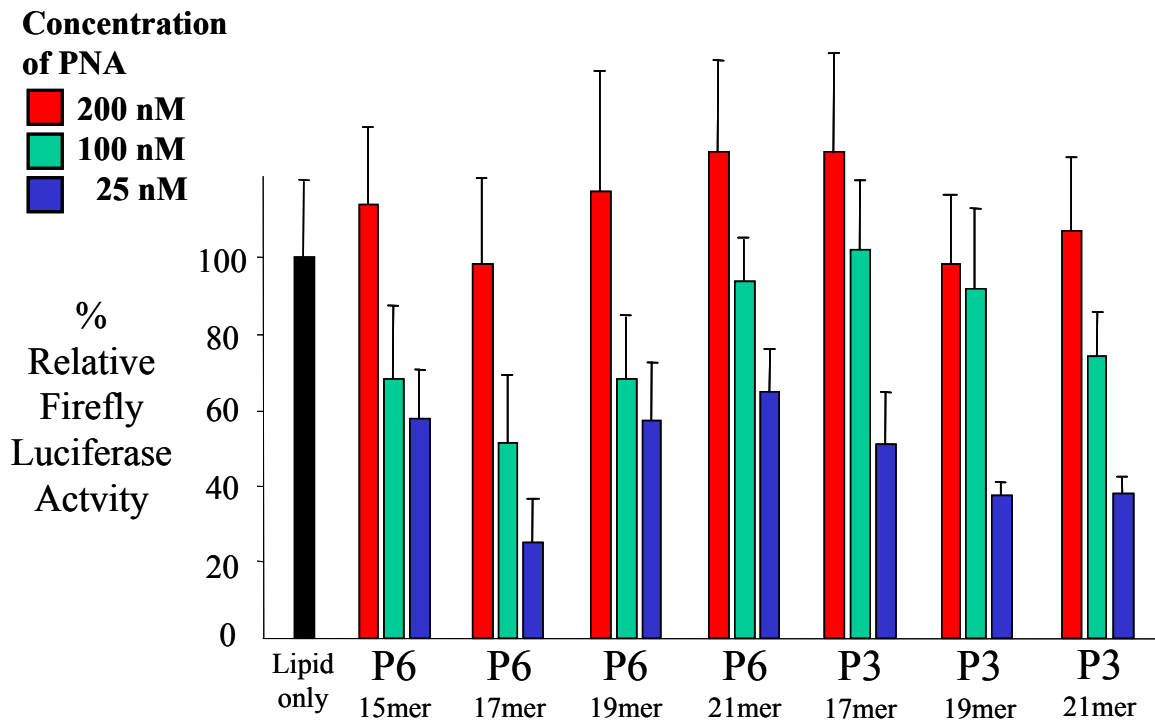


Figure 3-9. Effect of PNA length on IRES-dependent translation of Firefly luciferase. The % Relative Firefly Luciferase Activity is the ratio of Firefly:Renilla expression, normalized to lipid only control.

transcription, but that fifteen different 15-base PNAs targeted to downstream target sites were ineffective. From these previous experiments it was concluded that the one active PNA functioned by preventing 7^mG cap-dependent translation from initiating, and that binding of the inactive PNAs targeted to downstream sites was insufficient to prevent translation. Consistent with our previous findings, PNA P8, a 17-base PNA targeted to the luciferase coding region, was inactive (data not shown).

Inhibition of IRES-dependent translation by chimeric LNAs

LNAs provide another option for using high affinity hybridization to improve nucleic acid recognition. The LNAs used in these studies were chimeric molecules containing mixtures of DNA and LNA bases. The chimeric LNAs were designed to be analogous in sequence to PNAs P3-P7 (see **Table 3-2**). No chimeric LNA contained more than three contiguous DNA and any LNA-RNA hybrids formed would not be predicted to be good substrates for RNase H.

I transfected the chimeric LNAs into cells using the same lipid-mediated transfection protocol as the PNAs (but without the carrier DNAs) and observed the effect of their addition to cell culture on luciferase expression (**Figure 3-10. Effect of antisense chimeric LNAs on IRES-dependent translation of firefly luciferase**). Antisense chimeric LNA L3 did not substantially inhibit luciferase expression. Chimeric LNA L4 inhibited as well as PNA P4 with an IC₅₀ of approximately 200nM. Chimeric LNAs L6 and L7 were able to inhibit expression to some degree, but none as well as analogous PNAs P6 and P7. Our observation that inhibition by IRES-directed PNAs is more

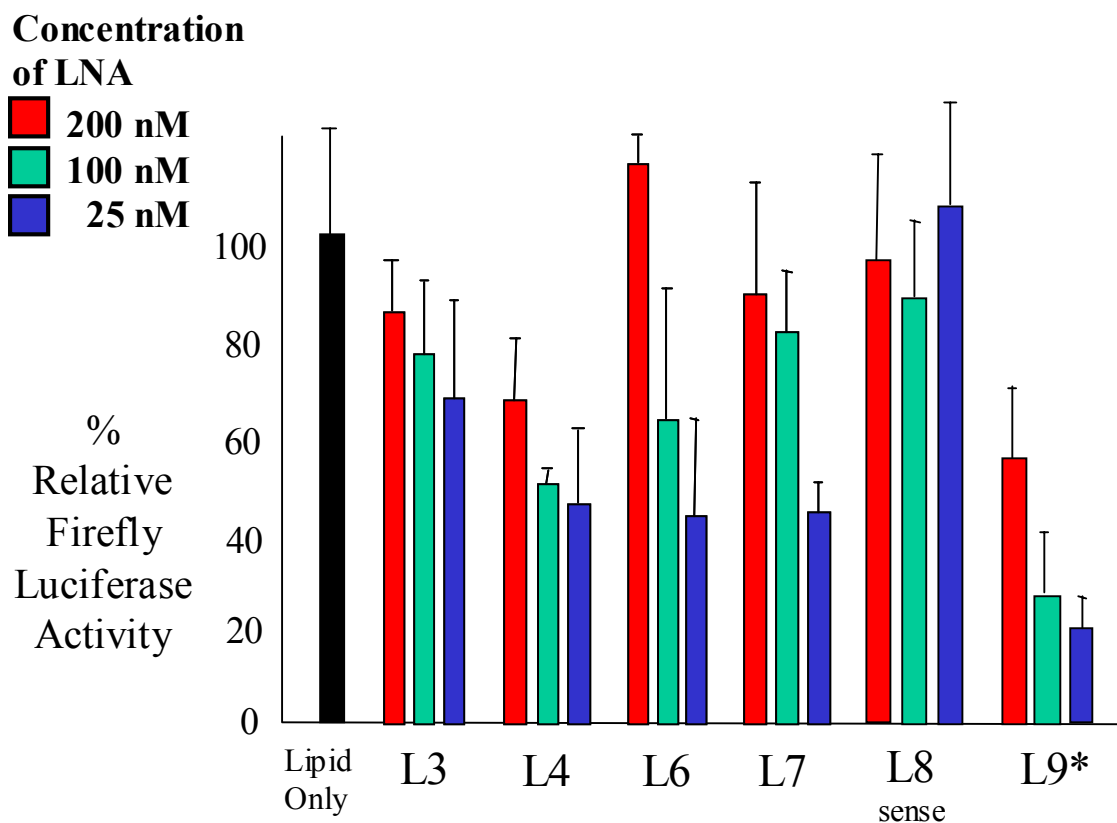


Figure 3-10. Effect of antisense chimeric LNAs on IRES-dependent translation of firefly luciferase. Positive control chimeric LNA L9* targets the coding region of Firefly luciferase and recruits RNase H for transcript cleavage. The % Relative Firefly Luciferase Activity is the ratio of Firefly:Renilla expression, normalized to lipid only control.

efficient than chimeric LNAs suggests that PNAs may be better able to invade the IRES, possibly due to their uncharged backbone linkages.

The control chimeric LNA L8-sense that was the same sequence as the target sense strand did not inhibit expression. The RNase H-activating chimeric LNA L9, targeting a sequence within the coding region of luciferase mRNA, was able to inhibit expression. This is in contrast to the PNA P8 targeting the same region. It is possible that L9 could be inhibiting Firefly expression by two possible mechanisms; sterically blocking translational machinery and by inducing RNase H cleavage of the transcript.

Factors governing the potencies of anti-IRES PNAs and LNAs

In this study, I observed that some PNAs and chimeric LNAs function better than others at inhibiting Firefly luciferase activity. A possible explanation for this is that some IRES RNA tertiary structures may be more accessible to hybridizing oligomers than others. For example, our results suggest that PNA P3 (specific for SL-III) only works moderately well, yet other studies have identified IRES domain SL-III as being the most accessible to ribozyme activity (58). Similarly, studies involving (siRNA-based) short hairpin RNA (shRNA) techniques to knock-down HCV replication found that all shRNAs targeting sequences in domain SL-IV or nearby coding sequences blocked viral replication. However, only one of seven shRNAs targeting sequences in domain SL-II or SL-III had a similar degree of antiviral activity, indicating that large sections of the HCV 5'-UTR/IRES are resistant to RNA interference (59).

It is also possible that the antisense PNAs and chimeric LNAs are hybridizing to their specific RNA target sequences intracellularly, but the bound oligomer does not

disrupt protein-RNA interactions or distort RNA secondary structure to cause a decrease in translation levels. This would suggest that some IRES RNA regions are more important for translation initiation than other RNA regions. Potential experiments such as the polyacrylamide gel shift assay of *in vitro* generated IRES (pRL-HL) transcripts incubated with antisense PNAs (or chimeric LNAs) would demonstrate the relative efficiency of hybridization of each oligomer for its particular RNA region. These experiments could be followed by *in vitro* translation of the bicistronic transcript (in the presence of antisense oligomers in cell extracts) and assaying for Firefly and Renilla activity to demonstrate the relative importance of each RNA region towards translation of the IRES. These simple experiments could give insight as to the inhibitory potential of a given oligomer (and target RNA sequence) without the confounding issues of transfection efficiency and cellular trafficking of the oligonucleotide.

IRES Sequences as targets for PNAs and chimeric LNAs

IRES sequences are a distinct class of cellular targets for recognition by oligonucleotides and PNAs. Because IRES sequences often direct the synthesis of viral proteins, compounds that efficiently bind to IRES sequences provide lead compounds for therapeutic development. The challenge for the design of these compounds is that they must be able to disrupt RNA secondary structure and compete with proteins for binding at their target sites.

Chimeric LNAs and PNAs share an ability to bind complementary sequences with high affinity, but also have many characteristics that differ. LNA monomers are conformationally restricted (i.e. fixed furanose ring), while PNAs are relatively flexible.

Chimeric LNA has negatively charged backbone linkages, whereas PNA linkages are uncharged. Finally, PNA is well known for its ability to invade duplex DNA. LNA has also been recently noted to bind duplex DNA (**50**), but the overall potential for chimeric LNA to bind structured nucleic acids is much less well characterized.

Our results demonstrate that PNAs and chimeric LNAs can inhibit IRES-mediate expression and achieving further improvement in the potency of IRES-targeted inhibition is a primary goal for future research. One strategy for improving the potency of inhibition by chimeric LNAs directed to IRES sequence is introduction of the ability to recruit RNase H. Others have noted that attachment of positive charges to PNAs can enhanced strand invasion of duplex DNA (**51, 52**), and similar modifications may also increase binding RNA structures within HCV IRES. Finally, others have shown that attachment of sugar moieties to PNAs allows liver cell-specific targeting through the asialoglycoprotein receptor (ASGP-R) and such modifications may be useful for in vivo testing of anti-IRES PNAs (**53, 54, 55**).

Given the numerous options for improving the efficiency of IRES-mediated inhibition, our results should only be viewed as a starting point. It is likely that further improvements in PNA and LNA chemistry and cellular delivery will lead to increasingly potent agents for IRES recognition.

Future Directions

Progressing antisense oligomers towards therapeutic applications not only requires improvements and greater scrutiny of existing protocols and techniques, but also technological advances to more complex model systems. Unfortunately, only a couple of alternative models for studying HCV exist.

Tissue culture systems are inefficient at supporting propagation of HCV virions. The next best model for studying oligomer-based antisense effects against HCV would be the HCV Replicon systems in Huh-7 cells (61). Replicons are autonomously replicating bicistronic HCV RNAs in which the structural proteins have been replaced with a selectable marker (neo). The HCV IRES sequence drives translation of the selectable marker while a second IRES (derived from the encephalomyocarditis virus- ECMV) drives translation for the non-structural proteins required to propagate the Replicon. As a high-throughput model, antisense oligomers could be targeted to any number of RNA sequences within the Replicon (including the highly conserved tertiary structure of the 3'-UTR and the ECMV IRES) and assessed for antisense activity (inhibiting translation or replication) by RT-PCR, Northern blots, or Western Blots. The HCV IRES could not be used as a target because it drives expression of the neo marker which is necessary for selection of cells harboring the Replicon.

A disadvantage to the Replicon system is that the RNA is prone to mutate over time which can alter translation and replication rates (60). While the Replicon might be expected to mutate the genome under selective pressure of an inhibitory oligomer “drug”, point mutations that occur outside the intended oligomer binding site may give inaccurate conclusions to antisense activity of a specific oligomer.

A chimeric mouse model for studying HCV has only recently been achieved (62). However, its robustness has not been scrutinized and it is not applicable to high-throughput analysis.

References for Chapter 3

- 1 Alter M.J., Kruszon-Moran D., Nainan O.V., McQuillan G.M., Gao F., Moyer L.A., Kaslow R.A., Margolis H.S. (1999) The prevalence of hepatitis C virus infection in the United States, 1988 through 1994. *New England Journal of Medicine*. 341:556-562.
- 2 Armstrong G.L., Alter M.J., McQuillan G.M., and Margolis H.S. (2000) The past incidence of hepatitis C virus infection: implications for the future burden of chronic liver disease in the United States. *Hepatology*. 31, 777-782.
- 3 Ikeda K., Saitoh S., Arase Y., Chayama K., Suzuki Y., Kobayashi M., Tsubota A., Nakamura I., Murashima N., Kumada H., and Kawanishi M. (1999) Effect of interferon therapy on hepatocellular carcinogenesis in patients with chronic hepatitis type C: A long-term observation study of 1,643 patients using statistical bias correction with proportional hazard analysis. *Hepatology*. 29, 1124-1130.
- 4 Gale M. Jr. and Beard M.R. (2001) Molecular clones of hepatitis C virus: applications to animal models. *Ilar. Journal*. 42(2):139-51.
- 5 Reed K.E. and Rice C.M. (2000) Overview of Hepatitis C Virus genome structure, polyprotein processing, and protein properties. *Current Topics in Microbiology and Immunology*. 242, 55-84.
- 6 Thompson S.R. and Sarnow P. (2000) Regulation of host cell translation by viruses and effects on cell function. *Current Opinion in Microbiology*. 3, 366-370.
- 7 Wang C., Sarnow P., and Siddiqui A. (1993) Translation of human hepatitis C virus RNA in cultured cells is mediated by an internal ribosome-binding mechanism. *Journal of Virology*. 67, 3338-3344.

- 8 Honda M., Ping L.H., Rihnbrand R.C., Amphlett E., Clarke B., Rowlands D., and Lemon S.M. (1996) Structural requirements for initiation of translation by internal ribosome entry within genome-length hepatitis C virus RNA. *Virology*. 222, 31-42.
- 9 Sarnow P. (2003) Viral internal ribosome entry site elements: novel ribosome-RNA complexes and roles in viral pathogenesis. *J. Virol.* 77, 2801-2806.
- 10 Vagner S., Galy B., and Pyronnet S. (2001) Irresistible IRES. Attracting the translation machinery to internal ribosome entry sites. *EMBO Rep.* 2, 893-898.
- 11 Spahn C.M., Kieft J.S., Grassucci R.A., Penczek P.A., Zhou K., Doudna J.A., and Frank J. (2001) Hepatitis C virus IRES RNA-induced changes in the conformation of the 40s ribosomal subunit. *Science*. 291, 1959-1962.
- 12 Buratti E., Tsminezky S., Zotti M., and Baralle F.E. (1998) Functional analysis of the interaction between HCV 5'UTR and putative subunits of eukaryotic translation initiation factor eIF3. *Nucl. Acids Res.* 26, 3179-3187.
- 13 Lukavsky P.J., Otto G.A., Lancaster A.M., Sarnow P., and Puglisi J.D. (2000) Structures of two RNA domains essential for hepatitis C virus internal ribosome entry site function. *Nat. Struct. Biol.* 7, 1105-1110.
- 14 McCaffrey A.P., Ohashi K., Meuse L., Shen S., Lancaster A.M., Lukavsky P J., Sarnow P., and Kay M.A. (2002) Determinants of hepatitis C translational initiation in vitro, in cultured cells and mice. *Mol. Ther.* 5, 676-684.

- 15 Blight K.J., Kolyhalov A.A., Reed K.E., Agapov E.V., and Rice C.M. (1998) Molecular virology of hepatitis C virus: an update with respect to potential antiviral targets. *Antivir. Ther.* 3 (Suppl 3), 71-81.
- 16 Gallego J. and Varani G. (2002) The hepatitis C virus internal ribosome-entry site: a new target for antiviral research. *Biochem. Soc. Trans.* 30, 140-145.
- 17 Klinck R., Westhof E., Walker S., Afshar M., Collier A., and Aboul-Ela F. (2000) A potential RNA drug target in the hepatitis C virus internal ribosomal entry site. *RNA*. 6, 1423-1431.
- 18 Martinand-Mari C., Lebleu B., and Robbins I. (2003) Oligonucleotide-based strategies to inhibit human hepatitis C virus. *Oligonucleotides*. 13, 539-548.
- 19 Marshall D.J., Heisler L.M., Lyamichev V., Murvine C., Olive D.M., Ehrlich G.D., Neri B.P., de Arruda M. (1997) Determination of hepatitis C virus genotypes in the United States by cleavage fragment length polymorphism analysis. *Journal of Clinical Microbiology*. 35(12):3156-62
- 20 Young K.K., Archer J.J., Yokosuka O., Omata M., and Resnick R.M. (1995) Detection of hepatitis C virus RNA by a combined reverse transcription PCR assay: comparison with nested amplification and antibody testing. *Journal of Clinical Microbiology*. 654-657, Vol. 33, No. 3.
- 21 Bukh J., Purcell R.H. and Miller R.H. (1992) Sequence Analysis of the 5' Noncoding Region of Hepatitis C Virus. *Proceedings of the National Academy of Sciences*. 89, 4942-4946
- 22 Hanecak R., Brown-Driver V., Fox M.C., Azad R.F., Furusako S., Nozaki C., Ford C., Sasmor H., and Anderson K.P. (1996) Antisense oligonucleotide inhibition of hepatitis C virus gene expression in transformed hepatocytes. *J. Virol.* 70, 5203-5212.

- 23 Michel T., Martinand-Mari C., Debart F., Lebleu B., Robbins I., and Vasseur J.J., (2003) Cationic phosphoramidate alpha-oligonucleotides efficiently target single-stranded DNA and RNA and inhibit hepatitis C virus IRES-mediated translation. *Nucl. Acids Res.* 31, 5282-5290.
- 24 Tallet-Lopez B., Aldaz-Carroll L., Chabas S., Dausse E., Staedel C., and Toulme J.J. (2003) Antisense oligonucleotides targeted to the domain III_d of the hepatitis C virus IRES compete with 40S ribosomal subunit binding and prevent in vitro translation. *Nucl. Acids Res.* 31, 734-742.
- 26 Choi K., Kim J.H., Li X., Paek L.Y., Ha S.H., Ryu S.H., Wimmer E., and Jang S.K. (2004) Identification of cellular proteins enhancing activities of internal ribosomal entry sites by competition with oligodeoxynucleotides. *Nucl. Acids Res.* 32, 1308-1317.
- 26 Nielsen P.G., Egholm M., Berg R.H., and Buchardt O. (1991) Sequence-selective recognition of DNA by strand displacement with a thymine substituted polyamide. *Science.* 254, 1497-1500.
- 27 Koshkin A.A. and Wengel J. (1998) Synthesis of Novel 2',3'-Linked Bicyclic Thymine Ribonucleosides. *J. Org. Chem.* 63, 2778-2781.
- 28 Obika S., Nanbu D., Hari Y., Andoh J., Morio K., Doi T., and Imanishi T. (1998) Stability and structural features of the duplexes containing nucleoside analogues with a fixed N-type conformation, 2'-O,4'-C-methylenribonucleosides. *Tet. Lett.* 39, 5401-5404.
- 29 Doyle D.F., Braasch D.A., Simmons C.G., Janowski B.A. and Corey D.R. (2001) Inhibition of gene expression inside cells by peptide nucleic acids: effect of mRNA target sequence, mismatched bases, and PNA length. *Biochemistry.* 40, 53-64.
- 30 Liu Y., Braasch D.A., Nulf C.J., and Corey D.R. (2004) Efficient and isoform-selective inhibition of cellular gene expression by peptide nucleic acids. *Biochemistry.* 43, 1921-1927.

- 31 Braasch D.A. and Corey D.R. (2001) Locked nucleic acid (LNA): fine-tuning the recognition of DNA and RNA. *Chem. Biol.* 8, 1-7.
- 32 Braasch D.B., Liu Y., and Corey D.R. (2002) Antisense inhibition of gene expression in cells by oligonucleotides incorporating locked nucleic acids: effect of mRNA target sequence and chimera design. *Nucleic Acids Res* 30, 5160-5167.
- 33 Wengel J. (1999) Synthesis of 3'-C- and 4'-C-branched oligodeoxynucleotides and the development of locked nucleic acid (LNA) *Accounts Chem. Res.* 32 301-10.
- 34 Wahlestedt C., Salmi P., Good L., Kela J., Johnsson T., Hokfelt T., Broberger C., Porreca F., Lai J., Ren K., Ossipov M., Koshkin A., Jakobsen N., Skouv J., Oerum H., Jacobsen M.H., Wengel J. (2000) Potent and nontoxic antisense oligonucleotides containing locked nucleic acids. *Proc. Natl. Acad. Sci. U.S.A.* 97(10):5633-8.
- 35 Kurreck J., Wyszko E., Gillen C., and Erdmann V.A. (2002) Design of antisense oligonucleotides stabilized by locked nucleic acids. *Nucl. Acids Res.* 30, 1911-8.
- 36 Grunweller A., Wyszko E., Bieber B., Jahnel R., Erdmann V.A., and Kurreck J. (2003) Comparison of different antisense strategies in mammalian cells using locked nucleic acids, 2'-O-methyl RNA, phosphorothioates and small interfering RNA. *Nucl. Acids Res.* 31, 3185-93.
- 37 Frieden M., Christensen S.M., Mikkelsen N.D., Rosenbohm C., Thruue C.A., Westergaard M., Hansen H.F., Orum H., and Koch T. (2003) Expanding the design horizon of antisense oligonucleotides with alpha-L-LNA. *Nucl. Acids Res.* 31, 6365-72.

- 38 Arzumanov A., Walsh A.P., Rajwanshi V.K., Kumar R., Wengel J., and Gait M.J. (2001) Inhibition of HIV-1 Tat-dependent trans activation by steric block chimeric 2'-O-methyl/LNA oligoribonucleotides. *Biochemistry*. 40, 14645-54.
- 39 Knudsen H. and Nielsen P.E. (1996) Antisense properties of duplex- and triplex- forming PNAs. *Nucl. Acids Res.* 24, 494-500.
- 40 Kim Y.K., Lee S.H., Kim C.S., Seol S.K., and Jang S.K. (2003) Long-range RNA-RNA interaction between the 5' nontranslated region and the core-coding sequences of hepatitis C virus modulates the IRES-dependent translation. *RNA*. 9, 599-606.
- 41 Honda M., Rijnbrand B., Abell G., Kim D., and Lemon S.M. (1999) Natural variation in translational activities of the 5' nontranslated RNAs of hepatitis C virus genotypes 1a and 1b: evidence for a long-range RNA-RNA interaction outside of the internal ribosomal entry site. *J. Virol.* 73, 4941-4951.
- 42 Collier A.J., Gallego J., Klinck R., Cole P.T., Harris S.J., Harrison G.P., Aboul-Ela F., Varani G., and Walker S. (2002) A conserved RNA structure within the HCV IRES eIF3-binding site. *Nat. Struct. Biol.* 9, 375-380.
- 43 Kieft J.S., Zhou K., Jubin R., Murray M.G., Lau J.Y., and Doudna J.A. (1999) The hepatitis C virus internal ribosome entry site adopts an ion-dependent tertiary fold. *J. Mol. Biol.* 292, 513-529.
- 44 Kolupaeva V.G., Pestova T.V., and Hellen C.U. (2000) An enzymatic footprinting analysis of the interaction of 40S ribosomal subunits with the internal ribosomal entry site of hepatitis C virus. *J. Virol.* 74, 6242-6250.

- 45 Wang C., Le S.Y., Ali N., and Siddiqui A. (1995) An RNA pseudoknot is an essential structural element of the internal ribosome entry site located within the hepatitis C virus 5' noncoding region. *RNA*. 1, 526-37.
- 46 Zhang H., Hanecak R., Brown-Driver V., Azad R., Conklin B., Fox M.C., and Anderson K.P. (1999) Antisense oligonucleotide inhibition of hepatitis C virus (HCV) gene expression in livers of mice infected with an HCV-vaccinia virus recombinant. *Antimicrob. Agents Chemother.* 43, 347-353.
- 47 Belitsky J.M., Leslie S.J., Arora P.S., Beerman T.A., Dervan P.B. (2002) Cellular uptake of N-methylpyrrole/N-methylimidazole polyamide-dye conjugates. *Bioorg. Med. Chem.* 10(10):3313-8.
- 48 Koppelhus U., Awasthi S.K, Zachar V., Holst H.U., Ebbesen P., Nielsen P.E. (2002) Cell-dependent differential cellular uptake of PNA, peptides, and PNA-peptide conjugates. *Antisense Nucleic Acid Drug Dev.* 12(2):51-63.
- 49 Honda M., Kaneko S., Matsushita E., Kobayashi K., Abell G.A., and Lemon S.M. (2000) Cell cycle regulation of hepatitis C virus internal ribosomal entry site-directed translation. *Gastroenterology*. 118, 152-162.
- 50 Hertoghs K.M., Ellis J.H., and Catchpole I.R. (2003) Use of locked nucleic acid oligonucleotides to add functionality. *Nucl. Acids Res.* 31, 5817-30.
- 51 Kaihatsu K., Shah R.H., Zhao X., and Corey D.R. (2003) Extending recognition by peptide nucleic acids (PNAs): binding to duplex DNA and inhibition of transcription by tail-clamp PNA-peptide conjugates. *Biochemistry*. 42, 13996-4003.

- 52 Bentin T. and Nielsen P.E. (1996) Enhanced peptide nucleic acid binding to supercoiled DNA: possible implications for DNA "breathing" dynamics. *Biochemistry*. 35, 8863-8869.
- 53 Zhang X., Simmons C.G., and Corey D.R. (2001) Synthesis and Intracellular Delivery of Lactose-Labeled PNAs. *Bioorg. Med. Chem. Lett.* 11,1269-1272.
- 54 Hamzavi R., Dolle F., Tavitian B., Dahl O., and Nielsen P.E. (2003) Modulation of the pharmacokinetic properties of PNA: preparation of galactosyl, mannosyl, fucosyl, N-acetylgalactosaminyl, and N-acetylglucosaminyl derivatives of aminoethylglycine peptide nucleic acid monomers and their incorporation into PNA oligonucleotides. *Bioconjugate Chemistry*. 14, 941-54.
- 55 Maier M.A, Yannopoulos C.G., Mohamed N., Roland A., Fritz H., Mohan V., Just G., Manoharan M. (2003) Synthesis of antisense oligonucleotides conjugated to a multivalent carbohydrate cluster for cellular targeting. *Bioconjugate Chemistry*. 14(1):18-29.
- 56 Hamilton S.E., Simmons C.G., Kathiriya I.S., Corey D.R. (1999) Cellular delivery of peptide nucleic acids and inhibition of human telomerase. *Chem. Biol.* 6(6):343-51.
- 57 Elayadi A.N., Braasch D.A., Corey D.R. (2002) Implications of high-affinity hybridization by locked nucleic acid oligomers for inhibition of human telomerase. *Biochemistry*. 41(31):9973-81.
- 58 Ryu K.J., Lee S.W. (2003) Identification of the most accessible sites to ribozymes on the hepatitis C virus internal ribosome entry site. *J. Biochem. Mol. Biol.* 36(6):538-44.
- 59 Kronke J., Kittler R., Buchholz F., Windisch M.P., Pietschmann T., Bartenschlager R., Frese M. (2004) Alternative approaches for efficient inhibition of hepatitis C virus RNA replication by small interfering RNAs. *J. Virol.* 78(7):3436-46.

- 60 Ma Y., Shimakami T., Luo H., Hayashi N., Murakami S. (2004) Mutational Analysis of Hepatitis C Virus NS5B in the Subgenomic Replicon Cell Culture. *J. Biol. Chem.* 279(24):25474-82.
- 61 Bartenschlager R., Lohmann V. (2001) Novel cell culture systems for the hepatitis C virus. *Antiviral Res.* 52(1):1-17.
- 62 Mercer D.F., Schiller D.E., Elliott J.F., Douglas D.N., Hao C., Rinfret A., Addison W.R., Fischer K.P., Churchill T.A., Lakey J.R., Tyrrell D.L., Kneteman N.M.. (2001) Hepatitis C virus replication in mice with chimeric human livers. *Nat Med.* 7(8):927-33.

CHAPTER 4 - OTHER MODELS AND APPLICATIONS FOR PNAs IN REGULATING GENE EXPRESSION (COLLABORATIONS)

	<u>Page</u>
Introduction	131
Comparison of PNAs with siRNA towards inhibiting isoform-specific expression of human caveolin-1 (Collaboration with Dr. Yinghui Liu, UT Southwestern Medical Center at Dallas)	133
The model target: Human caveolin-1	135
Design of PNAs and siRNAs to target sequences within the hCav-1 transcript	136
Inhibition of expression of hCav-1 isoforms by PNAs	136
Inhibition of expression of hCav-1 by siRNAs	139
The potency and duration of PNAs and siRNAs	139
Conclusions of comparisons	141
Comparison of PNAs with morpholinos for the inhibition of developmental genes in Zebrafish (collaboration with Dr. Stephen Egger, The University of Minnesota)	145
Background and chemistry of morpholino oligomers	145
Potential phenotypic outcomes of antisense experiments	147
Antisense effects of morpholinos and PNAs on Zebrafish development	148

Comparison of PNAs with 2'-<i>O</i>-(2-methoxyethyl) oligoribonucleotides (2'-MOE) for re-directing pre-mRNA splicing events (collaboration with Dr. Brett Monia, ISIS Pharmaceuticals)	152
Background and chemistry of 2'-<i>O</i>-(2-methoxyethyl) oligoribonucleotides (2'-MOE)	152
The model target: Human insulin receptor α-subunit	153
Efficiency of re-directing splicing events by PNAs and 2'MOE	156
The future of 2'MOE and PNAs as therapeutics	159
References for Chapter 4	161

Introduction

Controlling gene expression with nucleic acids is a simple yet powerful tool for investigating unknown protein functions inside cells. There are a variety of oligonucleotide-based technologies for controlling gene expression or studying gene function (1, 2, 3). In addition to the numerous chemically modified oligomers such as PNAs and LNAs (see Chapter 3), researchers are also using short inhibitory RNA (siRNA) (4, 5), small temporally regulated RNA (stRNA or microRNA) (6) and RNA or DNA decoys (7, 8) to study biological functions. Each technology has its own advantages ranging from ease of synthesis, greater sequence-specificity for target, and higher affinity for target, to cellular nuclease resistance, better *in vivo* pharmacokinetics, and lower toxicity effects. One technology may be more efficient at inhibiting gene expression versus another within a given model system depending on the chemical properties of an oligomer or the mechanism of inhibition. Several different oligomers chemistries may have to be tried to maximize inhibition effects.

While optimizing the efficiency of gene inhibition using an antisense approach is important, it is equally important to demonstrate that non-specific (or "off-target") effects are not the cause of reduced levels of expression (9, 10) and that other transcripts are not being unintentionally targeted (11, 12). One way of addressing these concerns is by comparing, in parallel, two oligomers of differing chemistry and/or mechanism of inhibition targeting the same RNA sequence. Different chemical properties and different mechanisms of inhibition of gene expression are unlikely to cause the same non-specific phenotype. Complementing antisense technologies validates the true "knock down" phenotype.

Having an in-house PNA synthesizer allows me to quickly generate PNAs for numerous collaborators. Most of the researchers requesting PNAs are interested in comparing oligonucleotide-based mechanisms of gene inhibition within their model systems. These collaborations are important for comparing and contrasting the advantages and disadvantages of oligomer-based mechanisms of inhibition. Understanding these differences can lead to the improvement of antisense reagents for cell culture or *in vivo* applications.

Comparison of PNAs with siRNA towards inhibiting isoform-specific expression of human caveolin-1 (Collaboration with Dr. Yinghui Liu, UT Southwestern Medical Center at Dallas) (see ref. 13)

Since the discovery of post-transcriptional gene silencing by short-inhibitory RNA (73, 74), siRNA has become popular as a robust and effective tool by researchers for regulating cellular gene expression (4, 77) (**Figure 4-1. The RNA interference pathway**). However, non-specific effects have been reported (11, 12). These non-specific effects may be associated with the mechanism of inhibition by siRNA, degradation of complementary RNA transcripts. Because PNAs do not cause degradation of target RNA, antisense effects by PNAs could be more specific for certain genes relative to siRNA.

Dr. Liu's interests include optimizing the use of antisense PNAs and siRNAs as molecular tools to study gene function. Previous reports demonstrated that microinjected PNAs could inhibit exogenous gene expression inside mammalian cells (14, 15). More recently, PNAs transfected into cell cultures could inhibit gene expression from a plasmid (16). However, the paucity of information for maximizing inhibitory effects by antisense PNAs inside cells requires continued experimentation in more complex models. This prompted the preliminary question, "Can antisense PNAs inhibit chromosomally expressed genes?"

My role in the project was to synthesize numerous PNAs targeting the RNA transcript of her model gene, human caveolin-1.

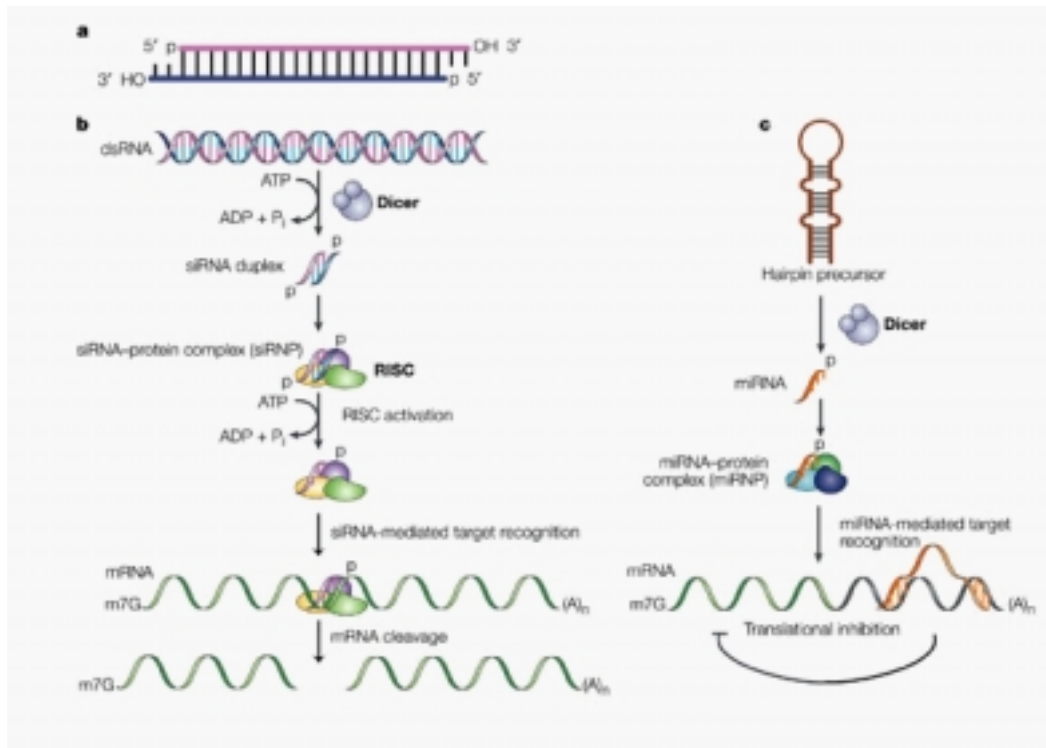


Figure 4-1. The RNA interference pathway. A.) Short interfering (si)RNAs. Molecular hallmarks of an siRNA include 5' phosphorylated ends, a 19-nucleotide (nt) duplexed region and 2-nt unpaired and unphosphorylated 3' ends that are characteristic of RNase III cleavage products. B.) The siRNA pathway. Long double-stranded (ds)RNA is cleaved by an RNase, Dicer, into siRNAs. These siRNAs are then incorporated into the RNA-inducing silencing complex (RISC). Once the siRNA duplex is unwound, the single-stranded antisense strand guides RISC to messenger RNA that has a complementary sequence, which results in the endonucleolytic cleavage of the target mRNA. C.) The micro (mi)RNA pathway. Although originally identified on the basis of its ability to process long dsRNA, Dicer can also cleave the 70-nt hairpin miRNA precursor to produce 22-nt miRNA. Unlike siRNAs, the miRNAs are single stranded and are incorporated into a miRNA-protein complex (miRNP). Partial sequence complementarity to target mRNA leads to translational repression without destruction of the transcript.

*From (ref. 72) Dykxhoorn D.M., Novina C.D., Sharp P.A. (2003) Killing the messenger: short RNAs that silence gene expression. *Nat. Rev. Mol. Cell Biol.* 4(6):457-67.

The model target: Human caveolin-1

Human caveolin-1 (hCav-1) is a protein that participates in the formation of caveole, flask-shaped invaginations of the plasma membrane (17, 18). It is expressed as two isoforms, a 24 kDa α -isoform and a 21 kDa β -isoform (19), that are differentially expressed in tissues (20). The two isoforms arise from two separate transcripts (21). The α -transcript has two AUG start sites, utilizing the upstream site to initiate translation to generate the α -isoform of hCav-1. The β -transcript of hCav-1 is a shortened form of the α -transcript and lacks the upstream AUG start site.

The function of each isoform of hCav-1 in normal and disease tissue and the significance of differential expression of α - and β -forms in tissues is not well known. It is known that caveolin-1 over-expression is linked to alterations of cholesterol distribution in the plasma membrane of brain cells and may be associated with the progression of Alzheimer's disease (72).

Using siRNA technology, previous reports demonstrated inhibition of human caveolin expression by addition of siRNA into cells (22). However, the destruction of the caveolin-1 transcript by siRNA caused both isoforms of caveolin-1 to be inhibited. Because the α - and β -isoforms could have individual and unique functions from one another, it may be beneficial to have an antisense oligomer that specifically inhibits for only one isoform. This prompted the second question by Dr. Liu, "Can antisense PNAs be as potent as siRNA and also be isoform-specific?"

Design of PNAs and siRNAs to target sequences within the hCav-1 transcript

Several antisense PNAs (19-mers) were designed and synthesized to target both AUG start site and several sites within the coding region (**Table 4-1. Sequences of PNAs, rational of use, calculated and observed molecular weights**) (**Figure 4-2a. Target sites of PNAs**). PNA-1 was designed to target the upstream AUG start site of the α -transcript while PNA-2 was complementary to the downstream AUG start site present in both transcripts. These PNAs were intended to prevent the ribosome from initiating protein translation by obstructing recognition of the start codon, a location known to be susceptible to antisense oligonucleotides (**23, 24**). PNA-3 and PNA-4 were complementary to sites within the coding region present in both transcripts. For controls, 2 base mismatch PNAs (for PNA-1 and PNA-2) were used to demonstrate specificity.

Inhibition of expression of hCav-1 isoforms by PNAs

Using a cationic lipid-based method to deliver antisense PNA:carrier DNA oligonucleotides into HeLa cells (**25, 26**) (see Chapter 3, Chapter 5), levels of α - and β -caveolin isoforms were assessed by Western blot (**Figure 4-2b. Target sites and inhibition of hCav-1 expression by PNAs**). As predicted, PNA-1 inhibited the α -isoform without affecting β -isoform expression levels (lane 1). PNA-2 and PNA-3 lowered expression levels of both isoforms, yet PNA-4 had no effect even though there was a complementary target sequence in both transcripts. The failure of PNA-4 to inhibit gene expression is unknown but does emphasize the importance of empirically testing several sequences within a transcript to target with antisense oligonucleotides to achieve maximal inhibition (**16**).

PNA	PNA sequence (N- to C-termini)	Comment/mRNA target site	Mass	
			calc	obs
1	TGCCCCCAGACATGCTGGC	α hCav-1 start codon	5293.8	5294.6
2	CTCGTCTGCCATGGCCTTG	β hCav-1 start codon	5290.7	5296.5
3	CTTCTCGCTCAGCTCGTCT	downstream of PNA 2	5225.6	5237.8
4	TGGTGTGCGCGTCGTACAC	downstream of PNA 3	5379.8	5395.5
5	TGCCCCCAGAC <u>GTGG</u> TGGC	mismatch analogue of PNA 1	5349.8	5367.4
6	CTCGTCTGCC <u>TTG</u> <u>AC</u> CTTG	mismatch analogue of PNA 2	5265.7	5266.6
7	TGCCCCCAGACATGC	15-base analogue of PNA 1	4193.6	4194.3
8	TGCCCCCAGACATGCTG	17-base analogue of PNA 1	4751.2	4758.2

Underlined letters represent mismatch bases

Table 4-1. Sequences of PNAs, rational of use, calculated and observed molecular weights.

*From: Liu Y., Braasch D.A., Nulf C.J., Corey D.R. (2004) Efficient and isoform-selective inhibition of cellular gene expression by peptide nucleic acids. *Biochemistry*. 43(7):1921-7.

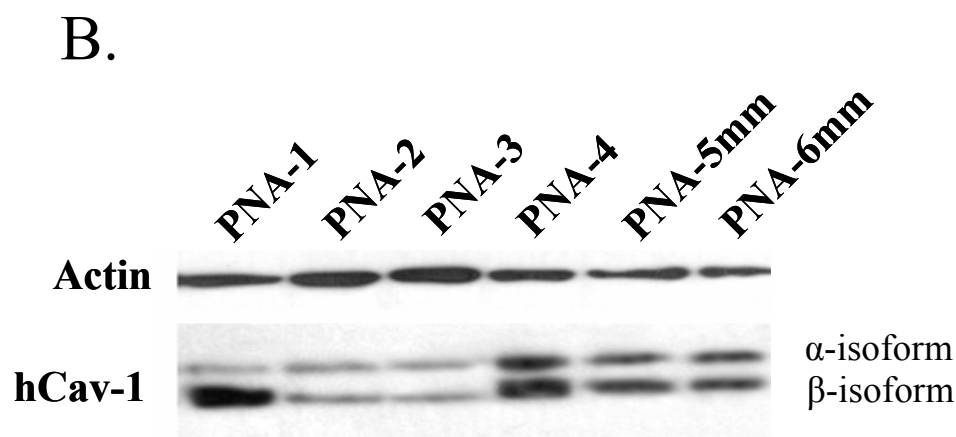
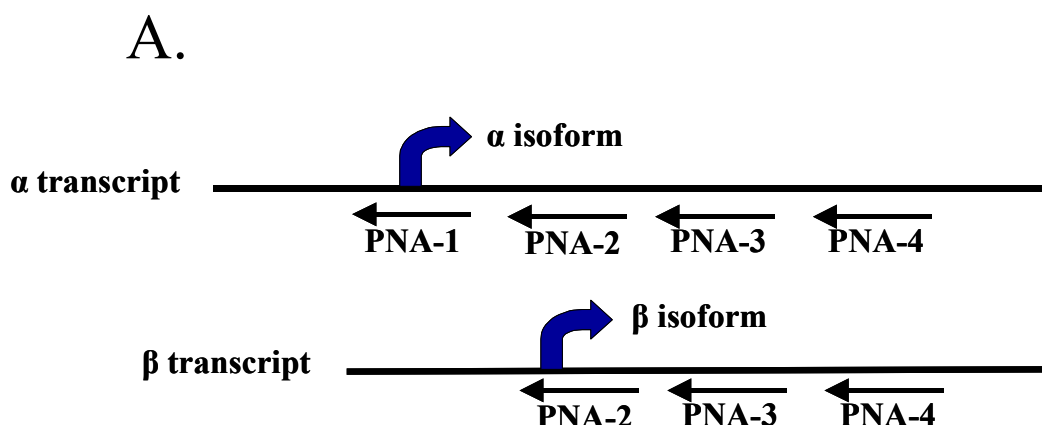


Figure 4-2. Target sites and inhibition of hCav-1 expression by PNAs. (A) Relative locations of the target sites for PNAs 1-4 within the mRNAs encoding the α - and β -isoforms of hCav-1. The two different start sites for the α - and β -isoforms are indicated. The schematic is not drawn to scale. (B) Western analysis of inhibition of hCav-1 gene expression by PNAs 1-4. Lane 1, PNA 1; lane 2, PNA 2; lane 3, PNA 3; lane 4, PNA 4; lane 5, mismatch PNA 5; lane 6, mismatch PNA 6.

*From: Liu Y., Braasch D.A., Nulf C.J., Corey D.R. (2004) Efficient and isoform-selective inhibition of cellular gene expression by peptide nucleic acids. *Biochemistry*. 43(7):1921-7.

Inhibition of expression of hCav-1 by siRNAs

For side-by-side comparison, siRNA with the same sequences as the PNAs were obtained. Using the same transfection protocol (replacing the PNA:carrier DNA duplex with siRNA) and concentrations, it was discovered that siRNA-1 (analogous to PNA-1) inhibited expression of both isoforms of caveolin even though the target sequence was not present in the β -isoform (**Figure 4-3. Comparison of inhibition of hCav expression by isoform-specific PNA 1 and analogous siRNA 1**). While the results are not fully understood, one possible explanation is that siRNA utilizing the endogenous ribosomal induced silencing complex (RISC) (27) may have indiscriminately found a similar (but not identical) target sequence in the β -isoform (28) but not the control gene actin. These results suggest that siRNA may not be as specific as PNAs in regulating gene expression and corroborate reports of gene expression profiling that suggest siRNA has non-specific transcript degradation (11). However, there are other reports with opposite views (29). When used as molecular tools, additional siRNA may need to be tested for specificity against a particular transcript (30).

The potency and duration of PNAs and siRNAs

The potency and duration of action of PNAs and siRNAs was next analyzed. Transfected PNAs are believed to partitioned into daughter cells with each cell division, reducing the effective concentration and efficacy in each daughter cell over time. The siRNA mechanism of action has been reported to amplify by an RNA-dependent RNA polymerase in plants (31). However, this mechanism appears to be dispensable in mammalian cells (32).

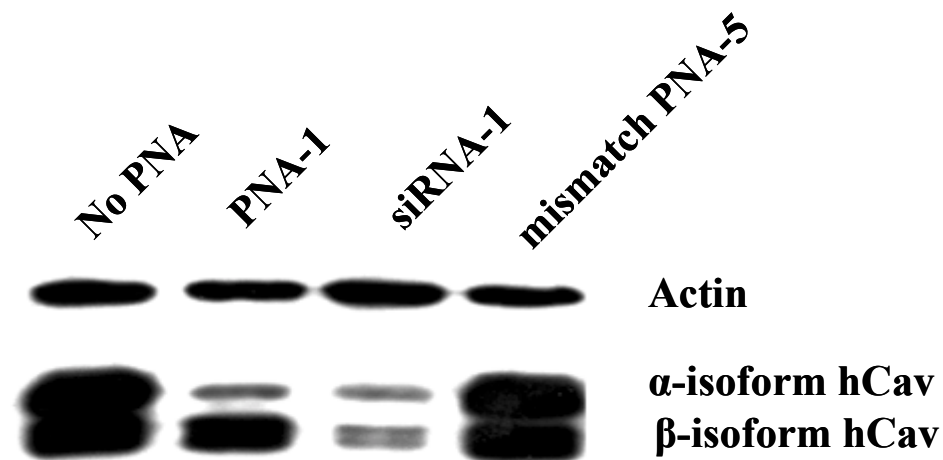


Figure 4-3. Comparison of inhibition of hCav expression by isoform-specific PNA 1 and analogous siRNA 1. Lane 1, no PNA; lane 2, PNA 1; lane 3, siRNA 1; lane 4, mismatch-containing PNA 5.

*From: Liu Y., Braasch D.A., Nulf C.J., Corey D.R. (2004) Efficient and isoform-selective inhibition of cellular gene expression by peptide nucleic acids. *Biochemistry*. 43(7):1921-7.

Caveolin levels from HeLa cells were analyzed by western blot 3 days after transfection of PNAs and siRNAs at various concentrations (**Figure 4-4. Inhibition of hCav-1 expression by varying concentrations of PNA 1, PNA 2, and siRNA 2**). Dose-response profiles reveal IC₅₀ values of approximately 25-30 nM for PNA-1, PNA-2 and siRNA-2 (with the same sequences as PNA-2). These IC₅₀ levels are consistent with other reports using chemically modified siRNA duplexes (**26**).

At days 3, 6, 9, 12 after PNA-1, PNA-2, and siRNA-2 were transfected into HeLa cells caveolin protein levels were assayed by western blot (**Figure 4-5. Time course of inhibition of hCav-1 expression by PNAs and siRNAs**). The results reveal that PNA-1, PNA-2, and siRNA have similar potencies at day 3 (90%, 87%, 87%, respectively) and day 6 (97%, 90%, 90%, respectively) at reducing protein levels of their targets.

However, at day 9 most of the caveolin levels have returned to normal, and at day 12 no inhibition was seen. Thus, transfected PNAs and siRNAs work equally well at reducing gene expression with similar potency and duration. Numerous other reports corroborate similar dose and duration when comparing "traditional" antisense oligonucleotide against siRNA molecules (**33, 34, 35**).

Conclusions of comparisons

The work by Dr. Liu emphasizes several similarities between antisense PNAs and siRNA molecules, including effective concentrations and duration of action. Fluorescence microscopy studies show similar perinuclear localizations of both fluorescently labeled PNAs (**36**) and siRNA (**26**) when transfected into cell cultures. *In vivo* biodistribution experiments of PNAs (**37**) and siRNAs (**38**) demonstrate similar

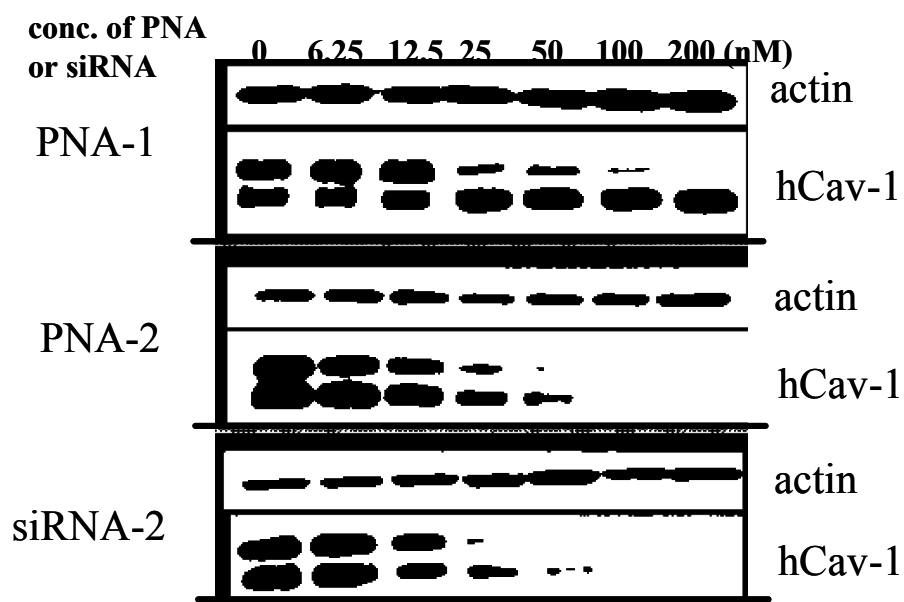


Figure 4-4. Inhibition of hCav-1 expression by varying concentrations of PNA 1, PNA 2, and siRNA 2.

*From: Liu Y., Braasch D.A., Nulf C.J., Corey D.R. (2004) Efficient and isoform-selective inhibition of cellular gene expression by peptide nucleic acids. *Biochemistry*. 43(7):1921-7.

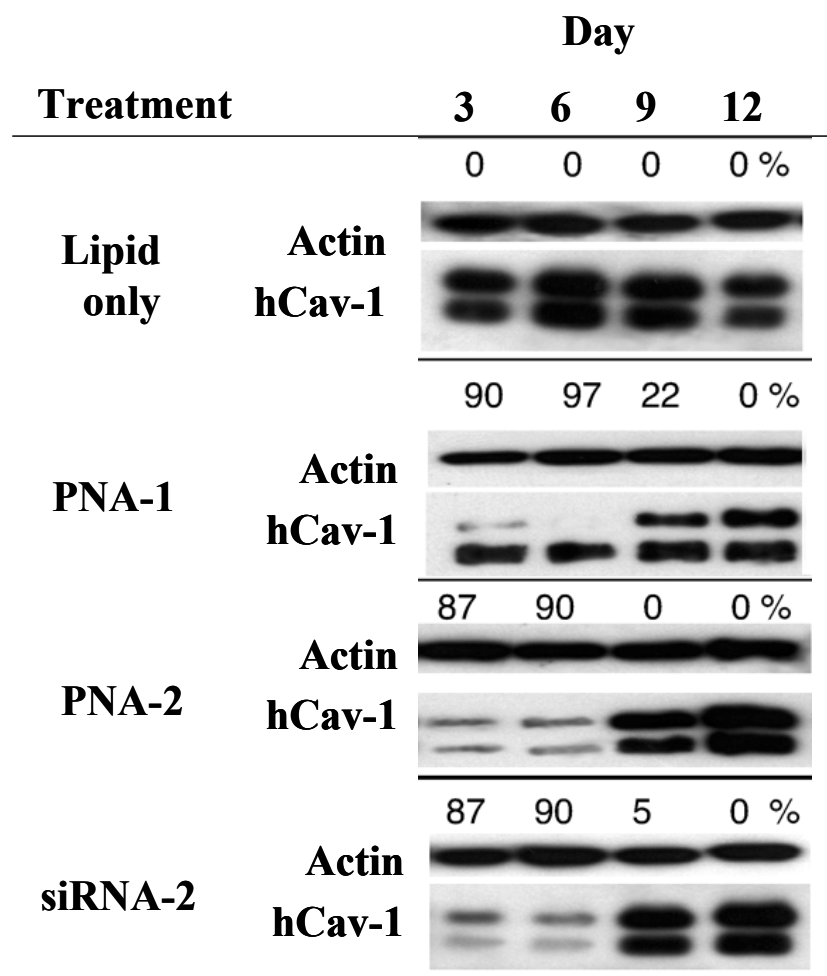


Figure 4-5. Time course of inhibition of hCav-1 expression by PNAs and siRNAs. Percent inhibition is noted above each lane. For cells treated with PNA 1, the percent inhibition refers to inhibition of the α -isoform. Percentages are calculated by comparison with cells treated with lipid alone. (A) Lipid only; (B) PNA 1 added; (C) PNA 2 added; and (D) siRNA 2 added.

*From: Liu Y., Braasch D.A., Nulf C.J., Corey D.R. (2004) Efficient and isoform-selective inhibition of cellular gene expression by peptide nucleic acids. *Biochemistry*. 43(7):1921-7.

tissue localization as other traditional antisense oligonucleotides (39, 40). Also, both PNAs and siRNA have demonstrated activity when administered *in vivo* (37, 41).

An important difference between PNAs and siRNAs is the mechanism by which inhibition is occurring. Destruction of a transcript may lead to unwanted phenotypes or misleading conclusions of gene function. This requires direct comparison of several antisense oligonucleotides with different mechanisms of action (e.g. steric, RNase-H activation, ribozyme-induced cleavage) for validating specificity of gene expression inhibition. Likewise, different chemically modified oligonucleotides will display different non-specific effects. Corroboration of a knock-down phenotype by different mechanisms strengthens the conclusions of a specific gene function.

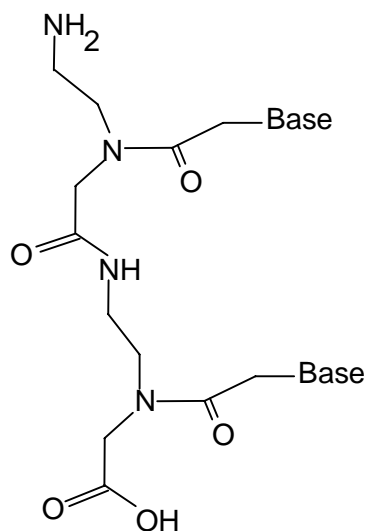
Comparison of PNAs with morpholinos for the inhibition of developmental genes in Zebrafish (with Dr. Stephen Ekker, The University of Minnesota)

Dr. Ekker at the University of Minnesota has interests in morpholino-based knock-down technology in Zebrafish embryogenesis (*Danio rerio*) (51). For comparison against known developmental phenotypes of knock-out mutants, Zebrafish embryos are microinjected with antisense morpholinos with the resulting knock-down phenotypes observed in F0 animals. Successful gene inactivation by morpholinos yields embryos with distinct morphologies termed "Morphants". His efforts have begun a genome-wide assignment of gene function based on sequence in a model vertebrate (52).

My role in the project was to synthesize PNAs targeting the chordino RNA transcript (among others) for direct comparison against antisense morpholinos.

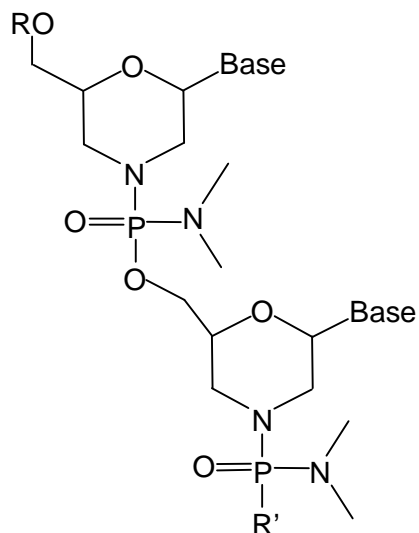
Background and chemistry of morpholino oligomers

Morpholino oligomers (Morpholinos - Gene Tools LLC) are synthetic DNA analogs with several shared biophysical properties as PNAs (56, for review 42). They are composed of a 6-member morpholine ring and a non-ionic phosphorodiamidate intersubunit linkage (Figure 4-6. Comparison of PNAs and morpholinos). Morpholinos bind to complementary nucleic acid sequences by Watson-Crick base-pairing. However, the affinity is no tighter than binding of analogous DNA and RNA oligonucleotides. The backbone makes morpholinos resistant to digestion by nucleases (43). Also, because the backbone lacks negative charge, it is thought that morpholinos are less likely to interact with cellular proteins, exerting low toxicity in cells.



Peptide Nucleic Acid (PNA)

2-aminoethyl glycine backbone
 Fmoc-based chemistries (compatible with
 peptide synthesis)
 Charge Neutral
 Increased nuclease and protease resistance
 Increased affinity



Morpholino

Non-ionic phosphorodiamidate intersubunit
 linkages of 6-member morpholino
 Phosphoroamidate chemical couplings
 Charge Neutral
 Increased nuclease and protease resistance
 Slight increased affinity

Figure 4-6. Comparison of PNAs and morpholinos. Morpholinos are proprietary to Gene Tools LLC, Corvallis, OR.

Analogous to antisense PNAs, antisense morpholinos exert a steric effect in blocking post-transcriptional activity and do not recruit RNase H (44). For example, morpholinos can be used to block pre-mRNA splicing events (45). When targeting intron-exon regions of the Zebrafish *fgf8* mRNA, 25-mer morpholinos can cause aberrantly spliced transcripts leading to a developmental phenotype similar to the mutant *fgf8*^{it282} (45, 49). Translation inhibition has also been demonstrated by morpholinos targeted to the 5'-UTR of transcripts. A 20-mer morpholino targeted to the 5'-UTR of c-myc lowered c-myc protein levels in treated cells and arrested cells in G0/G1 of the cell cycle (50). Binding prevents mRNA scanning by the 40S ribosomal subunit to the AUG start site. However, morpholinos targeting the coding region do not appear to stop ribosomal movement during protein synthesis (44). Compared to PNAs, most antisense applications use relatively long 25-base morpholinos for antisense gene inhibition. In spite of this, morpholinos have been used with great success in a number of animal models including zebrafish (45, 46), *Xenopus* (47), and rats (48).

Potential phenotypic outcomes of antisense experiments

When using antisense oligonucleotides to observe a knock-down phenotype, four situations could occur:

1. No effect, normal phenotype
2. Sequence-specific inhibition demonstrating mutant phenotype
3. Non-sequence-specific inhibition demonstrating mutant phenotype
4. Both specific and non-specific inhibition contributing to a mutant phenotype.

Distinguishing sequence-specific effects from non-specific effects is important for utilizing oligonucleotides as regulators of gene expression (53). Because PNAs have different backbone chemical composition from morpholinos, non-specific effects exerted by both will probably not overlap. Therefore, a common phenotype displayed by both antisense oligomers corroborates the true knock-down phenotype. While the work is still in progress, a couple of exciting results have been generated.

Antisense effects of morpholinos and PNAs on Zebrafish development

The chordino gene is an essential component of the dorsal organizer in Zebrafish (54). Mutations in the chordino gene give a morphological phenotype of abnormal u-shaped somites, reduced head, extremely expanded blood island, and abnormal tail fin (**Figure 4-7a, b. Morphologies of wild-type, mutant, and antisense morpholino-treated Zebrafish embryos**). Microinjecting an embryo with a 25-mer morpholino (1.5ng) targeting the AUG start site of the chordino transcript, recapitulates the same phenotype at 48 hours (**Figure 4-7c.**). Different degrees of severity in the phenotype can also be distinguished depending on experimental conditions (**Figure 4-8a. Degrees of severity of the chordino morphology phenotype**). To validate the specificity of the phenotype, 25-mer PNAs (1 ng) of the same sequence were microinjected into Zebrafish and the resulting phenotype was analyzed at 48 hours. With antisense PNAs, the same morphology as the Morphant was seen with different degrees of severity (**Figure 4-8b.**).



Figure 4-7. Morphologies of wild-type, mutant, and antisense morpholino-treated Zebrafish embryos. A.) Wild-type* B.) Chordino Mutant* C.) Chordino Morphant[‡]. Zebrafish were treated with morpholinos targeting Chordin RNA transcripts for 48 hours. Similar abnormal u-shaped somites, reduced head, extremely expanded blood island, and abnormal tail fin phenotype between the mutant and the morpholino-treated are seen.

*From: Schulte-Merker, et al. The zebrafish organizer requires chordino. Nature 387, 862-63 (1997).

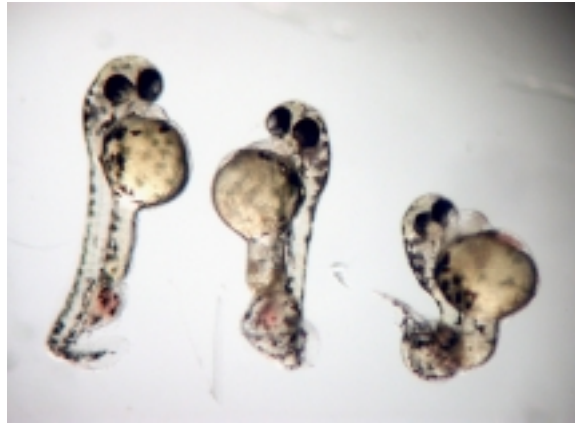
[‡]From: Ekker, Unpublished.

A.



Weak Moderate Severe

B.



Weak Moderate Severe

Figure 4-8. Degrees of severity of the mutant chordino morphological phenotype. Zebrafish embryos microinjected with either A.) antisense morpholinos or B.) antisense PNAs targeting chordino. The morpholino sequences and the PNA sequences are identical.

*From: Ekker, Unpublished.

These results suggest that the phenotype generated at 48 hours is the result of targeting the chordino transcript and not a non-specific result due to the morpholino chemical composition. Antisense PNAs targeting the Sonic Hedgehog (Shh) gene are still in progress.

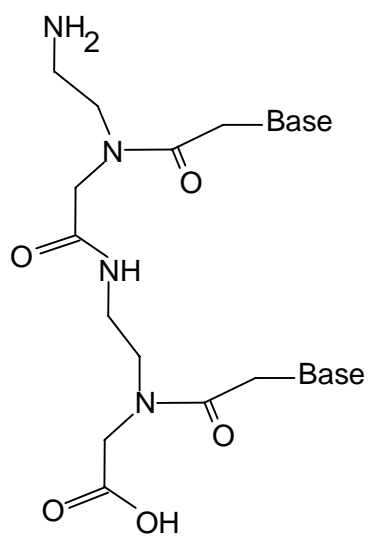
Researchers are currently using several other oligonucleotide analogs as tools to study developmental systems including those with positively charged backbones (76). While the use of morpholinos hasn't progressed as far as PNAs, there are a large number of on-going studies elucidating the potentials of morpholinos as tools for investigating gene function (55, 44).

Comparison of PNAs with 2'-O-(2-methoxyethyl) oligoribonucleotides (2'-MOE) for re-directing pre-mRNA splicing events (with Dr. Brett Monia, ISIS Pharmaceuticals)

At ISIS Pharmaceuticals, Dr. Brett Monia's interests involve drug target validation in cells by modified oligonucleotides. As the leaders in oligonucleotide antisense research and the only pharmaceutical company to have an FDA approved therapeutic antisense oligonucleotide (**60, 61**) there is the desire to find new and compelling genes that can be regulated by modified oligonucleotides. To corroborate recent findings in Dr. Monia's lab of alteration in splicing activity by 2'-O-(2-methoxyethyl) oligoribonucleotides (2'-MOE) (see below), I synthesized several PNAs that targeted the same RNA sequences for side-by-side comparisons.

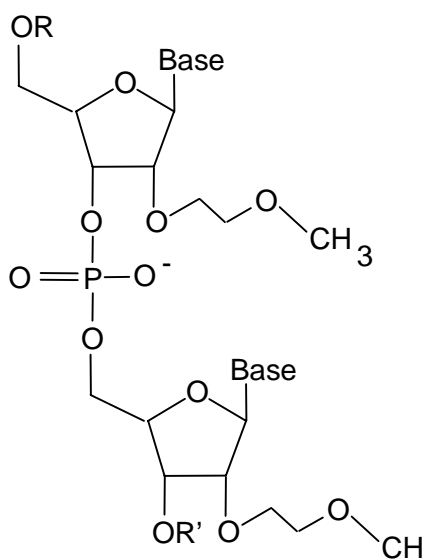
Background and chemistry of 2'-O-(2-methoxyethyl) oligoribonucleotides (2'-MOE)

The 'second generation' antisense oligonucleotides, 2'-O-(2-methoxyethyl) (2'-MOE), are a modification of the normal phosphodiester RNA molecule in that a methoxyethyl group extends from the 2'-OH of the ribose (**Figure 4-9. Comparison of PNAs and 2'-O-methoxyethyl RNA (2'-MOE)**). This alkyl modification in the sugar moiety adds affinity to the oligonucleotide for complementary target (**57**), increases nuclease resistance (**57**) and demonstrates lowered toxicity to cells than the 'first generation' phosphorothioates (**58**). Also, 2'-O-alkyl RNA cannot induce RNase H cleavage of the target RNA (**59**). So, like PNAs, 2'MOE's antisense mechanism of action is steric inhibition of translation.



Peptide Nucleic Acid (PNA)

2-aminoethyl glycine backbone
 Fmoc-based chemistries (compatible with
 peptide synthesis)
 Charge Neutral
 Increased nuclease and protease resistance
 Increased affinity



2'-O-methoxyethyl RNA (2'-MOE)

Phosphodiester backbone
 Phosphoramidate chemistries (compatible
 with DNA/RNA synthesis)
 Negatively charged
 2'OH group modified with methoxyethyl
 group
 Slight increased affinity for target
 Increased nuclease resistance

Figure 4-9. Comparison of PNAs and 2'-MOE.

The capacity of 2'-MOE oligonucleotides to inhibit translation initiation was first demonstrated when the expression of the intercellular adhesion molecule 1 (ICAM-1) was inhibited with an RNase H-independent 2'-*O*-methoxyethyl-modified antisense oligonucleotide that was targeted against the 5'-cap region (67). Another report illustrated the ability of 2'-MOE in altering splicing events when targeted to an aberrant splice site generated from a mutation in intron 2 of the β -globin gene, the cause of the genetic blood disorder β -thalassemia. Blocking the splice site corrects splicing of the β -globin transcript, reversing the disease (68).

The model target: Human insulin receptor α -subunit

Insulin resistance is a common abnormality in patients with myotonic dystrophy (DM). The most common form of DM is muscular dystrophy associated with an adult and congenital onset. The mechanism of insulin resistance in DM is unknown, but evidence supports alterations in surface receptor function (62). Alternative splicing events of the human insulin receptor α -subunit pre-mRNA (63) lead to the generation of two isoforms of the receptor: IR-A (without an additional exon) and IR-B (with an additional exon) (64) (**Figure 4-10. Alternative splicing mechanism of the human insulin receptor α -subunit**). The IR-B isoform is responsive to insulin and found predominantly in liver, skeletal muscle, and fat tissues. Isoform IR-A shows a decrease in signaling capacity to the inside of the cell upon insulin binding to the extracellular domain (65). A switch from the IR-B isoform to the IR-A isoform contributes to the decreased insulin sensitivity observed in DM patients (66).

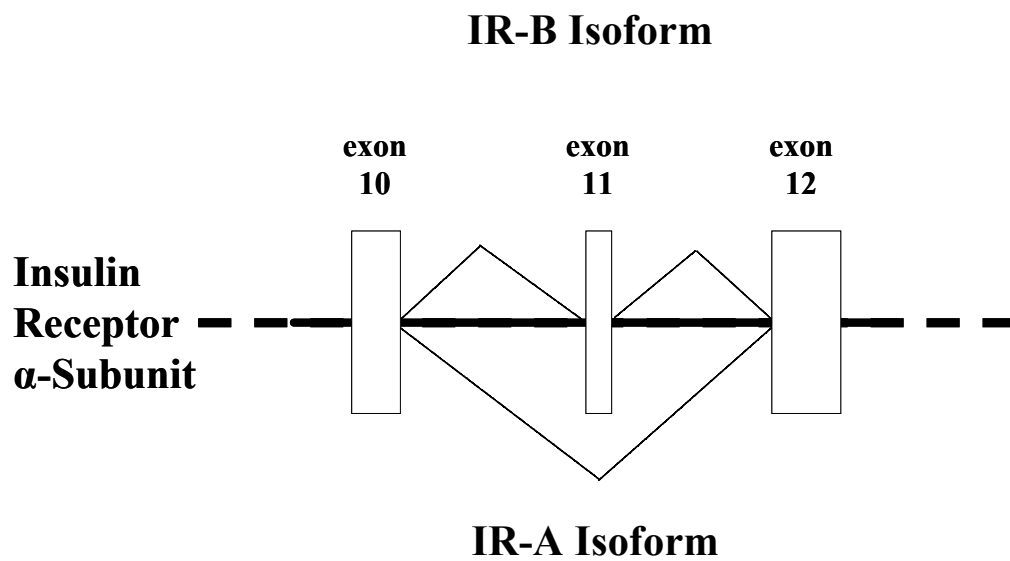


Figure 4-10. Alternative splicing mechanism of the insulin receptor α -subunit. The IR-B Isoform is insulin-responsive (found in muscle, liver, and adipose tissues). IR-A Isoform is not insulin-responsive (found in non-muscle tissue).

Efficiency of re-directing splicing events by PNAs and 2'MOE

To demonstrate the ability of an oligonucleotide to re-direct splicing events, 2'-MOE and PNAs were chosen to target the mouse Insulin Receptor (mIR) pre-mRNA transcript at the intron-exon 11 region. Because the best sequence to target by PNAs was unknown, several different PNAs were synthesized to the same intron-exon region for comparison to a 20-mer 2'-MOE (**Table 4-2. Comparison of the sequences of 2'-O-methoxyethyl and the PNA sequences and their relative position targeting the intron-exon junction**). Successful targeting of the intron-exon region re-directs RNA processing from IR-B (containing exons 10,11,12) to IR-A (containing exons 10 and 12). These molecules were electroporated into AML cell cultures and assayed for antisense activity by RT-PCR 20 hours later.

The 2'-MOE(205142) elicited the greatest effect in reducing IR-B mRNA and increasing IR-A mRNA relative to the untreated control cells (**Figure 4-11. Analysis of re-directed splicing event**). The scrambled control 2'-MOE(158641) also did not have effect on IR-B or IR-A mRNA levels suggesting that the activity of 2'-MOE(205142) is not a non-specific response to the oligonucleotide chemistry. PNA-BM01, a 20-mer PNA with the exact same sequence as the 2'-MOE, was approximately 85% as effective as the 2'-MOE in lowering IR-B and raising IR-A mRNA levels at 10 μ M concentrations.

Only modest altered splicing activities were demonstrated by the shorter 15-mer PNAs. The scrambled PNA control did not alter IR-B or IR-A mRNA levels (relative to the untreated control cells) suggesting that the activities elicited by the PNAs are not

Uniform MOE (5' to 3')

205412	(81666) <u>ACCTACTGTCCTCGGCACCA</u> (81685)	intron <u>exon11</u>
--------	---	-----------------------------

Corey PNA Oligos (N-termial amine to C-terminal lysine amide)

BM-01	<u>ACCTACTGTCCTCGGCACCA</u> - K	intron <u>exon11</u>
BM-02	<u>TGTCCTCGGCACCAT</u> – K	intron <u>exon11</u>
BM-03	<u>ACTGTCCTCGGCACC</u> – K	intron <u>exon11</u>
BM-04	<u>CTACTGTCCTCGGCA</u> – K	intron <u>exon11</u>
BM-05	<u>ACCTACTGTCCTCGG</u> – K	intron <u>exon11</u>
BM-06	<u>ATACCTACTGTCCTC</u> - K	intron <u>exon11</u>

Table 4-2. Comparison of the sequences of 2'-O-methoxyethyl and the PNA sequences and their relative position targeting the intron-exon junction. Bases in bold target the intron.

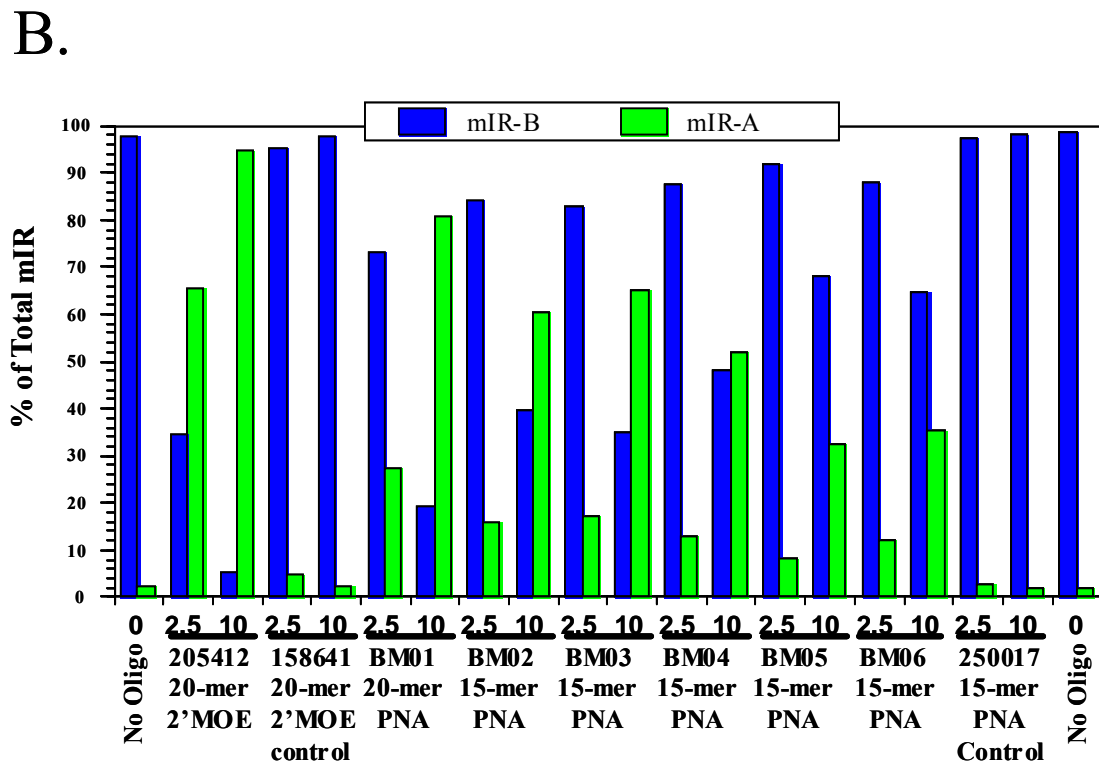
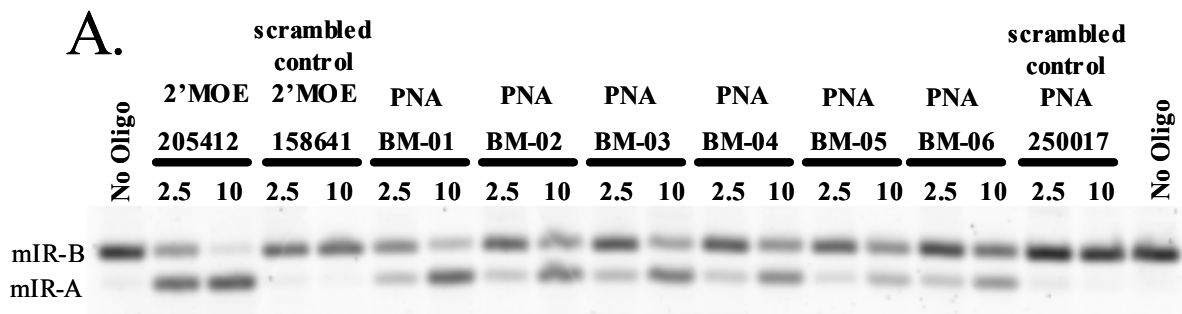


Figure 4-11. Analysis of re-directed splicing event A.) RT-PCR of mIR-B and mIR-A following treatment with 2'-MOE or PNA. AML cells were electroporated with either 2.5 or 10 μ M oligonucleotide and harvested at 20 hours. B.) Quantitation of mIR as a percent of total RNA. GraphPad Prism analysis program was used to analyze data.

*From: Monia, Unpublished.

result of the backbone chemistry. A comparison of the EC₅₀s for each oligonucleotide (**Figure 4-12. Comparison of oligonucleotide splicing inhibition EC₅₀s**) demonstrates that for this particular target, the 20-mer 2'-MOE oligonucleotide works slightly better than the PNAs at re-directing splicing activity.

The future of 2'MOE and PNAs as therapeutics

Recent experiments have progressed both 2'-MOE oligonucleotides and PNAs toward *in vivo* applications. When injected systemically into transgenic mouse, PNAs (with 4 lysines) efficiently targeting an aberrant splice site in a mutated intron of a human β -globin-eGFP transgene restored correct splicing events leading to expression of eGFP (37). 2'-MOE oligonucleotides demonstrated greater potency and lower toxicity versus phosphorothioates when targeting the apoptosis-inducing gene clusterin of prostate cancer xenografts *in vivo* (69). In addition, antisense oligonucleotides with 2'-*O*-methoxyethyl modifications mixed with phosphorothioate backbone after were shown to have antitumor activity in mice after oral administration (70). These successful results have lead to clinical trials of 'second generation' antisense oligonucleotides targeting TNF- α in treatment of rheumatoid arthritis. In January 2004, from Phase II clinical trials, data from ISIS Pharmaceuticals demonstrated that the 2'-MOE targeting TNF- α produced a statistically significant disease response in patients with rheumatoid arthritis (RA) with no serious adverse effects (71). Further experimentation will result in novel disease targets, better regulation of gene expression, and greater biodistribution for therapeutic use of chemically modified antisense oligonucleotides.

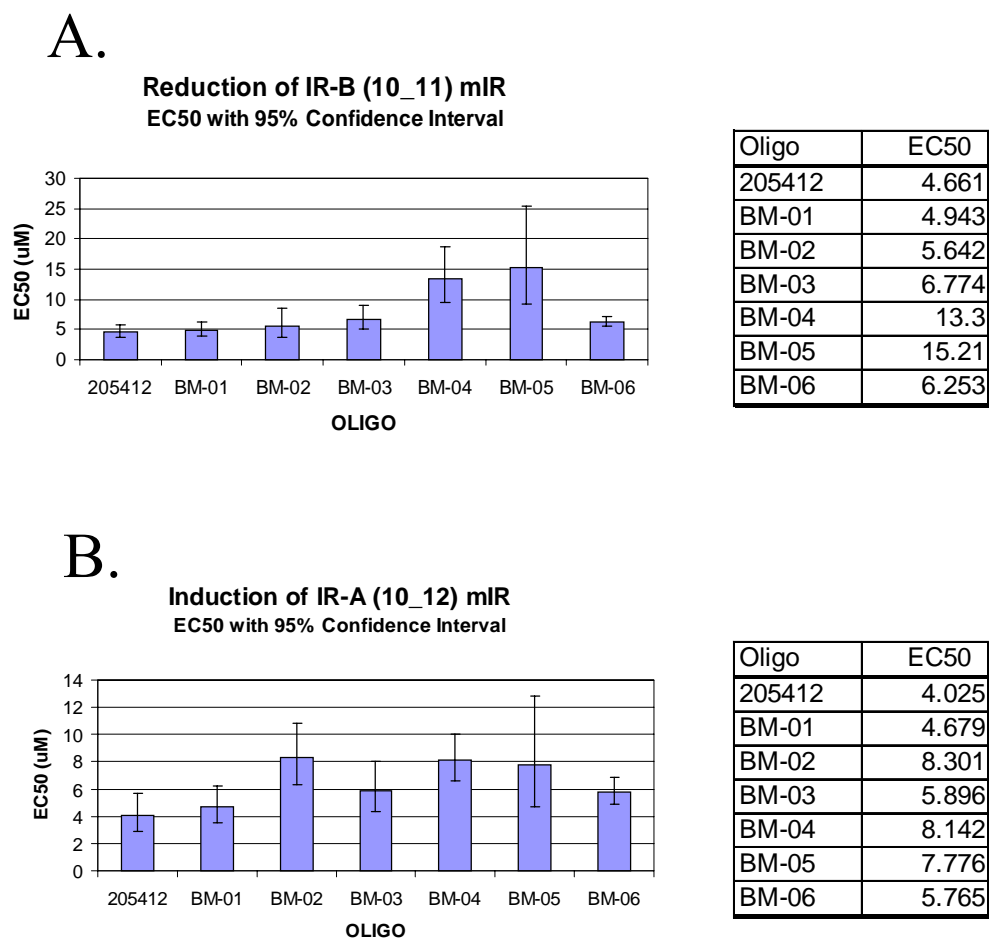


Figure 4-12. Comparison of oligonucleotide splicing inhibition EC₅₀s A.) the reduction of IR-B mIR levels and B.) the induction of IR-A mIR RNA levels. Splicing was quantitated by Taqman RT-PCR and EC₅₀s for reduction of IR-B mouse Insulin Receptor (mIR) mRNA (exons 10_11_12) splicing and induction of IR-A mIR mRNA (exons10_12) in AML cells electroporated with oligonucleotide.

*From: Monia, Unpublished.

References for Chapter 4

- 1 Kurreck J. (2003) Antisense technologies. Improvement through novel chemical modifications. *Eur. J. Biochem.* 270(8):1628-44.
- 2 Ravichandran L.V., Dean N.M., Marcusson E.G. (2004) Use of antisense oligonucleotides in functional genomics and target validation. *Oligonucleotides*. 14(1):49-64.
- 3 Lavery K.S, King T.H. (2003) Antisense and RNAi: powerful tools in drug target discovery and validation. *Curr. Opin. Drug Discov. Devel.* 6(4):561-9.
- 4 Elbashir S.M., Harborth J., Lendeckel W., Yalcin A., Weber K., Tuschl T. (2001) Duplexes of 21-nucleotide RNAs mediate RNA interference in cultured mammalian cells. *Nature*. 411(6836):494-8.
- 5 Elbashir S.M., Lendeckel W., Tuschl T. (2001) RNA interference is mediated by 21- and 22-nucleotide RNAs. *Genes Dev.* 15(2):188-200.
- 6 Lim L.P., Glasner M.E., Yekta S., Burge C.B., Bartel D.P. (2003) Vertebrate microRNA genes. *Science*. 299(5612):1540.
- 7 Lee S.W., Gallardo H.F., Gilboa E., Smith C. (1994) Inhibition of human immunodeficiency virus type 1 in human T cells by a potent Rev response element decoy consisting of the 13-nucleotide minimal Rev-binding domain. *J. Virol.* 68(12):8254-64.
- 8 Nishitsuji H., Tamura Y., Fuse T., Habu Y., Miyano-Kurosaki N., Takaku H. (2001) Inhibition of HIV-1 replication by 5'LTR decoy RNA. *Nucleic Acids Res. Suppl.* (1):141-2.

- 9 Sledz C.A., Holko M., de Veer M.J., Silverman R.H., Williams B.R. (2003). Activation of the interferon system by short-interfering RNAs. *Nat. Cell Biol.* 5: 834-839.
- 10 Agrawal S. (1999) Importance of nucleotide sequence and chemical modifications of antisense oligonucleotides. *Biochim. Biophys. Acta.* 1489(1):53-68.
- 11 Jackson A.L., Bartz S.R., Schelter J., Kobayashi S.V., Burchard J., Mao M., Li B., Cavet G., Linsley P.S. (2003) Expression profiling reveals off-target gene regulation by RNAi. *Nat. Biotechnol.*(6):635-7.
- 12 Saxena S., Jonsson Z.O., Dutta A. (2003). Small RNAs with imperfect match to endogenous mRNA repress translation: Implications for off-target activity of siRNA in mammalian cells. *J. Biol. Chem.* 278: 44312-44319.
- 13 Liu Y., Braasch D.A., Nulf C.J., Corey D.R. (2004) Efficient and isoform-selective inhibition of cellular gene expression by peptide nucleic acids. *Biochemistry.* 43(7):1921-7.
- 14 Hanvey J.C., Peffer N.J., Bisi J.E., Thomson S.A., Cadilla R., Josey J.A., Ricca D.J., Hassman C.F., Bonham M.A., Au K.G., et al. (1992) Antisense and antigene properties of peptide nucleic acids. *Science.* 258(5087):1481-5.
- 15 Bonham M.A., Brown S., Boyd A.L., Brown P.H., Bruckenstein D.A., Hanvey J.C., Thomson S.A., Pipe A., Hassman F., Bisi J.E., et al. (1995) An assessment of the antisense properties of RNase H-competent and steric-blocking oligomers. *Nucleic Acids Res.* 23(7):1197-203.
- 16 Doyle D.F., Braasch D.A., Simmons C.G., Janowski B.A., Corey D.R. (2001) Inhibition of gene expression inside cells by peptide nucleic acids: effect of mRNA target sequence, mismatched bases, and PNA length. *Biochemistry.* 40(1):53-64.

- 17 Smart E.J., Graf G.A., McNiven M.A., Sessa W.C., Engelman J.A., Scherer P.E., Okamoto T., Lisanti M.P. (1999) Caveolins, liquid-ordered domains, and signal transduction. *Mol. Cell Biol.* 19(11):7289-304.
- 18 Liu P., Rudick M., Anderson R.G. (2002) Multiple functions of caveolin-1. *J. Biol. Chem.* 277(44):41295-8.
- 19 Scherer P.E., Tang Z., Chun M., Sargiacomo M., Lodish H.F., Lisanti M.P. (1995) Caveolin isoforms differ in their N-terminal protein sequence and subcellular distribution. Identification and epitope mapping of an isoform-specific monoclonal antibody probe. *J. Biol. Chem.* 270(27):16395-401.
- 20 Ramirez M.I., Pollack L., Millien G., Cao Y.X., Hinds A., Williams M.C. (2002) The alpha-isoform of caveolin-1 is a marker of vasculogenesis in early lung development. *J. Histochem. Cytochem.* 50(1):33-42.
- 21 Aldred M.A., Ginn-Pease M.E., Morrison C.D., Popkie A.P., Gimm O., Hoang-Vu C., Krause U., Dralle H., Jhiang S.M., Plass C., Eng C. (2003) Caveolin-1 and caveolin-2, together with three bone morphogenetic protein-related genes, may encode novel tumor suppressors down-regulated in sporadic follicular thyroid carcinogenesis. *Cancer Res.* 63(11):2864-71.
- 22 Moskalenko S., Henry D., Rose C. Mirey C., Camonis J., and White M. A. (2002) The exocyst is a Ral effector complex. *Nature Cell Biology.* Vol 4:66-72.
- 23 DeMoor J.M., Vincent M.D., Collins O.M., Koropatnick J. (1998) Antisense nucleic acids targeted to the thymidylate synthase (TS) mRNA translation start site stimulate TS gene transcription. *Exp. Cell. Res.* 243(1):11-21.

- 24 Chavany C., Connell Y., Neckers L. (1995) Contribution of sequence and phosphorothioate content to inhibition of cell growth and adhesion caused by c-myc antisense oligomers. *Mol. Pharmacol.* 48(4):738-46.
- 25 Hamilton S.E., Simmons C.G., Kathiriya I.S., Corey D.R. (1999) Cellular delivery of peptide nucleic acids and inhibition of human telomerase. *Chem Biol.*(6):343-51.
- 26 Braasch D.A., Jensen S., Liu Y., Kaur K., Arar K., White M.A., Corey D.R. (2003) RNA interference in mammalian cells by chemically-modified RNA. *Biochemistry.* 42(26):7967-75.
- 27 Martinez J., Tuschl T. (2004) RISC is a 5' phosphomonoester-producing RNA endonuclease. *Genes Dev.* 18(9):975-80.
- 28 Persengiev S.P., Zhu X., Green M.R. (2004). Nonspecific, concentration-dependent stimulation and repression of mammalian gene expression by small interfering RNAs (siRNAs). *RNA.* 10: 12-18.
- 29 Chi J.T., Chang H.Y., Wang N.N., Chang D.S., Dunphy N., and Brown P.O. (2003) Genomewide view of gene silencing by small interfering RNAs. *Proc. Natl. Acad. Sci. U. S. A.* 100, 6343–6346.
- 30 Lassus P., Rodriguez J., Lazebnik Y. (2002) Confirming specificity of RNAi in mammalian cells. *Sci STKE.* (147):PL13.
- 31 Tang G., Zamore P.D. (2004) Biochemical dissection of RNA silencing in plants. *Methods Mol. Biol.* 257:223-44.

- 32 Chiu Y.L., Rana T.M. (2002) RNAi in human cells: basic structural and functional features of small interfering RNA. *Mol. Cell.* 10(3):549-61.
- 33 Vickers T.A., Koo S., Bennett C.F., Crooke S.T., Dean N.M., Baker B.F. (2003) Efficient reduction of target RNAs by small interfering RNA and RNase H-dependent antisense agents. A comparative analysis. *J. Biol. Chem.* 278(9):7108-18.
- 34 Xu Y., Linde A., Larsson O., Thormeyer D., Elmen J., Wahlestedt C., Liang Z. (2004) Functional comparison of single- and double-stranded siRNAs in mammalian cells. *Biochem. Biophys. Res. Commun.* 316(3):680-7.
- 35 Yokota T., Miyagishi M., Hino T., Matsumura R., Tasinato A., Urushitani M., Rao R.V., Takahashi R., Bredesen D.E., Taira K., Mizusawa H. (2003) siRNA-based inhibition specific for mutant SOD1 with single nucleotide alternation in familial ALS, compared with ribozyme and DNA enzyme. *Biochem. Biophys. Res. Commun.* 314(1):283-91.
- 36 Koppelhus U., Awasthi S.K., Zachar V., Holst H.U., Ebbesen P., Nielsen P.E. (2002) Cell-dependent differential cellular uptake of PNA, peptides, and PNA-peptide conjugates. *Antisense Nucleic Acid Drug Dev.* 12(2):51-63.
- 37 Sazani P., Gemignani F., Kang S.H., Maier M.A., Manoharan M., Persmark M., Bortner D., Kole R. (2002) Systemically delivered antisense oligomers upregulate gene expression in mouse tissues. *Nat. Biotechnol.* 20(12):1228-33.
- 38 Braasch D.A., Paroo Z., Constantinescu A., Ren G., Oz O.K., Mason R.P., Corey D.R. (2004) Biodistribution of phosphodiester and phosphorothioate siRNA. *Bioorg. Med. Chem. Lett.* 14(5):1139-43.

- 39 Lee P.A., Blatt L.M., Blanchard K.S., Bouhana K.S., Pavco P.A., Bellon L., Sandberg J.A. (2000) Pharmacokinetics and tissue distribution of a ribozyme directed against hepatitis C virus RNA following subcutaneous or intravenous administration in mice. *Hepatology*. 32(3):640-6.
- 40 Monteith D.K., Geary R.S., Leeds J.M., Johnston J., Monia B.P., Levin A.A. (1998) Preclinical evaluation of the effects of a novel antisense compound targeting C-raf kinase in mice and monkeys. *Toxicol Sci*. 46(2):365-75.
- 41 Zender L., Hutker S., Liedtke C., Tillmann H.L., Zender S., Mundt B., Waltemathe M., Gosling T., Flemming P., Malek N.P., Trautwein C., Manns M.P., Kuhnel F., Kubicka S. (2003) Caspase 8 small interfering RNA prevents acute liver failure in mice. *Proc. Natl. Acad. Sci. U.S.A.* 100(13):7797-802.
- 42 Summerton J. (1999) Morpholino antisense oligomers: the case for an RNase H-independent structural type. *Biochim. Biophys. Acta*. 1489:141-158.
- 43 Hudziak R.M., Barofsky E., Barofsky D.F., Weller D.L., Huang S.B., Weller D.D. (1996) Resistance of morpholino phosphorodiamidate oligomers to enzymatic degradation. *Antisense Nucleic Acid Drug Dev*. 6(4):267-72.
- 44 Summerton J., Stein D., Huang S.B., Matthews P., Weller D., Partridge M. (1997) Morpholino and phosphorothioate antisense oligomers compared in cell-free and in-cell systems. *Antisense Nucleic Acid Drug Dev*. 7(2):63-70.
- 45 Draper B.W., Morcos P.A., Kimmel C.B. (2001) Inhibition of zebrafish fgf8 pre-mRNA splicing with morpholino oligos: a quantifiable method for gene knockdown. *Genesis*. 30(3):154-6.

- 46 Nasevicius A., Ekker S.C. (2000) Effective targeted gene 'knockdown' in zebrafish. *Nat. Genet.* 26:216.
- 47 Heasman J., Kofron M., & Wylie C. (2000) β -Catenin signalling activity dissected in the early *Xenopus* embryo: a novel antisense approach. *Dev. Biol.* 222:124-134.
- 48 Arora V., Knapp D.C., Reddy M.T., Weller D.D., Iversen P.L. (2002) Bioavailability and efficacy of antisense morpholino oligomers targeted to c-myc and cytochrome P-450 3A2 following oral administration in rats. *J. Pharm. Sci.* 91(4):1009-18.
- 49 Reifers F., Bohli H., Walsh E.C., Crossley P.H., Stainier D.Y., Brand M. (1998) Fgf8 is mutated in zebrafish acerebellar (ace) mutants and is required for maintenance of midbrain-hindbrain boundary development and somitogenesis. *Development.* 125(13):2381-95.
- 50 Hudziak R.M., Summerton J., Weller D.D., Iversen P.L. (2000) Antiproliferative effects of steric blocking phosphorodiamidate morpholino antisense agents directed against c myc. *Antisense Nucleic Acid Drug Dev.* 10(3):163-76.
- 51 Ekker S.C. (2000) Morphants: a new systematic vertebrate functional genomics approach. *Yeast.* 17:302-306.
- 52 Ekker, S.C. The Morphant Database http://beckmancenter.ahc.umn.edu/morpholino_database.html
- 53 Branch A.D. (1998) A good antisense molecule is hard to find. *Trends Biochem. Sci.* 23:45-50.
- 54 Schulte-Merker S., Lee K.J., McMahon A.P., Hammerschmidt M. (1997) The zebrafish organizer requires chordino. *Nature.* 387(6636):862-3.

- 55 Stein D., Foster E., Huang S.B., Weller D., Summerton J.A (1997) Specificity comparison of four antisense types: morpholino, 2'-O-methyl RNA, DNA, and phosphorothioate DNA. *Antisense Nucleic Acid Drug Dev.* 7(3):151-7.
- 56 Summerton J., Weller D. (1997) Morpholino antisense oligomers: design, preparation, and properties. *Antisense Nucleic Acid Drug Dev.* 7(3):187-95.
- 57 Kurreck J., Wyszko E., Gillen C. & Erdmann V.A. (2002) Design of antisense oligonucleotides stabilized by locked nucleic acids. *Nucleic Acids Res.* 30, 1911-1918.
- 58 Levin A.A. (1999) A review of the issues in the pharmacokinetics and toxicology of phosphorothioate antisense oligonucleotides. *Biochim Biophys Acta.* 1489(1):69-84.
- 59 Zamaratski E., Pradeepkumar P.I., Chattopadhyaya J. (2001) A critical survey of the structure-function of the antisense oligo/RNA heteroduplex as substrate for RNase H. *J. Biochem. Biophys. Methods.* 48(3):189-208.
- 60 Geary R.S., Henry S.P., Grillone L.R. (2002) Fomivirsen: clinical pharmacology and potential drug interactions. *Clin. Pharmacokinet.* 41(4):255-60.
- 61 Marwick C. (1998) First 'antisense' drug will treat CMV retinitis. *J. Am. Med. Assoc.* 280, 871.
- 62 Moxley R.T., Corbett A.J., Minake, K.L. & Rowe J.W. (1984) Whole body insulin resistance in myotonic dystrophy. *Ann. Neurol.* 15, 157–162.
- 63 Seino S. & Bell G.I. (1989) Alternative splicing of human insulin receptor messenger RNA. *Biochem. Biophys. Res. Commun.* 159, 312–316.

- 64 Moller D.E., Yokota A., Caro J.F. & Flier J.S. (1989) Tissue-specific expression of two alternatively spliced insulin receptor mRNAs in man. *Mol. Endocrinol.* 3, 1263–1269.
- 65 Kellerer M., Lammers R., Ermel B., Tippmer S., Vogt B., Obermaier-Kusser B., Ullrich A., Haring HU. (1992) Distinct alpha-subunit structures of human insulin receptor A and B variants determine differences in tyrosine kinase activities. *Biochemistry.* 31(19):4588-96.
- 66 Savkur R.S., Philips A.V., Cooper T.A. (2001) Aberrant regulation of insulin receptor alternative splicing is associated with insulin resistance in myotonic dystrophy. *Nat. Genet.* 29(1):40-7.
- 67 Baker B.F., Lot S.S., Condon T.P., Cheng-Flournoy S., Lesnik E.A., Sasmor H.M. & Bennett C.F. (1997) 2'-O-(2-methoxy) ethyl-modified anti-intercellular adhesion molecule 1 (ICAM-1) oligonucleotides selectively increase the ICAM-1 mRNA level and inhibit formation of the ICAM-1 translation initiation complex in human umbilical vein endothelial cells. *J. Biol. Chem.* 272, 11994-12000.
- 68 Sierakowska H., Sambade M., Agrawal S. & Kole R. (1996) Repair of thalassemic human β -globin mRNA in mammalian cells by antisense oligonucleotides. *Proc. Natl Acad. Sci. USA.* 93, 12840-12844.
- 69 Zellweger T., Miyake H., Cooper S., Chi K., Conklin B.S., Monia B.P., Gleave M.E. (2001) Antitumor activity of antisense clusterin oligonucleotides is improved in vitro and in vivo by incorporation of 2'-O-(2-methoxy)ethyl chemistry. *J. Pharmacol. Exp. Ther.* 298(3):934-40.
- 70 Wang H., Cai Q., Zeng X., D. Agrawal S. & Zhang R. (1999) Antitumor activity and pharmacokinetics of a mixed-backbone antisense oligonucleotide targeted to the R1 α subunit of protein kinase A after oral administration. *Proc. Natl. Acad. Sci. USA.* 96, 13989-13994.

- 71 "ISIS Pharmaceuticals Reports Positive Data from Phase 2 Clinical Trial of ISIS 104838 in Rheumatoid Arthritis." Carlsbad, Calif., Jan. 5, 2004 /PRNewswire-FirstCall.
- 72 Gaudreault S.B., Dea D., Poirier J. (2004) Increased caveolin-1 expression in Alzheimer's disease brain. *Neurobiol. Aging*. 25(6):753-9.
- 73 Fire A., Xu S., Montgomery M. K., Kostas S. A., Driver S. E., and Mello C. C. (1998) *Nature*. 391, 806–811.
- 74 Hammond S.M., Bernstein E., Beach D., Hannon G.J. (2000) An RNA-directed nuclease mediates post-transcriptional gene silencing in *Drosophila* cells. *Nature*. 404(6775):293-6.
- 75 Dykxhoorn D.M., Novina C.D., Sharp P.A. (2003) Killing the messenger: short RNAs that silence gene expression. *Nat. Rev. Mol. Cell Biol.* 4(6):457-67.
- 76 Dagle J.M, Weeks D.L. (2000) Selective degradation of targeted mRNAs using partially modified oligonucleotides. *Methods Enzymol.* 313:420-36.
- 77 Caplen N.J., Mousses S. (2003) Short interfering RNA (siRNA)-mediated RNA interference (RNAi) in human cells. *Ann. N.Y. Acad. Sci.* 1002:56-62.

CHAPTER 5 – WORDS OF WISDOM FOR THE NEW USER

	<u>Page</u>
Introduction	172
Commit to details	173
Design simple protocols with sensitive assays	173
Oligomers as controls	175
Critique the work	176
Progress towards complexity	178
References for Chapter 5	180

Introduction

"It is a miracle that curiosity survives formal education."

-- Albert Einstein

Working with PNA oligomers over the past five years has given me the thrills and frustrations that I am sure to repeat throughout my career as a scientist. However, those interspersed moments of "insight" when an experiment works perfectly or an idea materializes, far exceeds cerebral fulfillment to those long stretches of time when confounding and perplexing data are the norm. It is probably this intellectual rollercoaster ride that will keep me in the lab for years to come.

My initial attraction to working with nucleic acid-binding PNA oligomers was the wide array of potential applications that could be explored. While the simplicity of antisense mechanisms to control viral gene expression was obvious to me (Chapter 3), the creative aspects of synthesizing PNAs as "molecular Legos™" to build supramolecular nanostructures revealed new (and then, underappreciated) interests in chemistry and biophysics of macromolecular assembly (Chapter 2). Recent advances in the emerging fields of nanoelectromechanical systems, DNA computing, and nanomedical applications (drug delivery systems and diagnostics) certainly have sparked my creative interests and broadened the number of possible career avenues to follow.

In the following chapter are a few "words of wisdom" for those individuals who want to embark into the creative world of PNAs. These are just a few of the scientific fundamentals that I found useful not only when designing experiments dealing with PNAs or antisense mechanisms, but as an inquisitive researcher seeking those moments of "insight".

Commit to the details

"If we knew what we were doing, it wouldn't be called research, would it?"

-- Albert Einstein

If there was one principal theme accentuated throughout my graduate career with PNAs, it is that commitment to details is critical for the success of experiments. PNAs are not difficult to work with so long as there is some dedication to the specifics of the protocols. Omitting the simple step of "heating the PNA solution, 5 minutes at 70°C prior to use" may cause weeks of negative experimental results, and even greater mental frustration when the error is discovered. Similarly, in an "antisense" lab where several parallel projects are on-going, the experimental protocols for one project may not be applicable to another. Each project will have different nuances relative to another, be they oligonucleotide chemistries, nucleic acid targets, mechanisms of action, cell lines, and reporter assays, to name just a few. Even something as (presumed) trivial as buffer solutions can alter experimental results. Oversimplifying the conclusions or interpretation of data from one project can lead to misinformation given to another. This necessitates the optimization of experimental conditions for each individual's project.

Design simple protocols with sensitive assays

"In the middle of difficulty lies opportunity."

-- Albert Einstein

The basic premise of PNA hybridization lends itself to innumerable creative directions for future applications. But, because researchers have been working with PNAs since 1991, it is often the fundamental principles that are assumed and forgotten to

make way for the much more complex, detailed, and so-called exciting experiments. The more complex an experiment is, though, the more difficult it is to troubleshoot when problems arise and the more difficult it is to explain confounding (or perhaps even conflicting) results. Designing simple assays with credible controls can go a long way to answering the question “Can my PNA hybridize to a nucleic acid target?”

For example, the concept of antisense gene regulation is simple in premise, but often difficult to demonstrate with convincing experimental evidence. The earliest reports of oligonucleotides inhibiting gene expression in tissue culture and *in vivo* were encouraging (1, 2), yet ultimately determined to be flawed and criticized due to lack of adequate controls for the complex biological systems (3, 4).

Although the Corey lab had already established itself with numerous publications in oligonucleotide-based antisense research (5, 6, 7, 8, 9), during the conception of my HCV IRES antisense project I made attempts towards increasing the credibility of results by simplify protocols and increasing sensitivity of the assays. For example, I chose to use a single plasmid for constitutive expression of both control and target genes, versus a complex chemically-inducible 3 plasmid co-transfection protocol described in a previous report (5). Using only one vector not only simplifies the transfection protocol (and prior plasmid preparations from E. Coli.) but also ensures that each transfected cell contains an identical number of both genes.

In addition, a bioluminescence-based assay for Renilla luciferase activity was chosen for the control gene rather than an assay based on colorimetric determination of β -galactosidase activity previously used (5, 6). The sensitivity of Renilla luciferase activity is approximately 100-1000 greater than β -galactosidase activity (attomoles vs.

femtomoles, respectively) (**10, 11**). Therefore non-specific inhibitory effects associated with PNAs and LNAs are likely to become more dramatic when measuring luminescence output from Renilla luciferase compared to the β -galactosidase colorimetric output.

Transfection efficiencies and sensitivity of reporter assays are critical parameters to consider when designing protocols for an antisense projects. They become important during interpretation of data reproducibility of results. They are also important considerations when comparing data to other published antisense reports. The differences in sequence-specific antisense effects (reported as a ratio of target gene to control gene assay read-outs) between published reports using different reporter assays could be a function of differences in protocols and assay techniques. However, the integrity and reliability of data stems from the simplicity, sensitivity, and believability of the assay and controls (**12**).

Oligomers as controls

"Reality is merely an illusion, albeit a very persistent one."

--Albert Einstein

Once a well-controlled antisense project is designed, there are two major challenges to successfully demonstrating antisense PNAs regulating a particular cellular mechanism. The first challenge is finding a PNA sequence that actually works. For a given RNA transcript several antisense PNAs will have to be synthesized and empirically tested to find the few PNAs that give the best results. PNA sequence and length are just two examples of a number of variables to consider and assess while designing oligomers for optimization of antisense activity.

The second (and much more demanding) challenge is demonstrating that the anticipated results seen are not due to other contributing cellular mechanisms unrelated to the antisense effect. Unfortunately, there is a paucity of published data concerning non-antisense affects of PNAs and LNAs, so assaying for each potential gene-inhibiting cellular process is impossible. Therefore, the numbers and types of negative controls to run per assay is based on practicality and convenience of obtaining the oligomers. Typically, the PNA (and chimeric LNA) negative controls include mismatched, scrambled, and sense-sequence oligomers. The negative control oligomers can rule out sequence-specific antisense effects, but there still may be some concern for non-antisense activity depending on the level of sensitivity (and credibility) of the non-targeted gene controls. Alternative assay platforms should also be performed (RNA levels, protein levels) and collectively presented to eliminate the most probable, non-sequence-specific affects of reduced gene expression by antisense oligomers.

Critique the work

"Imagination is more important than knowledge, for knowledge is limited while imagination embraces the entire world."

-- Albert Einstein

As a scientist, you should be your worst critic. Scrutinize the assumptions made within a series of experiments that led to a general conclusion, and then design simple experiments that can contribute to the believability of the conclusion. Assess all the possibilities that could be occurring, and then address the most probable with experimentation.

For example, my project involving antisense inhibition of IRES-dependent translation opened the door to a number a new questions to be addressed by other interested researchers. The initial conclusions drawn suggest that the HCV IRES sequence can be targeted by antisense oligomers to inhibit gene expression inside cells. Criticisms of the study include the inconclusive demonstration of the mechanism of action by the oligomers. The scrambled and sense-PNA (and chimeric LNA) negative controls suggest sequence-specific inhibition of the antisense oligonucleotide analogs. However, due to the limitation of the transfection assay (vector transcription of the RNA target) I could not illustrate direct evidence that the tertiary structure of the HCV IRES RNA was specifically bound by oligomers. It is also possible that the HCV RNA may be bound by oligomers just prior to RNA folding. This also limits any conclusions concerning the susceptibility (or difficulty) of HCV RNA tertiary structure to PNA or chimeric LNA binding.

Likewise, RNA levels of the target were not analyzed. Therefore, a steric mechanism of action could not be conclusively demonstrated for the antisense oligomers. While other published reports suggest that PNAs (and chimeric LNAs) do not recruit RNase H to targeted RNA sequences, the HCV IRES may be susceptible to alternative RNA degradation pathways if the tertiary structure is distorted by a bound oligomer or if particular RNA "stabilizing" factors are blocked (**13**).

All of these criticisms could be addressed (in part) by performing *in vitro* translation experiments in conjunction with gel shift assays. Radiolabeled transcripts generated from the T7 promoter of the pRL-HL vector (**14**) could be introduce into cell extracts, in the presence and absence of antisense oligomers, and assayed for both Firefly

and Renilla luciferase activity. This limits antisense oligomer hybridization to only correctly folded IRES-tertiary structure to elicit antisense activity.

Polyacrylamide gel electrophoresis could also demonstrate RNA degradation rates of the IRES transcript, with and without hybridizing oligomers. This should confirm previous reports of PNAs (and chimeric LNAs) inability to recruit RNase H (**15, 16**). Similarly, the gel electrophoresis may also demonstrate shifts in band migration rates if hybridized oligomers are sterically blocking translation factors from binding the IRES transcript. These simple experiments would lend strength to the mechanism of action by antisense PNAs and chimeric LNA oligomers at the HCV IRES.

Progress towards complexity

"Not everything that counts can be counted and not everything that can be counted counts."

--Albert Einstein

The big picture and future goal for PNAs is their potential use as therapeutics to treat microbial infections and diseases. The experimental progression from *in vitro*, to tissue culture systems, to small animal models, to “drug” can be excruciatingly slow to the excited researcher, however, necessary for understanding the activities of PNAs in a biological context. Moving from one platform to the next involves careful planning and thorough examination of the next best assay system available.

For example, while the bicistronic pRL-HL vector is useful in generating RNA transcripts to target with oligomers inside cells, it is artificial with respect to naturally occurring HCV viral infections in humans. A more advance system to use in studying inhibitory PNAs may be the HCV Replicon system. The self-propagating RNA transcript

(based on the HCV genome) replicates in the cytosol of cells in tissue culture, but can not form infectious virions. This platform has the advantages in that it resembles the normal lifecycle of HCV and lends itself to high-throughput analysis of inhibitory oligomers. Additionally, a greater number of RNA sequences could be targeted for studying antisense affects on HCV translation and replication.

While slow in execution, it is the “baby steps” of simple, sensitive, well-designed and progressively more complex experiments that, collectively, will lead to the full understanding and predictability of PNA hybridization to nucleic acid targets within a biological context. Only then can the creative aspects of peptide nucleic acids be fully appreciated and exploited for therapeutic uses.

References for Chapter 5

- 1 Crooke S.T. (1992) Therapeutic applications of oligonucleotides. *Annu. Rev. Pharmacol. Toxicol.* 32:329-76.
- 2 Stein C.A., Cheng Y.C. (1993) Antisense oligonucleotides as therapeutic agents--is the bullet really magical? *Science.* 261(5124):1004-12.
- 3 Eckstein F., Krieg A.M., Stein C.A., Agrawal S., Beaucage S., Cook P.D., Crooke S., Gait M.J., Gewirtz A., Helene C., Miller P., Narayanan R., Nicolin A., Nielsen P., Ohtsuka E., Seliger H., Stec W., Tidd D., Wagner R., Zon J. (1996) On the quality control of antisense oligonucleotides. *Antisense Nucleic Acid Drug Dev.* 6(3):149.
- 4 Stein C.A. (1995) Does antisense exist? *Nature Medicine.* 1(11):1119-21.
- 5 Doyle D.F., Braasch D.A., Simmons C.G., Janowski B.A. and Corey D.R. (2001) Inhibition of gene expression inside cells by peptide nucleic acids: effect of mRNA target sequence, mismatched bases, and PNA length. *Biochemistry.* 40, 53-64.
- 6 Braasch D.A., Liu Y., Corey D.R. (2002) Antisense inhibition of gene expression in cells by oligonucleotides incorporating locked nucleic acids: effect of mRNA target sequence and chimera design. *Nucleic Acids Res.* 30(23):5160-7.
- 7 Braasch D.A., Jensen S., Liu Y., Kaur K., Arar K., White M.A., Corey D.R. (2003) RNA interference in mammalian cells by chemically-modified RNA. *Biochemistry.* 42(26):7967-75.
- 8 Liu Y., Braasch D.A., Nulf C.J., and Corey D.R. (2004) Efficient and isoform-selective inhibition of cellular gene expression by peptide nucleic acids. *Biochemistry.* 43, 1921-1927.

- 9 Elayadi A.N., Braasch D.A., Corey D.R. (2002) Implications of high-affinity hybridization by locked nucleic acid oligomers for inhibition of human telomerase. *Biochemistry*. 41(31):9973-81.
- 10 Alam J., Cook J.L. (1990) Reporter Genes: Applications to the study of mammalian gene transcription. *Anal. Biochem*. 188, 245-254.
- 11 Ugarova N.N., Vozny Ya-V., Kutzova G.D., Dementieva E.I. (1991) in *Bioluminescence and Chemiluminescence: Current Status* (Stanley P.E., and Kricka L.J., Eds.), pp. 511-514, Wiley, Chichester.
- 12 Brysch W., Schlingensiepen KH. (1994) Design and application of antisense oligonucleotides in cell culture, in vivo, and as therapeutic agents. *Cell Mol. Neurobiol*. 14(5):557-68.
- 13 Mangus D.A., Evans M.C., Jacobson A. (2003) Poly(A)-binding proteins: multifunctional scaffolds for the post-transcriptional control of gene expression. *Genome Biol*. 4(7):223.
- 14 Honda M., Kaneko S., Matsushita E., Kobayashi K., Abell G.A., and Lemon S.M. (2000) Cell cycle regulation of hepatitis C virus internal ribosomal entry site-directed translation. *Gastroenterology*. 118, 152-162.
- 15 Knudsen H. and Nielsen P.E. (1996) Antisense properties of duplex- and triplex- forming PNAs. *Nucl. Acids Res*. 24, 494-500.
- 16 Kurreck J., Wyszko E., Gillen C., and Erdmann V.A. (2002) Design of antisense oligonucleotides stabilized by locked nucleic acids. *Nucl. Acids Res*. 30, 1911-8.

CHAPTER 6 – EXPERIMENTAL PROCEDURES

	<u>Page</u>
The Expedite 8909 PNA Synthesizer	183
Automated Synthesis of PNAs and bisPNAs	184
Manual Synthesis of PNAs	185
Reverse-Phase High Performance Liquid Chromatography (RP-HPLC) for the analysis and purification of PNAs	190
Matrix-Assisted Laser Desorption-Ionization Time-of-Flight (MALDI-TOF) Mass Spectroscopy of PNAs	191
Lyophilization of purified PNAs	192
Quantification of PNA concentrations by UV absorbance spectroscopy	192
Annealing of PNAs to complementary DNA oligonucleotides (PNA:DNA Duplex Formation)	193
Melting temperature analysis (T_m)	193
Preparation of radiolabeled (^{32}P) DNA oligonucleotides	194
Polyacrylamide gel electrophoresis of bisPNA:DNA hybridizations	195
Cesium-Chloride gradient preparation of supercoiled plasmid DNA	195
Detection of strand-invasion of PNA and bisPNA by the modified T7 Sequenase assay	196
Solution-phase N-terminal labeling of PNAs with Cy3 fluorophore	197
Thin-Layer Chromatography (TLC) detection of uncoupled Cy3	197

Maintenance and passaging of the CV-1 Cell Line	198
Cationic lipid-mediated transfection of PNA:DNA duplexes	198
and chimeric LNA oligonucleotides into CV-1 cells	
Cationic lipid-mediated transfection of reporter plasmid	199
pRL-HL into CV-1 cells	
Assessing Firefly luciferase and Renilla luciferase expression levels	201
Confocal fluorescence microscopy of cationic lipid-mediated uptake	202
of PNA-Cy3 into live CV-1 cells	
FACS analysis of LNA-Cy3 cellular uptake into CV-1 cells	202
References for Chapter 5	204

The Expedite 8909 PNA Synthesizer

PNAs were prepared by automated Fmoc-based solid-phase synthesis using an Expedite 8909 synthesizer (PE Biosystems, Foster City CA) (1). The Expedite synthesizer has been modified with proprietary software, designed to control delivery time and correct amounts of reagents across the solid-support resin for maximal efficiency of PNA synthesis. It is equipped with two ports such that two PNAs can be synthesized simultaneously. It also contains three additional bottle positions that can be used to introduce amino acids or linker molecules into the PNA oligomer during synthesis, provided that the molecules are compatible to Fmoc-based synthesis. On average, a 15-mer PNA oligomer takes approximately 6 hours to synthesize. Alternatively, manual synthesis of PNAs is also possible for larger scale synthesis (2).

Automated synthesis of PNAs and bisPNAs

Fmoc-protected PNA monomers with Bhoc-protected bases (A, T, G, and C), Fmoc-2-aminoethoxy-2-ethoxy acetic acid (Fmoc-AEEA-OH or Linker/Spacer molecule), HATU activator, Fmoc-XAL-PEG-PS resin (2 μ mol scale) and other reagents for PNA synthesis were obtained from PE Biosystems (Foster City, CA) (**3**). Each reagent was received in a pre-aliquoted amount, as are the Base solution (0.2 M DIPEA/0.3 M 2,6-lutidine), the Deblocking solution (20% v/v piperidine in DMF) and the Capping solution (5% v/v acetic anhydride/6% v/v 2,6-lutidine in DMF). Fmoc-amino acids were obtained from Advanced Chemtech (Louisville, KY) or Calbiochem-Novabiochem Corp. (La Jolla, CA).

It is essential to keep all reagents as anhydrous and amine-free as possible to minimize unwanted side-reactions. Powdered PNA monomers, HATU activator, linker molecule AEEA-OH, and amino acids were either lyophilized or placed in a Drierite dessicant container overnight. Each PNA monomer was dissolved in 3.75 mL Diluent (anhydrous NMP) (216 mM final) while HATU activator is dissolved in 13.5 mL anhydrous DMF (182 mM final). Fmoc-protected amino acids were dissolved in anhydrous DMF at a final concentration of 200 mM. Linker molecule AEEA is dissolved in 2.4 mL Diluent (209 mM final).

Upon completion of synthesis, the PNA-bound resin was washed with 20 mL DMF, followed by 20 mL isopropyl alcohol, and then dried in the lyophilizer. The resin was then transferred into a fritted (0.2- μ m) polytetrafluoroethylene (PTFE) spin column (Millipore). Addition of 250 μ L “cleavage cocktail” (20% (v/v) *m*-cresol (Sigma-Aldrich) in trifluoroacetic acid (TFA; Burdick Jackson) to the resin in the spin column sufficiently

releases the PNA from the resin within 5 minutes leaving a C-terminal amide functional group. An additional 90 minute incubation is necessary to remove the Bhoc-protecting groups from the nucleobases. A quick spin of the fritted PTFE column pulls the PNA solution into the bottom of the tube, separating it from the resin.

The PNA was then precipitated by addition of 1 mL ice cold (-20°C) diethyl ether. A cloudy white precipitate is demonstrative of a potential successful synthesis. Vortexing, followed by 5 minutes of microcentrifugation at 5000 rpm pelleted the crude PNA product to the bottom of the tube. The supernatant was decanted and the pellet was washed with another 1 mL ice-cold diethyl ether. The washing and centrifugation of the crude PNA product occurred three more times, discarding the supernatant each time. The PNA pellet was then air-dried for approximately 30 minutes to evaporate the volatile diethylether. Once dry, the PNA pellet was hydrated with 500 μ L dH₂O and stored at 4°C until use.

An important procedure for working with PNAs is that all PNA solutions must be heated to 80°C for 5 minutes on the day of use, prior to use. This will denature any aggregation of PNAs that may have occurred over time.

Manual Synthesis of PNAs

Manual synthesis of PNAs is advantageous because PNAs can be obtained in larger amounts (>2 μ mol) than on the Expedite 8909 synthesizer. By changing the amount of resin used, one can prepare as much or as little PNA as needed for each experiment.

Manual synthesis also avoids the need for a dedicated automated synthesizer. However, serious dedication is needed by the chemist performing the synthesis because of the repetitive nature of the protocol and the time constraints necessary for each coupling and deblocking step. For each cycle, the addition of a single PNA monomer to a growing resin-bound PNA oligomer takes approximately 1 hour.

As with automated synthesis, it is important to keep reagents and materials as anhydrous as possible. However, the coupling reactions are more exposed to atmospheric water. For manual syntheses *tert*-butoxycarbonyl (tBoc)-protected PNA monomers generally produce better yields than syntheses using Fmoc-protected PNA monomers. Dry all monomers and coupling reagents overnight *in vacuo* before beginning synthesis. All glassware, pipet tips, and 1.5-mL microcentrifuge tubes are dried in a 250°C oven overnight prior to use. Pipet tips and microcentrifuge tubes were flushed with nitrogen to ensure they are dry prior to synthesis.

Manual PNA synthesis is often so efficient that a capping step can be dispensed with. It is sometimes advisable, however, to include a capping step after coupling of the monomer to simplify the HPLC purification. The individual experimenter will have to determine the necessity for capping. It is typically necessary for long syntheses or for syntheses that have failed in the past.

Many different types of apparatus can be used for manual peptide synthesis, and it is likely that these can be adapted for PNA synthesis. The apparatus described here (**Figure 6-1. The apparatus for manual PNA synthesis**) uses common laboratory glassware and offers robust performance (2,3). While the details of manual synthesis will vary with apparatus, the outline of the procedure and the precautions that need to be taken

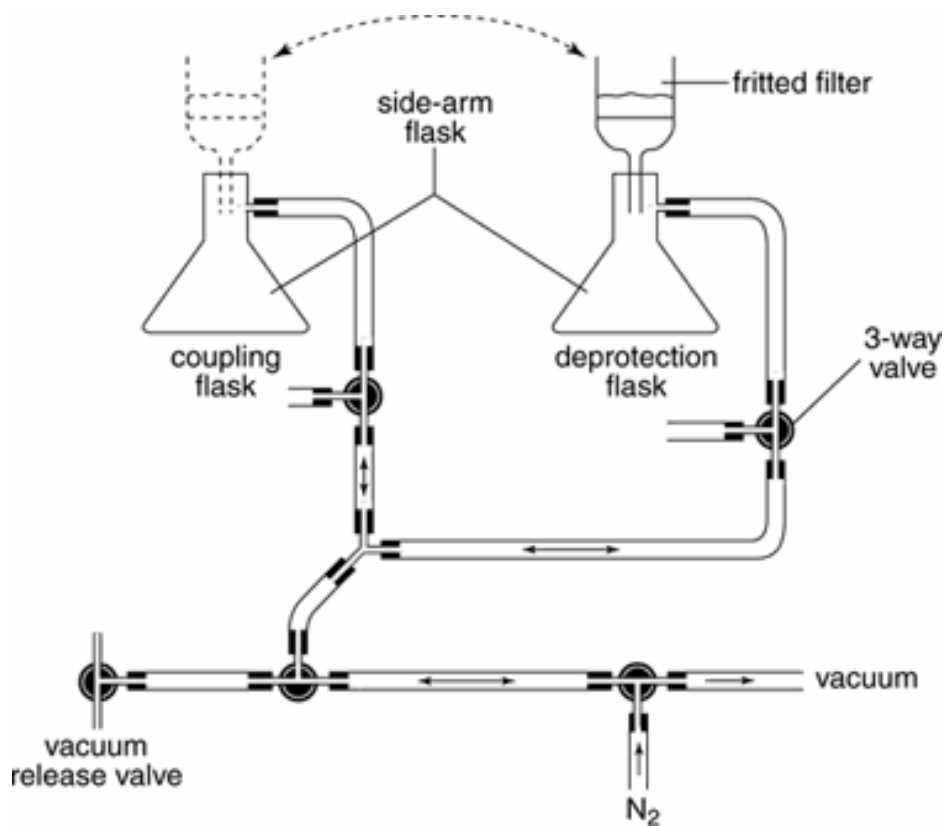


Figure 6-1. The apparatus for manual PNA synthesis. The fritted filter containing the growing resin-bound PNA is shuttled from one flask to another for the coupling reaction and the deprotection steps, respectively. Nitrogen gas is used to agitate (bubble) the reaction solutions. At the end of each reaction step, the solution is vacuumed into the flask, leaving the resin in the fritted filter.

From: Norton J.C, Waggenspack J.H, Varnum E., Corey D.R. (1995) Targeting peptide nucleic acid-protein conjugates to structural features within duplex DNA. *Bioorganic Medicinal Chemistry*. 3(4):437-45.

will remain the same. Because a single missed step can ruin a labor-intensive synthesis, I followed a detailed checklist for each step. The checklist provides a written record that all steps were performed. A sample spreadsheet detailing the amount of reagent needed for synthesis is shown (**Figure 6-2. Example spreadsheet for manual PNA synthesis**) (3).

The coupling, deprotection, and washing steps were performed in a 15 mL fritted glass filter fitted in the septa of a 100 mL flask. Mixing of solutions was achieved by nitrogen gas bubbling up through the filter and removed by applying a vacuum to pull the solution into a flask (bleeding). Two flasks (with septa) were employed, one for the coupling reactions and another for TFA deblocking reactions and washes. The fritted filter (with the resin) is transferred from one flask to the other for each step. The PNA monomers were activated by vortex mixing of 10 eq. DIPEA (relative to the resin active sites), 5-fold excess HOBt, and 4.5-fold excess HBTU in 1 mL DMF just prior to addition to the resin in the fritted filter. Each coupling reaction was done for 20 minutes with nitrogen bubbling. Resin was washed two times with 1 mL of 50:50 DMF/DCM. After transferring the fritted filter to the other flask, the removal of the protecting group was performed with 1 mL 5% m-cresol:TFA for 3 minutes, revealing an amine group for the next coupling reaction. The resin was washed six times with 1 mL of 50:50 DMF/DCM followed by washes of 1 mL pyridine and 1 mL anhydrous DMF. The fritted filter was then transferred back to the other flask for the subsequent coupling step.

Upon completion of synthesis a solution of TFMSA:TFA:m-cresol:thioanisole (2:6:1:1) was used to cleave PNAs from the resin and to remove the nucleobase protecting groups. PNAs were then precipitated and washed with 10 mL ice cold diethyl

	Monomer	Molecular Weight g/mol	PNA mass after each coupling g/mol
C-Terminus	terminal amide	17.00	–
1	lysine	128.00	145.00
2	A	275.32	420.32
3	A	275.32	695.64
4	C	251.30	946.94
5	A	275.32	1222.26
6	G	291.32	1513.58
7	A	275.32	1788.90
8	T	266.28	2055.18
9	T	266.28	2321.46
10	G	291.32	2612.78
11	G	291.32	2904.10
12	G	291.32	3195.42
13	A	275.32	3470.74
14	T	266.28	3737.02
N-Terminus			
			Total Mass 3737.02

Amount of Resin Used	10 mg
Substitution Number for Resin	0.66 mmol/g
Total Active Sites	0.0066 mmol
PNA Mass	3737.02 mg/mmol
Amount of PNA to be Synthesized	24.6 mg

	Equivalents	Amount Per Coupling
A Monomer	5.0	17.41 mg
G Monomer	5.0	17.94 mg
C Monomer	5.0	16.62 mg
T Monomer	5.0	12.68 mg
HBTU	4.5	11.26 mg
HOBt	5.0	4.46 mg
DIPEA	10.0	8.54 μ L
DMF	–	Up to 1 mL

Figure 6-2. Example spreadsheet for manual PNA synthesis. The PNA sequence is listed from C-terminus to N-terminus (including lysine at the C terminus) with the molecular weight of the PNA oligomer after each monomer coupling step. MALDI-TOF MS can be used to monitor the PNA synthesis after every few coupling reactions. The resin used in this example produces a theoretical yield of 24.6 mg of PNA upon cleavage.

From: Braasch D.A., Nulf C.J., and Corey D.R. (2002) *Current Protocols in Nucleic Acid Chemistry. Unit 4.11 Synthesis and Purification of Peptide Nucleic Acids.* pp.14.11.11-14.11.18, John Wiley & Sons, New York.

ether 3 times and air-dried. Analysis and purification of the PNA product was performed by RP-HPLC and MALDI-TOF MS.

PNAs oligomers can also be purchased directly from Applied Biosystems. Other vendors throughout the world have been licensed to sell PNAs. Currently, international vendors include Nippon Flour Mill, Omgen, Sawady Technologies, and OSWEL-University of Southhampton. Applied Biosystems can supply information for the vendor most convenient to a particular laboratory. Obtaining PNAs from commercial sources will probably be a less expensive option for laboratories that require a limited number of PNAs on a 2- μ mol scale, especially if the laboratories do not have experience making peptides.

Reverse-Phase High Performance Liquid Chromatography (RP-HPLC) for the analysis and purification of PNAs

Analogous to peptide purification, PNA oligomers, having both hydrophobic and hydrophilic properties, are analyzed and purified by reverse phase-high performance liquid chromatography (RP-HPLC). PNAs will adsorb to the hydrophobic C₁₈-column in an aqueous environment (running buffer), but can be competed off the column with an increasing gradient of non-polar ACN (stationary buffer). The flow-through is monitored by UV absorbance at λ_{260} , reading the nucleobases of the PNA. Longer PNAs, having greater hydrophobicity, will elute at higher ACN concentrations (longer elution times). Contaminating truncated PNA product from failed syntheses, having fewer hydrophobic monomers, will elute at lower ACN concentrations (shorter elution times) making it easy to separate undesired PNA from the full length PNA product. MALDI-TOF mass

spectroscopy (see below) of truncated PNA products can also assist in troubleshooting the Expedite 8909 synthesizer.

RP-HPLC of PNAs involved a running buffer of dH₂O:0.1%TFA (Buffer A) and an elution buffer of ACN:0.1%TFA (Buffer B) from a C₁₈-column (300-Å 5 µm Microsorb-MV column for analysis or a semi-prep C₁₈-column for PNA purification; Varian Analytical Instruments) inside a water jacket maintained at 55°C (to minimize PNA aggregation). The C₁₈-column was equilibrated with Buffer A for at least 20 minutes prior to injection of the PNA sample. Buffer A ran for 5 minutes after injection of the PNA sample, followed by a gradient ramping of Buffer B from 0% to 100% over 30 minutes with a flow rate of 1 mL/min for analysis or 2 mL/min for purification of PNAs. Elution of PNA from the C₁₈-column was monitored at 260 nm on a Dynamax UV-1 absorbance detector (Varian, Walnut Creek, CA) and flow-through corresponding the PNA product was collected. BisPNAs were purified in an analogous fashion.

Matrix-Assisted Laser Desorption-Ionization Time-of-Flight (MALDI-TOF) Mass Spectroscopy of PNAs

Mass spectrometry was performed by MALDI-TOF (**4**, **5**) on a Voyager-DE Workstation (Applied Biosystems, Foster City, CA) using a saturated solution (1:1 ratio of ACN and dH₂O, with 0.1% TFA) of either α-cyano-4-hydroxycinnamic acid or sinapinic acid (3,5-Dimethoxy-4-hydroxy-cinnamic acid) as a matrix (Sigma-Aldrich, St Louis, MO). On a gold-plated target, 1 µL of the PNA sample is mixed with 1 µL matrix and allowed to dry for at least 15 minutes until a crystal forms. MALDI-TOF analysis is sensitive to the concentration of the PNA solution so multiple concentrations of the PNA

solution are often spotted with matrix. The Voyager software was calibrated prior to each PNA analysis with a control standard peptide, porcine pancreas insulin (Sigma) with a known molecular weight of 5777.6 Daltons. All bisPNA were analyzed in the same manner.

Lyophilization of purified PNAs

The RP-HPLC flow-through peak corresponding to the correct PNA product was collected in 15 mL conicals. The purified PNA solution was frozen solid in a ethanol-dry ice bath, and placed within a lyophilizer until only a white, delicate solid remains in the conical. The PNA is then resuspended in Millipore dH₂O. PNAs should only be dissolved in dH₂O because higher pH solutions could cause precipitation of PNAs and unwanted intramolecular rearrangement side reactions resulting in truncated PNA (6).

Quantification of PNA concentrations by UV absorbance spectroscopy

The concentration of PNA solutions was measured using a Cary 100Bio UV-Visible spectrophotometer (Varian) at 260 nm and room temperature, using an extinction coefficient based on the sum of the extinction coefficients of each base monomer ($A = 13.7$, $C = 6.06$, $G = 11.7$, $T = 8.6$, mL/ μ mol \cdot cm). Concentrations of DNA, RNA, and chimeric LNA oligonucleotides were also measured by UV absorbance spectroscopy using extinction coefficients given by the manufacturer. Water (dH₂O) was used as the blank.

Annealing of PNAs to complementary DNA oligonucleotides (PNA:DNA duplex formation)

PNA:DNA duplex mixtures (50 μ M) in thin-walled PCR tubes were annealed in a thermocycler. Reductions in temperature occurred in 1 min. with the hold times indicated: 95°C, 5 min; 85°C, 1 min.; 75°C, 1 min.; 65°C, 5 min.; 55°C, 1min.; 45°C, 1 min.; 35°C, 5 min.; 25°C, 1 min.; 15°C, 1 min.; hold 15°C. After annealing, the PNA:DNA duplexes were maintained at 4°C until evaluation of T_m was performed, or until transfection.

Melting temperature (T_m) analysis

Melting temperature (T_m) experiments were performed by measuring the hyperchromic/hypochromic change in absorbance at 260 nm across a range of temperatures on a Cary 100Bio UV-Visible spectrophotometer (Varian Inc., Walnut Creek, CA) equipped with a 12-position sample holder and a Peltier temperature control accessory. PNA and complementary DNA oligonucleotides were suspended in Na_2HPO_4 buffer (100 μ M, pH 7.5) at 2 μ M each. Mineral oil was overlaid to minimize solution evaporation.

The temperature was initially held at 98°C for two minutes to dissociated PNAs and DNA oligonucleotides, and then ramped from 98°C to 14°C and back up to 98°C at a rate of 2°C/min with a 6 second hold at each reading. Data was collected in both directions (denaturation and renaturation) to ensure that the observed curves were reversible. Cary WinUV software was utilized to determine the T_m for each combination by calculating the first derivative of the absorbance versus temperature plot. The

calculated T_m of at least six runs was averaged to give a final T_m for each PNA:DNA combination. BisPNAs and chimeric LNA oligonucleotides were analyzed by the same method.

Preparation of radiolabeled (^{32}P) DNA oligonucleotides

DNA oligonucleotides were obtained from Integrated DNA Technologies (Coralville, IA) or Invitrogen-Life Technologies (Carlsbad, CA). All oligonucleotides received were resuspended in dH_2O , quantitated by UV absorption spectroscopy using extinction coefficients given by the manufacturer, and stored at -20°C until use. DNA oligonucleotides were radiolabeled using [$\gamma\text{-}^{32}\text{P}$]ATP (Amersham Pharmacia Biotech, Piscataway, NJ) and T4 polynucleotide kinase (Sigma-Aldrich).

Unincorporated [$\gamma\text{-}^{32}\text{P}$]ATP was removed by passing the oligonucleotides through a Bio-Spin 6 column (Bio-Rad Laboratories, Hercules, CA) that had been pre-equilibrated with distilled water. Equal amounts of unlabeled oligonucleotides were treated similarly and purified by Bio-Spin 6 column in parallel. These unlabeled oligonucleotides were used to estimate the concentration of the radiolabeled oligonucleotides that had been treated similarly. Unlabeled oligonucleotides were also used for gel shift experiments. For each 40-mer and 50-mer oligonucleotide the nucleobases were randomized, except for the complementary 12-mer target sequences, to minimize the potential for formation of specific secondary structures.

Polyacrylamide gel electrophoresis of bisPNA:DNA Hybridizations

Non-denaturing PAGE gel shift assays were performed to visualize bisPNA hybridization to individual single-stranded DNA oligonucleotides. BisPNA (150 nM final concentration) was mixed with ^{32}P -radiolabeled DNA oligonucleotides (150 nM final concentration) and unlabeled DNA oligonucleotide (0–25 μM) in a 20 μL , 50 μM Tris–HCl buffer (pH 8.0) reaction within a thin-wall PCR tube. Oligonucleotide strands were annealed using a PE 9600 Thermocycler (Perkin Elmer, Norwalk, CT) (95°C for 5 min, cooled to 4°C over a period of 60 min). The samples were then flash frozen in an ethanol and dry ice bath and stored at –20°C until use. On ice, 10 μL of a 30% glycerol tracking dye (0.05% bromophenol blue, 0.05% xylene cyanol and 0.05% orange G) was added, followed by a quick spin, before loading into a non-denaturing 10% (19:1) polyacrylamide gel (Bio-Rad). The gel was run at 4°C and 250 V for 3.5 h. The gel was analyzed by autoradiography using a Molecular Dynamics model 425F phosphorimager (Sunnyvale, CA).

Cesium-Chloride (CsCl) gradient preparation of supercoiled plasmid DNA

Supercoiled plasmid pUC19 DNA (**7**) was prepared by a mild lysis protocol (**8, 9**) followed by two successive CsCl gradient ultracentrifugations to minimized contamination of nicked or denatured plasmid (**10**). Ethanol-precipitated plasmid was resuspended in Tris-HCl (100 mM, pH. 7.5). Each plasmid preparation was run on 1% agarose and stained with ethidium bromide to qualify plasmid supercoil integrity.

Detection of strand-invasion of PNA and bisPNA by the modified T7 Sequenase assay

Supercoiled plasmid pUC19 (2 μ L of 400 nM) was incubated with PNA or bisPNA (1 μ L of 1 μ M) in 10 mM Tris-HCl (pH 7.5) buffer at 37°C for 60 minutes. Next, an oligonucleotide-peptide conjugate primer (5 μ L of 1 μ M) (**11**) was added to hybridize to the displaced DNA strand (P-loop) created by the PNA strand invasion, at 25°C for 30 minutes (Note: the peptide conjugate was previously demonstrated to increase hybridization rate of the oligonucleotide. It is only used here to decrease the assay time and does not influence the hybridization efficiency of the PNA). The radiolabeling reaction buffer consisting of MgCl₂ (8 mM), NaCl (80 mM), Tris-HCl (10 mM, pH 7.5), T7 DNA polymerase (Sequenase v2.0, US Biochemical, Cleveland, OH) (1 U/reaction), dNTPs, dideoxynucleotides (ddNTPs), and ³⁵S-dATP (Amersham Pharmacia) was added and the sequencing protocol proceeded (using the hybridized oligonucleotide-peptide conjugate primer) (**12, 13**). Equal amount of elongation product were loaded into a denaturing 6% polyacrylamide sequencing gel and resolved by electrophoresis. The gel was dried and visualized by autoradiography using a Molecular Dynamics model 425F phosphorimager (Sunnyvale, CA) (**14, 15**). The positive control for the assay was plasmid plus oligonucleotide-peptide conjugate primer only incubated at 37°C, the permissive hybridization temperature for the primer. The negative control is plasmid plus primer (in the absence of PNA strand invasion) incubated at 25°C, a non-permissive temperature for primer hybridization.

Solution-phase N-terminal labeling of PNAs with Cy3 fluorophore

For the confocal microscopy experiments purified PNA (100 nmoles, dissolved in dH₂O) with a free N-terminal amine was incubated with Cy3 NHS-ester mono-reactive molecule (Amersham Biosciences) in a 1 mL 10% N-Methylmorpholine (aq.) solution. The reaction proceeded for 1 hour in the dark at room temperature. PNA-Cy3 conjugates were repurified by RP-HPLC, analyzed by MALDI-TOF for the correct molecular weight, lyophilized overnight, resuspended in dH₂O, and stored at 4°C in the dark until use (personal communication with Ralph Casale, Applied Biosystems.).

Thin Layer Chromatography (TLC) detection of uncoupled Cy3

Due to the high Cy3:PNA molar ratio during the solution labeling process, some free Cy3 may associate non-specifically with the PNA even during the purification process or RP-HPLC. To insure that the purified PNA-Cy3 conjugate preparation does not contain free Cy3 molecules, 1 µL of the PNA-Cy3 solution was spotted on a normal phase TLC plate and allowed to dry for 30 minutes. In a TLC chamber, the spot is resolved with a 3:2 (DCM:methanol) solution containing 1% acetic acid. The PNA-Cy3 conjugate remains at the baseline while the free Cy3 molecule will migrate up the plate. There were no instances of residual free Cy3 in our preparations using the aforementioned protocol for “in-solution” labeling of PNAs with mono-reactive Cy3 (personal communication Ralph Casale, Applied Biosystems.)

Maintenance and passaging of the CV-1 cell line

CV-1 cells (African Green Monkey Kidney, normal) (American Type Culture Collection, Manassas, VA CCL-70) were maintained in Dulbecco's Minimal Essential Medium with phenol, supplemented with 4 mM L-glutamine, 10% fetal bovine serum (FBS) (Atlanta Biologicals, Norcross, GA), 500 U/mL penicillin, 0.1 mg/mL streptomycin, and 0.06 mg/mL tylosin (Sigma, St. Louis, MO). Cells were cultured at 37°C with 5% CO₂, and split 1:5 every three days.

Cationic lipid-mediated transfection of PNA:DNA duplexes and chimeric LNAs into CV-1 cells

Oligonucleotides transfections were previously described (16). Annealed PNA:DNA duplexes were prepared for transfection by equilibrating 12.8 µL of 50 µM PNA:DNA stock in 137.2 µL of Opti-MEM (Invitrogen). In a separate tube, 1.9 µL of LipofectAMINE (Invitrogen) was mixed with 148.1 µL Opti-MEM and vigorously mixed for 15 seconds followed by equilibration at room temperature for 5 minutes. The diluted PNA:DNA and LipofectAMINE solutions (150 µL each) were mixed together by agitating for 15 seconds. Lipid complexes were allowed to form by incubating the mixture at room temperature for 15 minutes in the dark. The solution containing the PNA:DNA:LipofectAMINE complex (300 µL) was diluted to 3.2 mL with Opti-MEM resulting in a final concentration of 200 nM. This 200 nM solution was serially diluted to the final working concentrations of 100 nM and 25 nM.

Chimeric LNAs conjugate were gifts from Dr. Khalil Arar and Alex Amiet of Proligo LLC (Boulder, CO). DNA oligonucleotides were obtained from Integrated DNA

Technologies (Coralville, IA). All oligonucleotides received were resuspended in dH₂O, quantitated by UV absorption spectroscopy, and stored at –20°C until use. Chimeric LNA oligonucleotide transfections were performed by the same protocol but without the addition of a complementary carrier DNA. Chimeric LNAs were heated to 90°C for 5 minutes prior to mixing with Opti-MEM to dissociate aggregated oligonucleotides.

CV-1 cells were plated at 10,000 cells/well in 48-well plates. Cells were incubated at 37°C at 5% CO₂ for a minimum of 8 hours prior to transfection. The cells were then washed once with 200 µL Opti-MEM, followed by 14-16 hour transfection with the PNA:DNA:lipid complex (or LNA:lipid complex) or lipid only control. Transfected cells were visualized by fluorescence microscopy, analyzed by FACS analysis, or re-transfected with reporter vector for luciferase assays (**Figure 6-3. The transfection protocol**).

Cationic lipid-mediated transfection of reporter plasmid pRL-HL into CV-1 cells

Plasmid transfections have been previously described (16). Plasmid pRL-HL (17) was obtained from Dr. Michael Gale (UT Southwestern Medical Center at Dallas, TX). Plasmid vector encoding luciferase was transfected 8 - 12 hours after transfection of PNA or chimeric LNA. The bicistronic vector pRL-HL was prepared for transfection by equilibrating plasmid DNA (120 ng/well) in 19.5 µL/well of Opti-MEM. Likewise, 0.2 µL of LipofectAMINE (7 ug/mL) was mixed with 19.8 µL Opti-MEM. The plasmid solution and the LipofectAMINE solution were mixed thoroughly and incubated for 20 minutes in the dark. The mixed solutions were diluted with Opti-MEM to a final

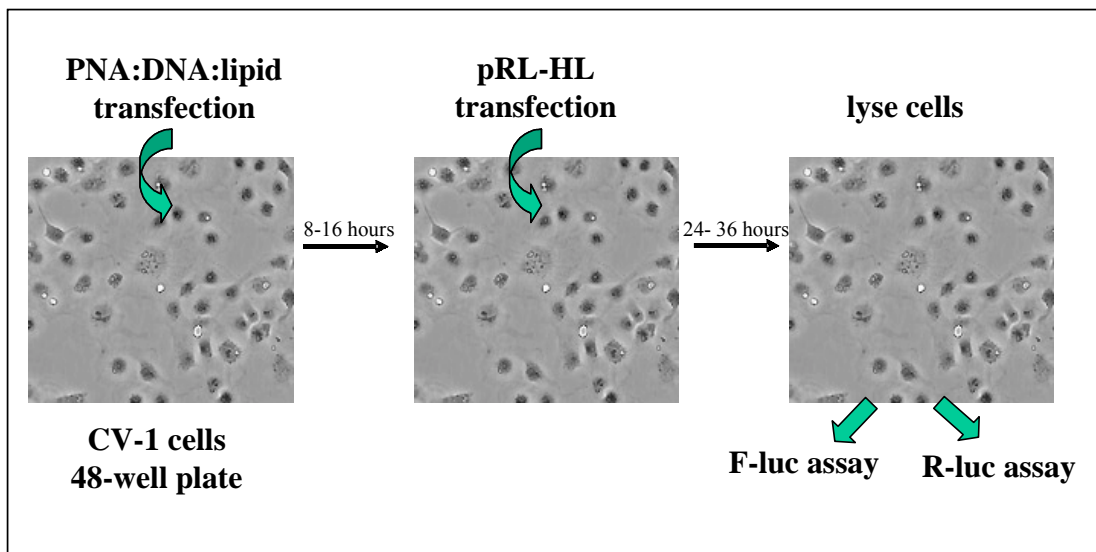


Figure 6-3 The transfection protocol. CV-1 cells are plated in a 48-well plate at 10,000 cells/well. 200 μ L of the PNA:DNA:LipofectAMINE dilutions (in Opti-MEM) is placed on top of the cells (in triplicate) and incubated overnight at 37° C, 5% CO₂. Transfection of the bicistronic expression (pRL-HL) occurs for 12 hours before the medium is replaced with fresh D-10 media. 24-36 hours post-transfection of the pRL-HL vector, the cells are lysed. 20 μ L of lysate is used for both Firefly luciferase and Renilla luciferase expression. Data is expressed as the ratio of Firefly:Renilla, normalized to cells treated with lipid only.

concentration of 120 ng/well at 50 μ L/well. Transfections were incubated for 8-10 hours before the transfection medium was aspirated and replaced with fresh media.

Assessing Firefly luciferase and Renilla luciferase expression levels

The cells were harvested 36 - 48 hours post-vector transfection and analyzed for Firefly luciferase and Renilla luciferase activities (At this time point, the cells are approximately 80% confluent). The media was aspirated and the cells were lysed using 100 μ L Passive Lysis Buffer (1x, PLB) (Promega) on ice for 20 minutes. Firefly luciferase assays were conducted in an opaque, flat-bottomed 96-well plate (Costar) with 20 μ L lysate, 100 μ L Firefly assay buffer (21.5 mM $MgCl_2$, 3.7 mM ATP in 0.1 M KH_2PO_4 , pH 7.8), and 100 μ L of 1 mM luciferin (Biosynth, Naperville, IL) dispensed via ML-3000 microplate luminescence system (Dynex technologies, Chantilly, VA). Data was recorded using enhanced flash parameters with BioLinx software v.2.22 and integrated from 0-5 seconds. Renilla luciferase assays were performed using 20 μ L lysate, 100 μ L Renilla assay buffer (0.1 M KH_2PO_4 , 0.5 M NaCl, 1 mM EDTA), and dispensed 100 μ L of 0.18 μ g/mL coelenterazine (Biosynth). Data was integrated from 0-5 seconds. All experiments were performed as least three times and reported as the ratio of Firefly luciferase to Renilla luciferase, normalized to the lipid only control.

Confocal fluorescence microscopy of lipid-mediated uptake of PNA-Cy3 into live CV-1 cells

The PNA-Cy3:DNA:LipofectAMINE complexes (100 nM, 500 μ L) were transfected into CV-1 cells that had been plated into a Lab-Tek 4-well chambered coverglass (Nalgene Nunc International, Naperville, IL) for 8 hours. The transfection solution was aspirated and replaced with fresh media for another 16 hours. Just prior to microscopy, cells were incubated for 30 minutes with 0.025 mg/ml Hoechst 33258 nuclear stain (Sigma) and 50nM LysoTracker (Molecular Probes, Eugene Oregon) at 37°C, and washed 3 times with 500 μ L room temperature Opti-MEM. Live cells were analyzed using a Zeiss Axiovert 200M inverted transmitted light microscope (Carl Zeiss MicroImaging, Thornwood, NY) equipped with a digital imaging system and Slidebook 4.0 imaging software (Intelligent Innovations, Denver, CO). Confocal mages were taken as 0.5 μ m intervals, from the bottom to the top of the cell, with the resulting images deconvoluted via the nearest neighbor algorithm. Each channel intensity was normalized to untransfected, "unstained" CV-1 cells.

FACS analysis of cationic lipid-mediated cellular uptake of LNA-Cy3 into CV-1 cells

CV-1 cells were plated in a 6-well plate (50,000 cells/well) and allowed to attach for at least 8 hours. Purified PNA-Cy3 conjugates were annealed to carrier DNA. The resulting PNA-Cy3:DNA duplex (4 μ L of a 50 μ M stock) was incubated with 1 μ L LipofectAMINE in 100 μ L Opti-MEM for 15-20 minutes after quickly agitating the mixture. CV-1 cells were washed once with room temperature Opti-MEM. PNA-

Cy3:DNA:lipid complexes were diluted with 2 mL Opti-MEM to a final concentration of 100 nM which was gently layered onto the CV-1 cells. Transfections were done at 37°C at 5% CO₂ for 8 hours.

Transfection media was aspirated and the cells were gently washed with 2 mL Opti-MEM. Cells were trypsinized (400 µL, 3 minutes, 37°C), harvested into a 15 mL conical, and thoroughly washed with 4 mL cold PBS 3 times. Cells were fixed in a freshly made 1% paraformaldehyde/PBS solution and stored at 4°C until flow cytometry was performed

Data was collected on a FACScan analyzer. Live cell population was gated and 5000 events were collected for data analysis. CellQuest software (Becton Dickinson) was used to collect and analyze the histogram plots.

References for Chapter 5

- 1 Mayfield L.D., Corey D.R. (1999) Automated synthesis of peptide nucleic acids and peptide nucleic acid-peptide conjugates. *Analytical Biochemistry*. 268(2):401-4.
- 2 Norton J.C, Waggenspack J.H, Varnum E., Corey D.R. (1995) Targeting peptide nucleic acid-protein conjugates to structural features within duplex DNA. *Bioorganic Medicinal Chemistry*. 3(4):437-45.
- 3 Braasch D.A., Nulf C.J., and Corey D.R. (2002) *Current Protocols in Nucleic Acid Chemistry. Unit 4.11 Synthesis and Purification of Peptide Nucleic Acids*. pp.14.11.11-14.11.18, John Wiley & Sons, New York.
- 4 Pieleus U., Zurcher W., Schar M., Moser H.E. (1993) Matrix-assisted laser desorption ionization time-of-flight mass spectrometry: a powerful tool for the mass and sequence analysis of natural and modified oligonucleotides. *Nucleic Acids Research*. 11, 21(14):3191-6.
- 5 Hathaway G.M. (1994) Characterization of modified and normal deoxyoligonucleotides by MALDI, time-of-flight mass spectrometry. *Biotechniques*. 17(1):150-5.
- 6 Christensen L., Fitzpatrick R., Gildea B., Warren B., Coull J. (1994) *Improved synthesis, purification and characterization of PNA Oligomers*. Christensen, L., Fitzpatrick, R., Gildea, B., Warren, B., Coull, J., Ed.; Mayflower Worldwide Limited, Birmingham, pp. 149-156.
- 7 Yanisch-Perron C., Vieira J., Messing J. (1985) Improved M13 phage cloning vectors and host strains: nucleotide sequences of the M13mp18 and pUC19 vectors. *Gene*. 33(1):103-19. (erratum appears in *Gene*. 1992, 114(1):81-3).

- 8 Panayotatos N., Wells RD. (1981) Cruciform structures in supercoiled DNA. *Nature*. 289(5797):466-70.
- 9 Lilley D.M. (1980) The inverted repeat as a recognizable structural feature in supercoiled DNA molecules. *Proceedings of the National Academy of Sciences of the United States of America*. 77(11):6468-72.
- 10 Murchie A.I., Lilley D.M. Supercoiled DNA and cruciform structures. (1992) *Methods in Enzymology*. 211:158-80.
- 11 Corey D.R., Munoz-Medellin D., Huang A. (1995) Strand Invasion by Oligonucleotide-Nuclease Conjugates. *Bioconjugate Chemistry*. 6, 93-100.
- 12 Smulevitch S.V., Simmons C.G., Norton J.C., Wise T.W., Corey D.R. (1996) Enhancement of strand invasion by oligonucleotides through manipulation of backbone charge. *Nature Biotechnology*. 14(13):1700-4.
- 13 Iyer M., Norton J.C., Corey D.R. (1995) Accelerated hybridization of oligonucleotides to duplex DNA. *Journal of Biological Chemistry*. 270(24):14712-7.
- 14 Ishihara T., Corey D.R. (1999) Strand invasion by DNA-peptide conjugates and peptide nucleic acids. *Nucleic Acids Symposium Series*. (42):141-2.
- 15 Zhang X., Ishihara T., Corey D.R. (2000) Strand invasion by mixed base PNAs and a PNA-peptide chimera. *Nucleic Acids Research*. 28(17):3332-8.

- 16 Doyle D.F., Braasch D.A, Simmons C.G., Janowski B.A. and Corey D.R. (2001) Inhibition of gene expression inside cells by peptide nucleic acids: effect of mRNA target sequence, mismatched bases, and PNA length. *Biochemistry*. 40, 53-64.
- 17 Honda M., Kaneko S., Matsushita E., Kobayashi K., Abell G.A., Lemon S.M. (2000) Cell cycle regulation of hepatitis C virus internal ribosomal entry site-directed translation. *Gastroenterology*. 118(1):152-62.

VITAE

Christopher Jon Nulf was born in Royal Oak, Michigan, on November 27, 1970, the son of Marilyn June Nulf and Larry Lee Nulf. After moving to Dallas, Texas in 1985 and completing high school at Plano East Senior High in 1989, he enrolled at Texas A&M University, College Station, Texas. In 1993 he graduated with a Bachelor of Sciences degree in Zoology. At the University of Texas Southwestern Medical Center at Dallas, he worked as a research technician in the lab of Dr. Peter Stastny for two and a half years before enrolling in the graduate program at UTSWMC in 1997. After studying under the guidance of Dr. David Corey, he was awarded the degree of Doctor of Philosophy in Molecular Microbiology in August 2004.

Permanent Address: 3240 N. Hall Street
Apartment #142
Dallas, Texas 75204